Mechanosensing in Plants

- Mechanosensitive Calcium Channels *versus* the Cell Wall-Plasma Membrane-Cytoskeleton Continuum

Zur Erlangung des akademischen Grades eines

DOKTORS DER NATURWISSENSCHAFTEN

(Dr. rer. nat.)

Fakultät für Chemie und Biowissenschaften

Karlsruher Institut für Technologie (KIT)-Universitätsbereich

genehmigte

DISSERTATION

von

Qiong Liu

aus

Xi'an, China

Dekan: Prof. Dr. Peter Roesky

Referent: Prof. Dr. Peter Nick

Korreferent: Prof. Dr. Reinhard Fischer

Tag der mündlichen Prüfung: 16. April. 2014

Die vorliegende Dissertation wurde am Botanischen Institut des Karlsruher Instituts für Technologie (KIT), Botanisches Institut, Lehrstuhl 1 für Molekulare Zellbiologe, im Zeitraum von April 2011 bis April 2014 angefertigt.

Hiermit erkläre ich, dass ich die vorliegende Dissertation, abgesehen von der Benutzung der angegebenen Hilfsmittel, selbständig verfasst habe.

Alle Stellen, die gemäß Wortlaut oder Inhalt aus anderen Arbeiten entnommen sind, wurden durch Angabe der Quelle als Entlehnungen kenntlich gemacht.

Diese Dissertation liegt in gleicher oder ähnlicher Form keiner anderen Prüfungsbehörde vor.

Karlsruhe, im März 2014

Qiong Liu

Acknowledgments

I would like to take this opportunity to express my gratitude to all those who offered me their help in any way during the entire course of my graduate study.

First and foremost, I would like to thank Prof. Peter Nick for his wonderful mentorship as well as this great opportunity to enhance myself both professionally and intellectually. I am truly humbled and inspired by his enthusiasm, sagacity, erudition, dedication, optimism, sympathy as well as patience and these are the things which I can benefit from for the rest of my life no matter what I do. Meanwhile, I deeply appreciate all the time and attention he devoted, all the suggestions and ideas he provided in supervising me as well as the freedom that he granted me to work on this project.

I am grateful that Prof. Reinhard Fischer agreed to be my co-examiner immediately and I really appreciate his time, devotion and expertise.

I thank Dr. Kateřina Schwarzerová, Dr. Jan Petrášek and Stanislav Vosolsobě for the wonderful time that I spend in their lab at the Charles University in Prague at the beginning of my work. My special thanks go to Ms. Gesine Preuss from the Institute of Mineralogy und Geochemistry, Karlsruhe Institute of Technology (KIT) for performing the atomic absorption analysis for determining the calcium and sodium content.

I would like to thank Dr. Jan Maisch, Dr. Michael Riemann, Dr. Kai Eggenberger and Dr. Fei Qiao for their help and suggestions during my work. I thank especially Dr. Jan Maisch and Dr. Kai Eggenberger for critical reading of this thesis. I appreciate the excellent work of our lab technician Sabine Purper and Sybille Wörner as well as our Azubi Isolde Konrad for her assistance in analyzing BY-2 cells.

My sincere thanks also go to all the doctoral students as well as all the members who work in Botanical Institute 1 for such a pleasant, friendly and helpful working atmosphere. I thank especially Ningning Gao for her support and accompany. We have kept each other going through a few bumps on the road. My special thanks also go to Yingnan Bai for his wonderful job with the visualization of one of the figures. My heartfelt thanks extend to Rita, Mohamed, Holger, Thomas, Bea and Katharina whom I learned many things as well as get help from so many times. Many thanks to Natalie, Sebastian, Fatemeh, Ye, Xiang and our Azubis for their excellent job in preparing the cell culture media which is a very important however tedious work.

Finally, I would like to thank my parents and my sister for their unconditional love and support. Thank you for being the rock of my life! Thank my little nephew Henry for adding another huge amount of fun to all our lives.

This work is financially supported by the China Scholarship Council (CSC) as well as the Sino-German Center for Science Funding, Programmme GZ614.

Qiong Liu

Table of Contents

Abbreviations

2, 4-D: 2, 4-dichlorophenoxyacetic acid

AFs: Actin filaments

BY-2: Tobacco *Nicotiana tabacum* L. cv. Bright Yellow 2

BA: Benzyl alcohol

CTK: Cytoskeleton

CW: Cell wall

cMTs: Cortical microtubules

DMSO: Dimethyl sulfoxide

ECM: Extracellular matrix

FM4-64: *N*-(3-triethylammoniumpropyl)-4-(6-(4-(diethylamino) phenyl) hexatrienyl) pyridinium dibromide

GFP: Green fluorescent protein

IAA: Indolyl-3-acetic acid

LatB: Latrunculin B

L_p: Hydraulic conductivity

MFs: Microfilaments

MS-Medium: Murashige and Skoog medium

MS: Mechanosensitive

MTs: Microtubules

NPA: 1-N-naphthylphthalamic acid

PA: Phosphatidic acid

PCV: Packed cell volume

PM: Plasma membrane

RFP: Red fluorescent protein

ROS: Reactive oxygen species

SA: Stretch activated

VM: Vacuole membrane

Zusammenfassung

Zu den unterschiedlichen natürlichen Faktoren, auf die Pflanzen innerhalb ihres Umfelds mit angepasster Entwicklung und Wachstum reagieren, zählen mechanische Kräfte zu den Wichtigsten. Im Laufe der Evolution haben Pflanzen dadurch ausgeklügelte Mechanismen entwickelt. Obwohl die molekularen Grundlagen der Reaktion auf verschiedene chemische Stoffe relativ bekannt ist, sind die schwer erkennbaren molekularen Mechanismen, die auf mechanische Stimuli folgen, weitestgehend unbekannt. Einige molekulare Akteure wie Gene, Proteine, Hormone oder nicht-organische Substanzen, die an der Signalverwertung mechanischer Stimuli beteiligt sind, konnten identifiziert werden. Dennoch sind die maßgeblichen Mechanorezeptoren sowie nachgeschaltete Signalwege weiter unbekannt.

Über die Mechanoperzeption in Pflanzen sind momentan zwei unterschiedliche Modelle im Gespräch. Eines beruht auf Ionenkanälen, das Andere auf Strukturen der sensorischen Tensegrität. Der Hauptbestandteil der sensorischen Tensegrität ist das pflanzliche Zytoskelett, das für die Volumenerhaltung der Zelle verantwortlich ist. In dieser Dissertation wird hydraulische Leitfähigkeit (L_p) als quantitative Größe herangezogen, um die Rolle des Zytoskeletts anhand von Volumenänderungen in Protoplasten zu erklären. Die Komplexbildung von Kalzium, die Unterdrückung der Kalziumkanäle, sowie die Manipulation der Membranfließeigenschaft haben die L_p nicht beeinflusst. Die Manipulation des Zytoskeletts auf direkte Art, über spezifische Pharmazeutika oder indirekt über den bakteriellen Elicitor Harpin oder die pharmakologische Aktivierung von Phospholipase D, haben demgegenüber einen Einfluss auf die L_p. Durch eine lokale Behandlung von Aktin mit einer photoaktivierbaren Form des Phytohormons Auxin wird die Symmetrie der Aktinorganisation unterbrochen, was zu einer lokalen Deformation der Zellform führt, und durch eine lokal erhöhte L_p angezeigt wird. In dieser Dissertation wird ein Modell aufgestellt, in welchem die unter der Membran liegenden Bestandteile des Zytoskeletts den intrazellulären

Membranspeicher während regulatorischen Volumenänderungen kontrollieren.

Um die Rolle zweier kalziumpermeabler Kanäle bei der Wahrnemung mechanisher Reize aufzuklären, wurden die dazugehörenden Gene NtTPC1A (*Nicotiana tabacum* Two Pore Channel 1A) and NtMCA2 (*Nicotiana tabacum* Mid1 Complementing Activity 2) stabil in BY2-Tabakzellen (*Nicotiana tabacum* L. cv. Bright Yellow 2) transformiert. Eine folgende fluoreszenzmikroskopische Analyse zeigt die Lokalisation von NtTPC1A-GFP am Tonoplast. Im Gegensatz dazu befindet sich ein Großteil des GFP-NtMCA2 Fusionsproteins an der Zellmembran, bewegt sich aber dennoch zyklisch zwischen intrazellulären Kompartimenten und der Zellmembran. Die Überexpression von NtTPC1A und NtMCA2 führt zu erhöhter Toleranz gegenüber Gd^{3+} und Al^{3+}, sowie zu einer verbeserten Salztoleranz in BY2-Tabakzellen. Ebenso führt sie zu vermindertem Zelllängenwachstum und zu einer verminderten Kalziumkonzentration, was durch Zugabe von Kalzium ausgeglichen werden kann. Aus diesen Resultaten lässt sich schlussfolgern, dass beide Ionenkanäle *in vivo* vermutlich nicht als Monomere funktionieren, sondern dass eine Komplexbildung erfolgt. Die Bildung und Funktion dieses Komplexes unterligen vermutlich ausgeklügelten Regulierungsmechanismen. Die Verminderung der Zellgröße, sowie die Salztoleranz lassen vermuten, dass die Kanäle auch in Mechanismen der Antwort auf in- und externe Reize involviert sind.

Mit der Beteiligung der Ionenkanäle am Mechanosensing wird ein Model bevorzugt, indem nicht nur Ionenkanäle der Zellmembran, sondern auch Ionenkanäle im Tonoplast am Komplex der dynamischen Tensegrität beteiligt sind. Es konnte gezeigt werden, dass die Integrität dieses tensegralen Systems, besonders in Gegenwart der Zellwand, wesentlich für die Signalverarbeitung von mechanischen Kräften ist. Dies wird durch den Vergleich der Kalzium-Unabhängigkeit der L_p in Protoplasten mit der Kalzium-Beteiligung an der Zellantwort auf mechanische Stimuli, die am Beispiel der Zellwand gezeigt werden konnte, deutlich. Die Verbindung zwischen Zellwand, den beiden Kalziumkanälen und dem Zytoskelett benötigt jedoch weitere Forschungsarbeiten.

Abstract

Among a wide range of diverse factors of distinct nature which plants rely on to perceive their surroundings and adjust their growth and development accordingly, mechanical force is the most ancient, fundamental, and constantly encountered one. Plants have been well equipped with intricate mechanisms during the course of evolution to perceive and respond to external as well as internal mechanical forces of various amplitudes and durations. However, unlike the well understood molecular bases of sensing soluble ligands, the very different molecular mechanisms make how exactly mechanical stimuli are sensed and transduced a long standing question. Molecular players participating mechanoresponses in plants have been identified successively, like genes, proteins, hormones as well as inorganic signaling molecules. However, the identity of genuine mechanoreceptors and the exact downstream signaling pathways remained a field which needs further investigation.

Two models proposed interpreting mechanoperception in plants, one relying on mechanosensitive ion channels and one depending on sensory tensegrial structures were expounded. As the main component of the tensegrial structures, the role of the cytoskeleton in mechanosensing was probed using volume regulation as exemplary phenomenon. Employing hydraulic conductivity (L_p) as quantitative readout, a role of the cytoskeleton in protoplast swelling was demonstrated. Chelation of calcium, inhibition of calcium channels, or manipulation of membrane fluidity, did not significantly alter L_p, whereas direct manipulation of the cytoskeleton via specific chemical reagents, or indirectly, through the bacterial elicitor Harpin or activation of phospholipase D, was effective. By optochemical engineering of actin using a caged form of the phytohormone auxin the symmetry of actin organization can be broken resulting in a localized deformation of cell shape indicative of a locally increased L_p. These findings are interpreted in terms of a model, where the submembraneous

cytoskeleton controls the release of intracellular membrane stores during regulatory volume change.

Meanwhile, two putative calcium permeable channel encoding genes, namely *NtTPC1A* (*Nicotiana tabacum* Two Pore Channel 1A) and *NtMCA2* (*Nicotiana tabacum* Mid1 Complementing Activity 2) were stably overexpressed in tobacco BY-2 (*Nicotiana tabacum* L. cv. Bright Yellow 2) suspension cells respectively in order to exam their roles in mechanosensing. Fluorescent microscopic studies revealed the tonoplast localization of NtTPC1A-GFP fusion proteins. The GFP-NtMCA2 fusion proteins predominantly locate at the plasma membrane and are constantly cycling between the intracellular compartments and the plasma membrane. On the one hand, overexpression of NtTPC1A and NtMCA2 lead to increased tolerance to Gd^{3+} and Al^{3+} as well as to mild salt stress in tobacco BY-2 cells. On the other hand, it results in inhibited cell elongation as well as decreased intracellular calcium content which can be restored by calcium supplements. These results indicate that both channel proteins function not as monomers *in vivo* and instead form multimers which are subjected to intricate regulating mechanisms. The inhibition of cell elongation growth as well as improved salt tolerance suggest alterations in sensing internal as well as external mechanical forces. Therefore, it is speculated that they both are involved in mechanosensing.

Based on the investigations of these two players speculated to be involved in mechanosensing, a dynamic tensegrial based entity for sensing mechanical stimuli in plants involving not only plasma membrane ion channels but also vacuolar membrane ion channels is proposed. Meanwhile, the integrity of this tensegrial structure, the presence of the cell wall in particular, is shown to be vital for mechanotransduction when comparing the independency of L_p on calcium observed in the protoplasts with the involvement of calcium in mechanosensing demonstrated for walled cells. However, the link between the cell wall, these two calcium channels and the cytoskeleton needs further investigation.

1. Introduction

Owning to their sessile lifestyle, adaptation has become an eternal theme for plants that are successful in surviving this ever-changing environment which is most of the time absolutely not amiable for them. To master the developmental flexibility required for adaptation, plants must be able to integrate the signaling triggered by different environmental factors at certain time into a balanced and appropriate response. As a prerequisite for mounting the appropriate biochemical, physiological, morphological as well as developmental responses leading to adaptation under a multitude of abiotic and biotic stimuli, perception is undoubtedly of pivotal importance. Among the wide range of diverse factors of distinct nature which plants rely on to perceive their surroundings and adjust their growth and development, such as temperature, the quality, intensity and periodicity of light, water and CO_2 availability, nutrient levels, wounding, pathogen, symbiotic microorganisms and so on, mechanical force is the most ancient, fundamental, and constantly encountered one. Therefore, sensing and responding to mechanical forces had become the most fundamental skills of terrestrial plants. In fact, all living creatures are able to sense mechanical forces regardless of whether they are imposed externally or generated from within and adjust their biological processes accordingly; no matter they are complicated multicellular organisms like us humans or simple single cell microbes as bacteria.

As plants living in the wild, they are constantly exposed to mechanical forces, from the perpetual presence of gravity, to a sudden gush of wind, from herbivores attack to the gentle rub of animals walking by. As a result of evolution, plants have developed very intricate mechanisms to perceive and respond to mechanical stimuli of various amplitudes and durations, ranging from these intense enough to cause tissue damage to those gentle as light brush, from those ephemeral as pollinators landing to the perpetual pulling of gravity. The omnipresent mechanical

forces had hence become a critical signal profoundly affecting morphogenesis (Hamant & Traas, 2010) and growth (Moulia *et al.*, 2006) in plants. Comprehensive descriptions about gravity and mechanical-driven growth in plants have been known for over a hundred years (Darwin & Darwin, 1880; Knight, 1806), like wind sculpturing a tree, a tendril used by the climbing plants twining around the support, the roots navigating their way through obstacles in the soil. The long standing questions behind these observations are how these mechanical stimuli are sensed by plants and what do plants rely on to respond appropriately to them. Unlike the well understood molecular bases of sensing soluble ligands through the lock-and-key binding of certain ligands to specific receptors on the plasma membrane (PM), the very different and diverse mechanosensory phenomena make how exactly mechanical stimuli are transduced and sensed on the molecular level only started to be unraveled till quite recently. Although molecular players participating in mechanoresponses have been identified successively, like genes, proteins, hormones, inorganic signaling molecules, such as reactive oxygen species (ROS), and Ca^{2+} ions (Braam, 2005; Kung, 2005; Telewski, 2006; Chehab *et al.*, 2009; Monshausen & Gilroy, 2009; Mirabet *et al.*, 2011; Strohm *et al.*, 2012; Baldwin *et al.*, 2013; Hamant, 2013; Kurusu *et al.*, 2013; Toyota & Gilroy, 2013; Shigematsu *et al.*, 2014), the identities of genuine mechanoreceptors and the downstream signaling pathways remained an intensively investigated field.

1.1 Mechanical load on the membrane - not only for evident mechanical forces sensing

Life requires an internal space which is chemically differentiated from the external surroundings as well as the ability to buffer internal homeostasis against fluctuations of the external environment (Lintilhac, 1999) which are achieved by semipermeable biomembranes and are therefore subjected to mechanical force imposed by osmotic imbalances. In multicellular animals, cells are protected from

osmotic challenges by excretion organs which establish an isotonic intercellular environment for the wall-less cells. However, this strategy is not possible for bacteria, fungi, and plants which have to cope with strong variations of osmotic conditions. Upon sufficient supply with water, the cell membrane of these organisms experiences considerable pressure from the cell interior against the constraint of the cell wall. In contrast, when these cells are exposed to extreme hyperosmotic stress or high salinity, especially outside a tissue context, the protoplast shrinks and even detaches from the cell wall. In order to maintain a functional metabolism, the cells must be able to sense osmotic changes in the first place. It is therefore not surprising that already prokaryotes have evolved mechanisms to sense osmotic forces at the PM reviewed in (Kung, 2005). Concomitantly with the osmotic gradient generated due to the separation of the PM is the segregation of charged particles across the membrane which creates spatial gradient of voltage and consequently tremendous electrical forces across the PM which had been shown to play an important role in mediating various cellular functions, such as driving ions and nutrients translocation across the PM, response to stimuli (Behrens *et al.*, 1985; Okazaki *et al.*, 2002; Carpaneto *et al.*, 2007; Kupisz & Trebacz, 2011) as well as organizing PM microdomains (Grossmann *et al.*, 2007).

Other than the forces caused by electrochemical gradients at the PM due to segregation, since the very beginning of all life forms, gravity with its constant direction and magnitude has become a rather important clue for plant morphogenesis especially after they left water for land. No buoyancy is available on land to counterbalance the gravity caused by self-weight. Consequently, territorial plants had to develop stronger structures for mechanical support and better strategies to arrangement the load bearing elements spatially. Gravisensibility guarantees that most shoots grow upwards and most roots grow downwards (Moulia & Fournier, 2009; Hashiguchi *et al.*, 2013) meanwhile optimizes the arrangement of load bearing elements in space for maximal

exposure to the sun for photosynthesis at minimum cost of biomass.

It is natural to link many environmental factors, such as gravity, osmolarity, wounding, wind, touch, invasion of pathogen, or density of the substrate/medium with sensing mechanical load on the PM. However, other factors influencing PM fluidity can also be sensed as a mechanical load upon the PM (Los & Murata, 2004). Many experiments using membrane fluidizers and rigidifiers suggested that membrane rigidification might be involved in the perception of cold stress (Monroy & Dhindsa, 1995; Orvar *et al.*, 2000; Sangwan *et al.*, 2002; Sangwan *et al.*, 2001). Due to the constant existence of mechanical load on the membrane, many membrane embedded proteins have involved the ability to exploit this mechanical force for the benefit of the organism. The best known examples are the bacterial mechanosensitive (MS) channels with large-, small- and mini-conductance which protect *Escherichia coli* against osmotic pressure with even the ability to distinguish strong fluctuations from mild ones (Berrier *et al.*, 1996). Taking it all together, it is clear that mechanosensing is an indispensable skill of all living organisms which plays very important roles particularly in plant growth, morphogenesis as well as responses to both abiotic and biotic stresses that are perceived as mechanical load on the membrane even not ostensibly.

1.2 How do plants sense mechanical stimuli?

Plants' responses to mechanical stimuli mainly fall into two broad categories. The first type is characterized by extremely rapid movements of organs in response to mechanical stimulation, like the folding of *Mimosa pudica* leaflets when they are touched (Braam, 2005) or the closing of the Venus fly trap seconds after a prey walked in (Forterre *et al.*, 2005). The other type involves morphogenetic changes which progress over a long period of time, ranging from days to weeks even throughout the whole life of plants. The fast mechanical responses often rely on specialized organs or appendages such as trigger hairs, snap tentacles, or

adhesive emergences (Krol *et al.*, 2012; Poppinga *et al.*, 2012). And in contrast, mechanical responses of most plants do not require special structures and occur in a slow manner often not being noticed if not given time and effort. However, the capability of sensing and responding to mechanical forces in non-specialized plant cells have been shown to be critical for fundamental processes such as turgor regulation, cellular expansion and morphogenesis down to the single cell level. Experimental evidences have been provided in suspension cultured soybean and parsley cells (Gross *et al.*, 1993; Yahraus *et al.*, 1995), meristematic and fully differentiated shoot and root cells (Braam & Davis, 1990; Legue *et al.*, 1997; Ditengou *et al.*, 2008; Hamant *et al.*, 2008; Haswell *et al.*, 2008), even in protoplasts (Haley *et al.*, 1995; Wymer *et al.*, 1996). Therefore, it is very important to understand the molecular mechanisms of how non-specialized plant cells sense mechanical stimuli of various amplitudes and durations originated from both external and internal. Elucidating such a fundamental process could help to answer how plants respond to mechanical stimuli on the whole organismal level.

As above pointed out, all types of plant cells are capable of sensing mechanical forces, not only those located in specialized sensing organs or tissues, which when looking at on the single cellular level, is not so easy to achieve due to obstacles from two aspects that plants have to conquer as summarized in Nick (2013). It is generally believed that the original inputs from mechanical stimuli are minute changes in geometry of the membrane, where the perception mechanism is speculated to be located. In other words, the energy of the primary input is extremely small and therefore has to be efficiently amplified to stand out the bilayer tension fluctuations. This general problem of mechanosensing is even accentuated in plants, because plant cells are subject to continuous pressure simultaneously both from the inside (produced by the expanding protoplast) and the outside (produced by the tissue tension from expanding neighboring cells). These pressures are in the range of several bars, and provide large background forces against which the minute changes of mechanical energy must be

discriminated. A further challenge to mechanical sensing peculiar for plants is the lack of specialized sensory organs. Sensing is diffusely spread over a large number of cells. Thus, each individual cell has to cross the threshold for sensing without support from its neighbors (Nick, 2013). Based on these considerations, a highly sensitive device for detecting and effectively magnifying these minute changes must exist in plant cells for sensing mechanical stimuli.

Unlike signaling events triggered by the binding of a ligand to its receptor, for a mechanical stimulus triggered response, no matter rapid or slow, the crux is that the detected physical input has to be firstly translated into a signaling output of biochemical quality and subsequently being processed intracellularly. This is achieved in a two-step approach: in the first step, the physical energy is transformed into a chemical signal in a process that has been named ‘susception’. It relies on mechanoreceptors/mechanosensors which the stimulus has been transmitted to. As a second step, perception in the strict sense is triggered by this transformed input (Nick, 2013) namely the mechanical signal transduction pathway. Our understandings about how plant cells sense forces, transmit them into the cell interior or to other cells, and translate them into chemical signals which impact a wild range of cellular responses on the molecular level rely on the comparison with mechanosensory transduction mechanisims as well as mechanosensors recognized in other organisms such as *E. coli* and *Saccharomyces cerevisiae* as well as mammalian cells. The speculated major molecular players include the cytoskeletons, ion channels, osmotic sensors, cell-wall associated kinases and so on (Monshausen & Haswell, 2013).

We have learned that the critical elements for an effective mechanotransduction event are speed and sensitivity. There are two popular hypotheses of how mechanotransduction is achieved in mammalians. The first one is via direct activation of a membrane ion channel due to mechanical force induced tension in the lipid bilayer. The second is via linking or tethering of a channel protein to the

extracellular matrix and/or the intracellular cytoskeletons which then directly leads to the opening of the channel and allows ionic influx (Gillespie & Walker, 2001; Welsh *et al.*, 2002; Barritt & Rychkov, 2005; Martinac, 2014). In the following sections, current ideas originated from these two hypotheses about how mechanotransduction could be achieved in plants will be introduced.

1.2.1 Models for plant mechanosensing I: mechanosensitive ion channels

Mechanosensing relies on diverse types of transducer molecules and MS ion channels are considered as the most important primary transducers which convert mechanical force into an electrochemical signal in mammalian cells for hearing, touch, and other mechanical senses (Sukharev & Corey, 2004). And ion flux, especially calcium, has been associated with mechanical stimuli in many studies in plants as well (Trewavas & Knight, 1994; Fasano *et al.*, 2002; Kurusu *et al.*, 2013; Toyota & Gilroy, 2013). Consequently, ion channels, embedded at the site where mechanical stimuli are detected and gated in response to mechanical force converting mechanical force into electrochemical signals by allowing ions to flow through an ideal candidate for mechanosensors to achieve rapid and efficient mechanotransduction (Gillespie & Walker, 2001).

As a matter of fact, such kind of channel has been located within a wide variety of mechanotransduction complexes in a large number of species. Disruption of these channels has been shown to result in alterations in the detection of the mechanical environment (Brierley, 2010). The activation of MS ion channels by motion of starch filled plastids (amyloplasts) has been proposed as mechanism for gravity sensing in root tips (Boonsirichai *et al.*, 2002). The rapid ionic flux occurred upon altered gravity vector also fits the profile of MS ion channels (Toyota & Gilroy, 2013). However, the revealing of the molecular identity of genuine MS ion channels in plants remains arduous. Several promising candidates for mechano- and osmo- sensitive channels proposed in a range of species, like the transient receptor potential (TRP) channels in animal cells (and

the yeast TRPY homolog), the DEG/ENaC voltage-independent Na^+ channel family and the TREK K^+ channel family, which are all lack of homologs in any of the currently sequenced plant genomes (Monshausen & Gilroy, 2009). The best-understood MS channels are the MscS and MscL from *E. coli* which serve as osmotic safety valves. By releasing cytoplasmic low-molecular-weight contents to the extracellular medium they help to prevent cellular lysis during hypoosmotic shock (Corry & Martinac, 2008). The gating mechanism is well characterized for these channels as well. Tension in the membrane leading to phospholipids pulling on the transmembrane domains of the channel, causing it to open in an iris-like fashion without assistance from any other proteins (Kung *et al.*, 2010). Bacteria MscS played an important role in identifying at least one family of plant mechanosensor candidates whose existence has been corroborated by accumulating evidences obtained via many electrophysiological evidences in plants and algae as summarized in Toyota *et al*. (2013). At the moment, the top two candidates for MS ion channels in plants are the MSL and MCA.

The *MSLs* (*MscS*-like) genes are plant homologs of the bacteria MS channels which are composed of multimers with an iris-like pore, gated by increasing tension in the membrane as the cells subjected to hypotonic stress (Haswell & Meyerowitz, 2006). 6 and 10 *MSLs* homologous genes were found in rice and *Arabidopsis* respectively (Pivetti *et al.*, 2003). *MSC1*, an *MscS* family member from green algae *Chlamydomonas*, together with *AtMSL2* and *AtMSL3* were reported to be implicated in the control of organelle size, shape, and perhaps division during normal plant development (Haswell & Meyerowitz, 2006; Nakayama *et al.*, 2007) probably by modulating ion flux in response to membrane stretch and protecting them from hypoosmotic stress that occurs during normal plant growth (Veley *et al.*, 2012). AtMSL9 and MSL10 locate in the PM of root cells. They possess distinct stretch activated (SA) channel activities in protoplasts derived from root cells and appeared to be involved in mechanosensitive gating of Cl^- conductance, whilst no global physiological functions were detectable

(Haswell *et al.*, 2008).

A year after the cloning of MSLs in *Arabidopsis*, a PM protein designated as MCA1 (MID1-Complementing Activity 1) was cloned through a screen for proteins which are able to rescue the lethal mutation in yeast lacking a putative Ca^{2+} permeable SA channel component called MID1 using cDNAs of *Arabidopsis* (Kanzaki *et al.*, 1999; Nakagawa *et al.*, 2007). MCA1 has been shown to be correlated with Ca^{2+} influx in *Arabidopsis* root cells (Nakagawa *et al.*, 2007). Via blast search, a single paralog of MCA1 in *Arabidopsis* was identified and designated as MCA2. Reduced calcium uptake in roots was also observed in *mca2* mutants. Overexpressing MCA1 results in the upregulation of touch responsive genes such as TCH3 (CML11), and heterologous expression of MCA1 in mammalian CHO cells leads to a novel stretch-induced Ca^{2+} current. Shortly after, two MCA homologs in tobacco BY-2 cells named NtMCA1 and NtMCA2 were isolated (Kurusu *et al.*, 2012c). Meanwhile, the sole rice homolog of MCA1 in *Arabidopsis* was isolated and the Ca^{2+} uptake activity in the OsMCA1-overexpressing cells was shown to be higher than in the GUS-expressing control cells (Kurusu *et al.*, 2012b).

In summary, the structural similarity between MSL and bacteria MS channel and the strong link between calcium fluxes and MCAs are indications that these two channels may function as MS ion channels. However, whether these proteins *per se* form SA ion channels and function alone like bacteria MscS and MscL rather than requiring tether to other intra- or extracellular components for gating is not clear. Taking into consideration that the physiological functions of the most MSL proteins remain enigmatic and the touch responsive TCH3 also respond to environmental stimuli such as darkness as well as to developmental regulation (Lee *et al.*, 2005), the possibilities of these two channels as genuine MS ion channels become less certain according to the criteria set for bacterial MS channels (Arnadottir & Chalfie, 2010).

1.2.2 Models for plant mechanosensing II: sensory tensegrial structure

A mechanical model of cell structure based on tensegrity architecture has been used to explain how cell shape, movement and cytoskeletal mechanics are controlled, as well as how mammalian cells sense and respond to mechanical forces (Ingber, 1993). Tensegrity is a term in architecture coined from “tension” and “integrity” by the American architect and engineer Richard Buckminster Fuller who used it to describe self-supporting structures that were able to stabilize their shape by continuous tension or ‘tensional integrity’ rather than by continuous compression (Fuller, 1961). They consist of continuous networks of tensile elements (which can transmit forces by pulling) interconnected to a discontinuous system composed of stiff components (which can transmit forces by compression) (Nick, 2011) resulting in a dynamic prestress state which mechanically stabilizes all constituents. The simplicity of tensegrial structures by using materials at the most economical way beautifully exemplifies the balance of underlying force, which is based on local compression and continuous tension. In such a structure, all elements are in a state of isometric tension and disturbance of any individual element would results in immediate alterations in all other elements within the same structure. In the cellular tensegrity model, tensional forces are borne by cytoskeletal microfilaments and intermediate filaments. These forces are well balanced by interconnected structural elements that resist compression, most notably, internal microtubule struts and extracellular matrix (ECM) adhesions in mammalian cells (Ingber, 2003a). This well balanced cellular tensegrial structure is highly responsive to mechanical disturbance and allows the forces to propagate and to be transduced in relatively long distances along filaments within an organism or directly to the nucleus from the outer surface of a cell (Ingber, 2008; Wang *et al.*, 2009).

Although the cellular tensegrity model was proposed based on experiments performed in mammalians, the molecular resemblance motivated the application

of this theory in plants. The cytoskeletons as major components of the cellular tensegrial structure are composed of microfilaments and microtubules in plants whereas the structurally more stable intermediate filaments are absent. Like in mammalian cells, the plant cytoskeleton undergoes constantly remodeling and contributes to cell shape, cell division and expansion, intracellular organization and trafficking, as well as signal transduction in plant cells. Due to the existence of the mechanically stable cell wall, the tensegrial function accomplished by the interphase cytoskeleton in mammalian cells is mostly taken over by the cell wall in plants. Therefore, the plant cytoskeleton is not obligated to provide mechanical support to the cell structure and thus free to adopt other roles, like to function as sensory tensegrity in plant cells (Nick, 2011). Accumulating evidences have shown that the plant cytoskeletons participate in sensing and responding to both biotic as well as abiotic stimuli (Kobayashi *et al.*, 1997; Komis *et al.*, 2002b; Schmelzer, 2002; Nick, 2008; Berghofer *et al.*, 2009). And the role of MTs as sensor for abiotic stimuli is reviewed in Nick (2008).

Due to the completely different lifestyles which plants and animals adopted, their cellular structures and functions have meanwhile evolved accordingly to better serve their distinct ways of living. The cell wall is probably the most prominent structural element which distinguishes plant cells from animal cells. Meanwhile, our understanding about the cell wall has evolved from the boring, lifeless, static, supporting enclosure to highly dynamic structures constantly undergoing changes required by growth and development as well as responding to a plethora of external stimuli (Seifert & Blaukopf, 2010). More importantly, the mechanical property of the ECM has been shown to affect internal activity, shape, alignment and adhesion to the ECM in mammalian cells (Bershadsky *et al.*, 2003; Engler *et al.*, 2004; Discher *et al.*, 2005; Vogel & Sheetz, 2006). Besides, an external mechanical perturbation will first inevitably act on the plant cell wall before reaching the PM and the cytoskeleton (CTK). All these considerations lead to the attempt to examine the role of plant cell wall in mechanosensing using the

mammalian ECM as a reference.

Cell walls are highly heterogeneous, dynamic and intricate structures, which have the remarkable property of combining extreme tensile strength with extensibility. Not only the composition of plant cell walls in different species exhibits a large diversity, it also varies in different cell types, and even in different subcellular cell wall domains and over time during cellular growth and differentiation (Freshour *et al.*, 1996; Somerville *et al.*, 2004; Derbyshire *et al.*, 2007; Pelletier *et al.*, 2010). The typical plant cell wall is made of an ordered array of stiff and tensionally strong cellulose microfibrils, interconnected with a matrix consisting of hemicellulose and/or pectin, and, in certain cell types, lignin, decorated with structural proteins and phenolic compounds (Cosgrove, 2005). From the chemical point of view, the compositions of mammalian ECM and plant cell wall are very different yet they could all be described as complex continuous networks composed of macromolecules organizing into fibrillar like meshes (Reuzeau & Pont-Lezica, 1995). This structural similarity between mammalian ECM and plant cell wall has been shown by high resolution stereomicroscopy (Kachar *et al.*, 1990; McCann *et al.*, 1990). The mechanical properties of the basic macromolecules composing the plant cell wall resemble the properties featured for the components of tensegrial structure. Therefore, the cell wall forms another tensegrial structure in plants both on the single cell and organismal level and has been shown to be able to influence cellular behaviors (Berger *et al.*, 1994; Brownlee, 2002). Accumulating evidences have emerged supporting that similar as the mammalian ECM, the plant cell wall with its specific texture and composition may influence the way mechanical signals are propagated and transduced to the cell (Hamant, 2013). Together with subcellular cell wall microdomains bearing modified mechanical properties as well as associated proteins, the cell wall has been shown to participate in various cell signaling events, mechanosensing included (Rodakowska *et al.*, 2009; Wolf *et al.*, 2012).

1.3 The cell wall (CW)-plasma membrane (PM)-cytoskeleton (CTK) continuum and mechanosensing

MS channels unequivocally responding to membrane tension without other proteins were first characterized in *E. coli* (Martinac *et al.*, 1990) and then later were found in *Archaea* (Le Dain *et al.*, 1998) as well as in eukaryotes (Zhang & Hamill, 2000). Based on these findings, Hamill & Martinac (2001) suggested that sensing the bilayer tension by mechano-gated channels may have first evolved in bacteria and *Archaea*, and then been preserved in eukaryotes providing a fundamental prototype for the evolution of more elaborate and sensitive mechanisms based on channel-ECM and channel-CTK association. It is natural that more diverse mechanosensing phenomena as observed both in humans and plants as well as more delicate precision demands required by these phenomena call for more complex mechanosensing device than SA channels in bacteria whose major task is to simply prevent cells from lysis. Actually, the study of more complex organism *Caenorhabditis elegans* revealed a mechanoreceptive complex composed of MS ion channel connected to both cytoskeletal components and ECM proteins forming a mechanical force transduction apparatus (Chalfie, 1997; Tavernarakis & Driscoll, 1997). Accumulating evidences have substantiated that a continuum between the CTK and the ECM plays a central role in mechanoperception in mammalian cells for various purposes (Geiger & Bershadsky, 2001; Chen *et al.*, 2004; Ingber, 2006; Geiger *et al.*, 2009; Mammoto & Ingber, 2010; Bukoreshtliev *et al.*, 2013). Despite that the molecular composition of mammalian ECM and plant CW differs and the intermediate filaments are missing in the cytoskeletal tensegrity in plants, a new concept had emerged in plant research that has been depicted as a counterpart of the extracellular matrix (EMC)-plasma membrane (PM)-cytoskeleton (CTK) continuum in mammalians, which is the cell wall (CW)-plasma membrane (PM)-cytoskeleton (CTK) continuum.

The EMC-PM-CTK continuum has been shown to play a central role in mechanosensing in mammalian cells. One of the most important components for a functioning MS tensegrial structure is the linker protein which connects the EMC with the CTKs on the other side of the PM (Geiger & Bershadsky, 2001; Ingber, 2003b; Geiger *et al.*, 2009; Goldmann, 2012a; Goldmann, 2012b). Integrins and cadherins through ligands binding connect cells with other cells as well as with the ECM in mammalian cells. Meanwhile, they are linked to the cytoskeleton from the cytoplasmic side. They are well positioned to mediate mechanotransduction and have been shown are intrinsically mechanosensitive (Schwartz & DeSimone, 2008). Cytoskeletal structures that adhesion receptors universally connected to allowing adhesions to resist deformation from applied forces are strongly implicated in mechanotransduction as well. The major linker proteins forming focal adhesions found in mammalian cells include integrin, talin, vinculin, filamin, actinin, and tensin whose true homologs were found to be absent through screening the *Arabidopsis* Genome Database available (Hussey *et al.*, 2002). However, evidences for the existence of the plant proteins sharing similar motifs with animal integrins have been provided (Canut *et al.*, 1998; Laval *et al.*, 1999; Clark *et al.*, 2001; Gentzbittel *et al.*, 2002; Knepper *et al.*, 2011) suggesting the existence of proteins in plants which may have a similar structure and function to integrins in animals. Baluska *et al.* (2003) summarized in a review that WAKs (cell-wall-associated kinases, a subfamily of the receptor-like protein kinases, RLK family), pectins, AGPs (arabinogalactan proteins), cellulose synthase, formins, plant-specific myosins of class VIII, phospholipase D, and callose synthase being the potential candidates of the obscure linker between the CTK and the CW. And a couple of years later Baluska *et al.* (2005) were able to show that a plant-specific myosin of class VIII and formins were the strongest candidates as the elusive adhesive molecules connecting the PM with CTK in plants. Deeks *et al.* (2005) reported that Group 1 formins proteins AtFH4 and AtFH8 are rich in the cross walls of roots, hypocotyls, and shoot cells of *Arabidopsis.* Among these two proteins, AtFH4 binds to profilin, influencing the

polymerization of actin. The extensin-like domain of the group 1 formins is predicted to insert into the cell wall which supports the putative role of formins as molecules linking the cell wall and the cytoskeleton (Cvrckova, 2000; Cvrckova *et al.*, 2004).

In the search for this elusive linker, Gens *et al.* (2000) first proposed the concept of plasmalemmal reticulum which was then refined by Pickard (2008) who described it as an elaborately patterned peripheral structure of the cell with cytoskeleton based components connecting the cell wall, periplasm, PM, cortex, and cytoplasm featured by adhesive components (such as arabinogalactan proteins and wall-associated kinases) and the functional analogues of integrins, as well as mechanosensory calcium channels. And some evidences for the existence of such signaling complex in tobacco cells are provided (Gens *et al.*, 2000; Pickard & Fujiki, 2005).

If verified in plants, mechano-gated channels like those found in bacteria and *Archaea* will become undisputable MS channels. However, few eukaryotic channels meeting the criteria set for MS channels in bacteria are confirmed, not only in plants but also in mammalians (Arnadottir & Chalfie, 2010). It is probably due to the fact that neither bacteria nor *Archaea* have the cytoskeleton in the eukaryotic sense and their cellular structures are vastly different. Multicellular eukaryotes probably do not directly employ such simple SA channels adopted by prokaryotes and instead they use the ECM/CW-PM-CTK continuum for mechanoperception which is more likely capable of providing a more sensitive, efficient and most importantly, more diverse mechanisms for mechanosensing. This tensegrial continuum composed of the CW, PM and the CTK as well as all sorts of linker proteins together with ion channels makes both the whole plant organism as well as the individual building blocks of the organism one giant or mini tensegrial structure. Here is one of the scenarios of how such a CW-PM-CTK continuum could operate in mediating plants' mechanoresponses. Ion channels

are tethered to the cytoskeletal components (MTs and AFs) which are responsible for perceiving, focusing as well as amplifying mechanical stimuli both from internal and external. Altered mechanical tension leads to the opening of the ion channels by the pulling force of the anchored cytoskeleton which then triggers ion flux thus completes the two-step mechanotransduction process and initiates downstream signaling pathways. In this case, the ion channel is considered as MS only because it is a component of the tensegrial structure and is not intrinsically mechano-gated by membrane tension *per se*. The localization of MS ion channels in this sense is not limited to the PM but also endomembrane located ion channels could be involved. A membrane embedded ion channel tethered to the CTK being the mechanotransducer with its ability to initiate ion flux seems to be a very direct and efficient model to accomplish the transduction of mechanical stimulus into an electrochemical signal in plants. The dynamic properties of the cytoskeletons *per se* as well as the possible ways they are connected to the channels and/or CW render huge diversity and flexibility to this sensory tensegrity.

1.4 Scope of this study

Mechanosensing is ubiquitous which takes place on many levels, from single cell, to tissue, till the entire organism. Consequently, it plays critical roles in regulating growth, development as well as response to stimuli of many kinds. As previously depicted, MS ion channels, the cytoskeletons and adhesion proteins, such as members of the RLKs family, are speculated to be most probable candidates for mechanosensors in plant cells. Two hypothetical models for mechanisms underlying mechanosensing were illustrated, namely through MS ion channels or via sensory tensegrial structure, which are in fact not mutually exclusive (Nick, 2013). A dynamic model in which the cytoskeleton tethered ion channels for mechanoperception is proposed as one of the scenarios of such a tensegrial entity in operation. However, the exact molecular components as well as their

action modes are far from being understood. Therefore, in this dissertation, two of the critical components, namely, the cytoskeleton and two selected putative ion channels will be examined in details in the context of mechanosensing and mechanoresponses.

1.4.1 Is the cytoskeleton involved in mechanosensing?

Sense osmotic alterations in the surrounding environment and adjust their volume correspondingly by actively change volumes have been commonly observed in mammalian cells reviewed in (Henson, 1999). Already several decades ago, wall-free plant protoplasts were shown to swell or shrink considerably within seconds in response to fluctuations of osmotic potential without losing their spherical shape (Wolfe *et al.*, 1986). Osmotic swelling or shrinkage of spherical protoplasts proceed within a couple of minutes, and must therefore be caused either by insertion of additional membrane material (in case of swelling) or by internalization of excess membrane material (in case of shrinking) (Wolfe *et al.*, 1986; Kubitscheck *et al.*, 2000; Shope *et al.*, 2003). This rapid osmotic swelling differs from the slow swelling reported for protoplasts generated from guard cells in response to blue light that requires 1 to 2 h and probably involves gene regulation (Zeiger & Hepler, 1977). The situation in osmotically challenged plant protoplasts is different from that in animal cells, where large proportions of the cell membrane are folded into filopodia, ruffles, and other protrusions, such that considerable increases in cell volume can be accommodated without the need for adjusting the cell surface reviewed in (Koivusalo *et al.*, 2009).

Prokaryotes respond to osmotic stress by active transport of ions and osmolytes as shown for the MS channel of large conductance, MscL, in *E. coli* (Kung, 2005). In animal cells, such concentration changes remain minute (Koivusalo *et al.*, 2009), and are therefore thought to be of minor impact as compared with the yielding of membrane protrusions and ruffles. Since animal cells lack cell walls and the PM itself cannot provide a mechanical barrier, the actin cytoskeleton has

been proposed to be involved in the mechanism that allows shape control after osmotic challenges (Henson, 1999; Koivusalo *et al.*, 2009). In plant cells as well, a hyperosmotic shock was shown to cause bundling of actin (Komis *et al.*, 2002b) and microtubules (Komis *et al.*, 2002a), indicating a connection between cytoskeleton and membrane tension.

In previous works from our group, it was shown for tobacco BY-2 cells that stabilization of actin by either Phalloidin (Berghofer *et al.*, 2009), or by inducible expression of an actin-bundling domain (Hohenberger *et al.*, 2011) also stabilizes the PM against electric permeabilization. By total internal reflection fluorescence microscopy (TIRF), a subset of the cytoskeleton that was directly adjacent to the PM was visualized (Hohenberger *et al.*, 2011). Stabilization of the submembraneous cytoskeleton caused an increase in the apparent thickness of the cell membrane. In fact, the actin filaments concentrated in the submembraneous cell cortex region has been suggested to be an appealing candidate for controlling the shape changes associated with alterations in cell volume (Henson, 1999). Since the elementary membrane cannot be resolved by light microscopy, these changes of apparent thickness must be caused by membrane topologies, leading to a model of tubulovesicular membrane folds or invaginations that increase membrane surface and might be structurally maintained by actin filaments (Hohenberger *et al.*, 2011).

This model predicts that the swelling response of protoplasts which are subjected to hypoosmotic shock should depend on the status of the submembraneous cytoskeleton. The permeability of the membrane to water is conventionally described as hydraulic conductivity (L_p) used as indicator for membrane behavior. The permeability of the membrane to water has been successfully used to quantify the activity of aquaporins (Maurel, 1997). A variation of this approach used osmolytes with variable hydrodynamic radii to estimate the size of the pores induced by nanosecond pulsed electrical fields (nsPEFs) (Nesin *et al.*, 2011).

When the cytoskeletons participate in volume control by regulating the insertion or release of submembraneous resources of membrane material, pharmacological manipulation of the cytoskeletons should result in changes of L_p. In fact, more than two decades ago, water permeability in the two poles of internodal cells in *Characean* algae had been reported to depend differentially on actin (Wayne & Tazawa, 1988). In these giant cells that often are 100 mm in length, actin is organized into prominent cortical bundles driving the rapid cytoplasmic streaming essential to provide nutrient transport. Whether this phenomenon is specific for this peculiar and highly specific cell type or whether it is general for cells from higher plants, has remained unclear.

The North American grape *Vitis rupestris* inhabits sunny rocks and slopes and is therefore used in viticulture as drought-tolerant rootstock. In contrast, the North American *Vitis riparia*, growing in alluvial forests, is less adapted to drought. It has been shown previously (Ismail *et al.*, 2012) that a cell line derived from *V. rupestris* is more salt tolerant as compared to a cell line derived from *V. riparia*. In the current work, these two grapevine cell lines are uses to probe for the role of the submembraneous cytoskeleton in volume regulation using L_p as indicator for the status of the cytoskeleton. To test the influence of actin organization on membrane geometry directly, optochemical engineering of actin organization was used as a strategy. The plant hormone indolyl-3-acetic acid (an inducer of actin dynamicity) was released from an inactive caged precursor (Kusaka *et al.*, 2009) at one flank of the protoplast by a localized pulse of short-wavelength light, and the temporal changes of cell geometry at the illuminated versus the opposite non-illuminated flank of the protoplast was followed. Elucidating the link between the plant cytoskeleton and volume control could contribute to understand the elusive volume sensory and regulatory machinery in plant cells.

1.4.2 Are these two putative calcium permeable channels players in plant mechanosensing?

A large number of candidates of MS ion channels in the PM of plant cells have been revealed using patch clamp analyses (Monshausen *et al.*, 2008) and among which the MS ion channels with calcium permeability has caught special attention. Because an immediate, transient cytosolic calcium increase that lasts for a few seconds is often observed accompanies mechanical stimulation caused by contact, touch, wobbling, bending or wind. Depending on the type of the stimulus, this initial increase in cytosolic calcium concentration may be followed by a slower and more sustained elevation lasting tens of seconds (Monshausen *et al.*, 2008). Bedsides the short term mechanical stimulus, cytosolic calcium increase was also reported to be responsible for gravity sensing (Plieth & Trewavas, 2002; Toyota *et al.*, 2008). Calcium imaging revealed that point contact elicits a localized Ca^{2+} increase spreading from the contact point throughout the whole cell (Monshausen *et al.*, 2009). Bending leads to biphasic Ca^{2+} increase only in cells under stretching tension (Monshausen *et al.*, 2009; Richter *et al.*, 2009). In contrast, cells undergoing compression do not experience cytosolic Ca^{2+} increase. Such a spatial distribution of Ca^{2+} increase consists with a role of MS calcium permeable channel.

The molecular identities of stretch-activated (SA) channels had been speculative due to the unavoidable highly artificial conditions used in electrophysiological experiments to verify their existence. One exception is the MscS-like proteins which had been found located in the plastid envelope in *Arabidopsis* and are able to restore osmotic-shock sensitivity of a bacterial mutant lacking MS ion channel activity (Haswell & Meyerowitz, 2006). Roughly at the same time, a PM protein designated as MCA1 was cloned by functional complementation of a lethal mutation in yeast which lacks a putative Ca^{2+} permeable SA channel component called MID1. It has been shown to be correlated with Ca^{2+} influx in *Arabidopsis*

root cells (Nakagawa *et al.*, 2007). Roots of knockout mutants of *MCA1* showed a reduced ability to penetrate a layer of hard agar, suggesting some defect in either growth or mechanical responsiveness. However, plants constitutively overexpressing MCA1 exhibited more obvious defects in development, like short stems, small rosettes, no petals and shrunken seed pods. The sole paralog of MCA1 in *Arabidopsis*, MCA2 which when knocked out, however did not affect the roots' ability to penetrated hard agar like in the *mca1* mutant indicating that it has a distinct role in Ca^{2+} up take in roots (Yamanaka *et al.*, 2010). Both of them were able to complement the yeast *mid1* mutant (Nakagawa *et al.*, 2007; Yamanaka *et al.*, 2010) and therefore have been suggested as another potential candidate for MS ion channel in plants despite the fact that both MCA1 and MCA2 bear very low structural similarity to MID1. Right after that, two MCA homologs in tobacco BY-2 cells named NtMCA1 and NtMCA2 were isolated and suggested to play roles in Ca^{2+}-dependent cell proliferation and mechanical stress-induced gene expression in BY-2 cells, probably by regulating the Ca^{2+} influx through the PM (Kurusu *et al.*, 2012c). Meanwhile, the Ca^{2+} uptake activity of OsMCA1 was also suggested by overexpression in rice (Kurusu *et al.*, 2012b). Nakagawa *et al.* (2007) reported that MCA1 has at least two potential transmembrane segments. And *in silico* study indicates that the C-terminal half of MCA1 shows similarity to the PLAC8 (for human placenta-specific gene 8) region which is a cysteine-rich domain of unknown function found in 127 plant and animal proteins (Marchler-Bauer *et al.*, 2005). The N-terminal half was predicted to have an EF hand-like motif and is similar to a functionally unknown N-terminal domain found in many putative rice protein kinases (Kurusu *et al.*, 2013). In contrast, not so much is known about the NtMCA2 and it is therefore intriguing to characterize it as a component of the tensegrial entity for mechanosensing given its identity as a putative calcium channel. This would help to exam the proposal that ion channels tethered to the cytoskeleton could be used as a potential mechanism of mechanosensitivity.

Another type of putative calcium permeable channel, the TPC1 (two pore channel 1) channel from tobacco BY-2, has also been brought to my attention due to its controversial localization and elusive contribution to calcium hemostasis in plants. Furuichi *et al.* (2001) first reported that a full length cDNA encoding a putative voltage sensitive Ca^{2+} channel (AtTPC1) was isolated from *Arabidopsis* which shares high structural similarities with TPC1 cloned from rat kidney (Ishibashi *et al.*, 2000). Following that, by designing primers based on cDNA sequence of the conserved domain of AtTPC1 and rat TPC1, Kadota *et al*. (2004) was able to isolate two homologous genes NtTPC1A and NtTPC1B from *Nicotiana tabacum.* Nearly at the same time, TPC1 channels were found in rice and wheat successively (Kurusu *et al.*, 2004; Wang *et al.*, 2005). Similar as AtTPC1 and TPC1 in rat, the TPC1 channels found in tobacco, wheat and rice all comprise of two homologous domains, each containing six transmembrane segments (S1-S6) with a loop between S5 and S6 (Kurusu *et al.*, 2012a; Kurusu *et al.*, 2012c; Furuichi *et al.*, 2001). This overall structure of known plant TPC1s is very similar to the structural arrangement of half of the α_1 subunit of voltage-gated calcium channels in mammalian cells (Catterall, 2000).

AtTPC1 was able to rescue the yeast *cch1* mutant which encode a protein together with Mid1 constitute a protein complex responsible for Ca^{2+} transport activity across the PM in yeast indicating AtTPC1 has Ca^{2+} uptake activity. This was corroborated by the induced luminescence intensity in aequorin-expressing *Arabidopsis* leaves overexpressing AtTPC1 (Furuichi *et al.*, 2001). Furuichi *et al.* (2001) suggested that AtTPC1 is a voltage-activated calcium channel located in the PM. GFP tagged AtTPC1 expressed in tobacco BY-2 cells was found to be localized in the PM and and the authors also suggested that the TPC1 channel family are the only ROS-responsive Ca^{2+} channels and are the possible targets of Al^{3+}-dependent inhibition (Kawano *et al.*, 2004). OsTPC1 was proposed to localize in the PM when transiently introduced into onion epidermal cells and participate in the regulation of elicitor induced defense response (Kurusu *et al.*,

2005). Hashimoto *et al*. (2005) also reported that OsTPC1 localized predominantly to the PM using an immunoblott with a newly developed antibody against the linker domain of OsTPC1 and indirect immunofluorescence confocal microscopy of rice protoplasts. In contrast, stably expressed OsTPC1-GFP was found to be targeted to the vacuole membrane (VM) in tobacco BY-2 cells lately (Kurusu *et al.*, 2012a). TaTPC1 was reported to be located at the PM and mediates response to abiotic stress in wheat (Wang *et al.*, 2005). When revisiting the topic of AtTPC1 channels, Carter *et al.* (2004) and Peiter *et al.* (2005) reported the vacuolar localization of the TPC1 channels. Peiter *et al.* (2005) showed that a *tpc1* knockout mutant lacks functional slow vacuolar channel activity and was defective in both abscisic acid-induced repression of germination and in the response of stomata to extracellular calcium. Therefore, a role in Ca^{2+}-activated Ca^{2+} release from intracellular Ca^{2+} stores has been suggested. A couple of years later, Ranf *et al.* (2008) confirmed the vacuolar localization of AtTPC1 channel in *Arabidopsis*. However, the authors disproved the role of AtTPC1 in modulating $[Ca^{2+}]_{cyt}$ homeostasis in response to both biotic and abiotic stimuli under physiological conditions. In contrast, NtTPC1s have been proposed to contribute to the $[Ca^{2+}]_{cyt}$ elevation through allowing Ca^{2+} permeate across the PM in response to cold shock, sucrose, H_2O_2, salicylic acid and elicitors (Kadota *et al.*, 2004; Kawano *et al.*, 2004; Lin *et al.*, 2005; Hamada *et al.*, 2012; Kurusu *et al.*, 2012a). Even though tobacco has been used as a host to investigate the localizations of TPC channels from other species, the localization of NtTPC1s has not yet been clearly demonstrated. In addition, the reports about their involvement in calcium homoeostasis are also controversial.

Evidences are accumulating which hint the possibilities of NtMCAs' participation in mechanoperception and NtTPC1s' involvement in intracellular Ca^{2+} homeostasis. However, many aspects of these two putative calcium channels were not fully understood, such as their structure, oligomeric states, gating mechanisms, whether they contribute to intracellular Ca^{2+} homeostasis in a

cooperated fashion like the CCh1 and Mid1 in yeast, whether they are involved in mechanosensing and if so, how do they contribute to mechanoperception and so on. Therefore, it is both intriguing and important to search for answers to those questions in order to understand how molecular players speculated to participate in calcium signaling are implicated in mechanosensing in plants.

A large number of MS channels from various organisms of different origins have been identified at the molecular level benefitting from the development in sequencing technology and bioinformatics. However, the structure of only a few of them has been made clear because of the difficulties in resolving the structures of membrane proteins. Great efforts have been made to understand the function of these potential MS channels using different experimental approaches, with the exception of bacterial MS channels, yet still very little is known about how exactly these channels sense mechanical forces and whether other cellular components are required for their function and if so, how do they contribute to the function of MS ion channels in multicellular eukaryotes. In this study, how the CTK, as the major component of the proposed dynamic sensory tensegrial entity, is involved in mechanosensing in plants will be investigated using volume regulation in protoplasts as exemplary phenomenon. In the meantime, two selected putative calcium channels, NtTPC1A and NtMCA2 will be characterized relying on plant transformation and fluorescence microscopy. Some light will hopefully be shed on their functions *in vivo* through analyzing tobacco BY-2 cells overexpressing these two channel proteins.

2. Materials and Methods

2.1 Cell cultures

Tobacco BY-2 (*Nicotiana tabacum* L. cv BY-2) suspension cultures (Nagata *et al.*, 1992) were maintained in liquid medium containing 4.3 g/l Murashige and Skoog salts (Duchefa Biochemie, Haarlem, the Netherlands), 30 g/l sucrose, 200 mg/l KH_2PO_4 , 100 mg/l inositol, 1 mg/l thiamine, and 0.2 mg/l 2,4-D, pH 5.8. The cells were subcultivated on a weekly basis by inoculating 1.0 to 1.5 ml of stationary cells into 30 ml fresh medium contained in 100 ml Erlenmeyer flasks using oblique cut tips. The cells were incubated at 26 °C in darkness on an orbital shaker (IKA Labortechnik, Staufen, Germany) rotating constantly at 150 rpm. The stock BY-2 calli were maintained on the same medium solidified with 0.8 % (w/v) agar (Roth, Karlsruhe, Germany) and subcultivated monthly. Transgenic suspension cells and calli were cultivated on the same medium as above mentioned with only addition of corresponding antibiotics (for more details, see Appendix 5.1, p.117).

Suspension cell cultures of *V. rupestris* and *V. riparia* were cultivated in the same liquid medium as tobacco cells. Cultures were also subcultivated weekly, however 8-10 ml of stationary cells were inoculated into 30 ml of fresh medium held in 100 ml Erlenmeyer flasks during subcultivation.

2.2 Protoplast generation and determination of expansion velocity

2.2.1 Generating protoplast

Protoplasts of *Vitis* were obtained by digesting suspension culture cells at specific time points after inoculation (day 7 to 9) with 1 % w/v cellulase and 0.3 % w/v

macerozyme in slightly hypertonic medium (0.45 M mannitol) for 3-4 h in darkness at 25 °C on an orbital shaker at 100 rpm. For tobacco cells, 3-day-old cell culture was digested with 1 % w/v cellulase and 0.1 % w/v pectolyase in slightly hypertonic medium (0.45 M mannitol) for about 2 h under the same condition. Progression of digestion was followed by light microscopy till the majority of the cells displayed a perfectly spherical shape. The liberated protoplasts were filtered with a nylon mesh of 70 µm pore width and washed twice in slightly hypotonic medium (0.3 M mannitol). For the washing steps, protoplasts were collected by centrifugation at 300 rpm for 15 min. After the second washing step, the protoplasts were resuspended in a minimal amount of 0.3 M mannitol supplemented with 10 % (v/v) of enzyme solution (1 % w/v cellulase and 0.3 % w/v macerozyme in 0.3 M mannitol) to suppress regeneration of new cell walls. If the protoplasts were to be used for microscopic studies directly, cultivation medium is used to dilute the protoplasts till appropriate density for observation.

2.2.2 Determination of expansion velocity

To observe protoplast expansion, 5 µl of protoplast suspension was mixed with 45 µl of double distilled water, and 20 µl of the mixture was transferred into a hemocytometer (Fuchs-Rosenthal), and observed by differential interference contrast (DIC) microscopy (Axioskop FS 2, Zeiss, Jena, Germany). The time of mixing was defined as starting time t = 0, images were recorded from 1 min after mixing at intervals of 30 s over the following 3 min. Protoplast diameters were determined using the AxioVision Rel. 4.8 software (Zeiss, Jena, Germany).

Osmolality of the solutions (c_σ) administered to the protoplasts was measured by a vapour pressure osmometer (Vapro 5520; Wescor Inc.). The readout values were converted to osmotic pressure and then used for calculating hydraulic conductivity L_p as described in (Taiz & Zeiger, 2002).

Protoplast expansion velocity was calculated based on hydraulic conductivity L_p

(Taiz & Zeiger, 2002):

$L_p=(dV/dt)/(-\Delta\Pi S)\approx[(V90s-V60s)/30s]/[S(Oms_o-Oms_i)]$

with V: protoplast volume; S: protoplast surface area; Π: osmotic pressure; Osm_o-Osm_i: osmotic gradient (outside-inside).

2.3 Analysis of membrane turnover by quantifying intensity of the FM4-64 tracer

Protoplasts of tobacco BY-2 cells were prepared as described above. They were then subjected either to hypoosmotic stress (final concentration of 0.15 M mannitol), or to hyperosmotic stress (final concentration of 0.5 M mannitol) in the presence of low concentrations (5 µM) of the membrane tracer FM4-64 (N-(3-triethylammoniumpropyl)-4- (6-(4-(diethylamino) phenyl) hexatrienyl) pyridinium dibromide) (Molecular Probes/Invitrogen, Carlsbad, CA, USA). Time-lapse series were recorded at intervals of 10 s, and average fluorescent intensities from at least 20 protoplasts were determined for each time point using the software Image J (Abramoff *et al.*, 2004). Relative fluorescent intensity compared to that of the first image was plotted over time.

2.4 Constructs

2.4.1 RNA extraction and cDNA synthesis

3-day-old tobacco BY-2 wild type (WT) cells undergoing exponential growth were harvested by centrifugation at 4000 rpm for 2 min in a 2 ml Eppendorf reaction tube. After removing the medium, the cells were immediately frozen in liquid nitrogen and homogenized with Tissue Lyser (Qiagen/Retsch Hilden, Germany). mRNA was extracted using the innuPREP Plant RNA kit (Analytic, Jena) following the manufacturer's instruction and the optional on-column digestion of genomic DNA was performed via incubating with RNase-free DNAse I (Qiagen) for 30 min

at 30 °C. Purity and integrity of the RNA samples were determined by agarose gel electrophoresis. For cDNA synthesis, the DyNAmo™ cDNA Synthesis Kit (Finnzymes, Vantaa, Finland) was used and 1 µg of RNA was taken as template.

2.4.2 Cloning procedure

Plasmids for stable transformation of tobacco BY-2 WT cells were constructed using the Gateway®-Cloning technology (Invitrogen Corporation, Paisley, UK). The sequences encoding the genes of interest (Appendix 5.2, p.117) were amplified via PCR (for PCR program, see Appendix 5.4, p.118) using oligonucleotide primers with Gateway®-specific flanks (Appendix 5.3, p.118). The size of the amplicons were verified by electrophoresis and purified using the NucleoSpin® Extract II (Macherey-Nagel, Düren, Germany) kit according to the manufacturer instructions. The resulting coding sequences were inserted into the binary vector pK7FWG2,0 (Karimi *et al.*, 2002), pH7RWG2,0 (Karimi *et al.*, 2002), pK7WGF2,0 (Karimi *et al.*, 2002) following the manufacturer's instructions. A complete overview of all constructs generated from this study can be found in (Appendix 5.5, p.119).

2.5 Transformation and establishment of stable transgenic tobacco BY-2 cells

2.5.1 Biolistic, transient expression

Gold particles (1.5-3.0 µm; Sigma-Aldrich, Taufkirchen, Germany) were coated with the corresponding plasmid DNA according to the standard manual of Bio-Rad (PDS-1000/He Particle Delivery System manual; for details, see Appendix 5.6, p.120) with the following modifications. 12.5 µl (1.5 mg) of gold suspension particles was coated with 1 µg of plasmid-DNA and dispersed throughout the macrocarriers (Bio-Rad, Hercules, CA, USA). 800 µl of 3-day-old

non-transformed tobacco BY-2 WT cells was allowed to settle for 5 min in a 2 ml Eppendorf reaction tube. After that, 300 µl of the supernatant was removed. The remaining 500 µl of cells was resuspended and then evenly disseminated onto the PetriSlides™ (Millipore, Billerica, USA) in which 1.5 ml of above mentioned solid medium for BY-2 calli were inlaid in advance. Both the loaded PetriSlides™ and macrocarriers were transferred into a chamber custom-made according to Finer *et al*. (1992) and bombarded three times at pressure of 1.5 bar in a vacuum chamber at -0.8 bar. After the bombardment, the cells were first incubated for 16-24 h at 26 °C in darkness and then observed under fluorescence microscope.

2.5.2 *Agrobacterium*-mediated, stable expression

Stable cell lines over expressing NtTPC1A-GFP, NtTPC1A-RFP and GFP-NtMCA2 were obtained through method developed by Buschmann *et al*. (2010) with several modifications for better performance. 1.5 ml of 7-day-old BY-2 WT cells instead of 1 ml was used during subcultivation and kept for 3 days under the same conditions as normal suspension cell culture. Afterwards, 3 flasks each containing 31.5 ml cell culture were pooled together and washed twice with 200 ml of washing media (4.3 g/l Murashige and Skoog salts (Duchefa Biochemie, Haarlem, the Netherlands), 10 g/l sucrose, pH 5.8) each time. The washing steps were performed using a scientific Nalgene® filter holder (Thermo Scientific, Langenselbold, Germany) combined with Nylon mesh with pores of diameter of 70 µm. The washed cells were then resuspended in 15-18 ml of washing medium yielding a 5- to 6- fold concentrated cell suspension. 6 ml of these concentrated cell suspension was mixed with cell suspension of *Agrobacterium tumefaciens* transformants prepared as following.

100 µl electro-competent *A. tumefaciens* (strain LBA 4404; Invitrogen Corporation, Paisley, UK) was thawed on ice and incubated with 100 ng binary expression vectors containing genes of interests on ice for another 20 min. Following that, the mixture was transferred into electroporation cuvette with 2 mm electrode gap

(Peqlab, Erlangen, Germany) pre-cooled on ice and exposed to electric pulses of 2.5 kV, 200 Ω for 5 ms (Gene Pulser Xcell™ electroporator, Bio-Rad, Laboratories, Hercules, CA, USA). After incubation, spread the bacteria onto solid LB (Lennox Broth, Roth, Karlsruhe, Germany) agar medium containing antibiotics (100 µg/ml rifampicin, 300 µg/ml streptomycin and 100 µg/ml spectinomycin) and incubate for 3 days at 28 °C in the dark. One of the single colonies was inoculated into 5 ml LB liquid medium supplied with the same selective antibiotics and incubated at 28 °C agitated vigorously overnight. The OD_{600} of the overnight culture was determined and certain amount of the overnight culture was inoculated into 5 ml of fresh LB-medium (without antibiotics) to reach an OD_{600} of 0.15. After approximately 5 h of growth, 6 ml of the transformed *A. tumefaciens* bacteria was harvested at an OD_{600} of 0.8 by centrifugation at 8000 g (Heraeus Pico 17 Centrifuge, 600 Thermo Scientific, Langenselbold, Germany) for 7 min in a 50 ml falcon tube at 28 °C. The bacteria were then resuspended in 180 µl washing medium by mixing vigorously using a bench-top vortexer (Bender & Hobein Zurich, Switzerland) till the suspension becomes homogeneous.

Mix the prepared BY-2 cells with the homogenized bacteria suspension and incubate the falcon tube on an orbital shaker at a 30° angle above the horizontal at 100 rpm for 5 min till fully mixed. Subsequently, this mixture was dropped with sterile oblique cut tips onto petri dishes inlaid with washing medium solidified with 0.5 % (w/v) Phytagel (Sigma P8169) without any antibiotics on which a single layer of sterile filter paper was placed in advance. Those plates were sealed with parafilm and incubated at 22 °C in the dark instead of 27 °C as recommended in the original publication. 3 to 4 days later, the cell plaques together with the filter paper were transferred on to MS agar plates supplied with 300 µg/ml cefotaxime together with either 100 µg/ml kanamycin or 60 µg/ml hygromycin and incubated at 26 °C in the dark. After approximately 3 weeks incubation, the appeared calli were transferred onto fresh MS agar plates (with corresponding antibiotics and cefotaxime) for further growth and a suspension culture was then established

from the calli after enough of them had grown into appropriate sizes.

2.6 Phenotyping of tobacco suspension culture

2.6.1 Determination of division synchrony, cell length and width

For the determination of cell division synchrony, 500 µl aliquot of cells from each sample were collected from day 1 to day 4 after subcultivation/treatment (diluted in MS medium if necessary) and immediately viewed under AxioImager Z.1 microscope (Zeiss, Jena, Germany). Frequency distributions over the number of cells per individual file were constructed (excluding rare files with more than 10 cells) from images obtained from differential interference contrast (DIC) by a digital imaging system (AxioVision; Zeiss). For each picture, the MosaiX module of the AxioVision software was used to cover a 4x4 mm area with 121 single pictures at an overlay of 10 % to monitor division synchrony (Campanoni *et al.*, 2003; Maisch & Nick, 2007). Each data point represents at least 1500 cell files from three independent experimental series.

For cell width and cell length, 500 µl aliquot of cells from each sample were collected immediately after subcultivation and viewed under AxioImager Z.1 microscope (Zeiss, Jena, Germany). Cell length and width were measured from the image of the central section of the cells using the length measurement function of the AxioVision software according to Maisch and Nick (2007). And each data point represents mean and standard error from at least 1500 individual cells obtained from three independent experimental series. The results were tested for significance using Student's *t*-test at 95 % and 99 % confidence level.

2.6.2 Determination of cell mortality and packed cell volume

To quantify cell mortality, aliquots of cells at indicated time points after subcultivation/treatment were collected and the medium was drained in a

custom-made staining chamber using mesh with a pore-size of 70 µm as bottom (Nick *et al.*, 2000), and then transferred into 1 ml of 2.5 % Evans Blue (w/v) (Sigma-Aldrich) dissolved in millipore water for 1 min. After washing 3 times with fresh millipore water the cells were viewed under AxioImager Z.1 microscope (Zeiss, Jena, Germany) and mosaic pictures were obtained as described above. Cell mortality was calculated as the number of dead cells divided by the total number of cells. Each time point represents at least 3000 cells obtained from at least three independent experimental series.

Growth of the BY-2 cell culture was approximated by measuring the packed cell volume (PCV) (Jovanovic *et al.*, 2010) at day 5 after subcultivation/treatment. Equal amounts of cell culture were poured from the Erlenmeyer flasks directly into a 15 ml falcon tube and kept vertically at 4 °C for a time period between 48 h and 72 h (depending on the density of the cell culture) till the upper surface can be clearly distinguished from the cells sediment and the PCV were read directly using the scale of the 15 ml falcon. And each data point represents mean and standard error obtained from at least three independent experimental series. The results were tested for significance using Student's *t*-test at 95 % and 99 % confidence level.

2.7 Treatments with membrane agents, elicitor and cytoskeletal drugs

2.7.1 Cell membrane agents

Benzyl alcohol (BA) is an amphiphilic molecule, which has been used often to investigate cellular responses to membrane fluidity. Benzyl alcohol can be used as a membrane "fluidizer" that affects lipid bilayer structures (Ebihara *et al.*, 1979). In contrast, dimethyl sulfoxide (DMSO), a polar aprotic solvent, is a well-documented membrane rigidifier (Lyman *et al.*, 1976). Aliquots of protoplast

were treated with various concentrations of BA and DMSO for 30 min prior to the measurement of expansion velocity.

2.7.2. Elicitor treatment

Harpin is a protein from the phytopathogenic bacterium *Erwinia amylovora* and can induce the so called effector-triggered immune responses (Wei *et al.*, 1992). A prominent feature of this type of immunity is the induction of rapid actin bundling (Guan *et al.*, 2013). Aliquots of protoplast were treated with 9 µg/ml Harpin (Messenger, EDEN Bioscience Corporation, Washington, USA; 3 % of active ingredient Harpin protein, dissolved in MS liquid medium to a concentration of 300 mg/ml as a stock solution, the active Harpin protein concentration equals to 9 mg/ml) for 30 min and then used for further analysis.

2.7.3. Cytoskeletal drugs

Latrunculin B (LatB) binds actin monomers near the nucleotide binding cleft with 1:1 stoichiometry and prevents actin from polymerizing, resulting in progressive elimination of the actin filaments depending on their innate turnover. Phalloidin binds specifically at the interface between F-actin subunits, locking adjacent subunits together, which prevents the depolymerization of actin filaments. Aliquots of protoplast were treated with either 1 µM of Phalloidin (Sigma-Aldrich, Steinheim, Germany) or LatB (Sigma-Aldrich) for 30 min and then used for experiments.

Taxol stabilizes the microtubule polymer against disassembly. Oryzalin sequesters the dimer of plant tubulin at the plus end, whereas depolymerization at the minus ends proceeds resulting in progressive elimination of microtubules depending on their innate turnover. Aliquots of protoplast were treated with either 10 µM of Taxol (Sigma-Aldrich) or Oryzalin (Sigma-Aldrich) for 30 min and then used in the following experiments.

All cytoskeletal drugs are not readily water soluble and have thus to be dissolved in DMSO as stock solutions and stored at 4 °C. For this reason, a solvent control with DMSO was included in the experiments to probe for potential effects of the solvent. The temporal length of treatments using the above mentioned agents was indicated in the legend accordingly except for the determination of expansion velocity for which the time of treatment was fixed at 30 min.

2.8 Atomic absorption spectrometry (AAS) for intracellular ion content determination

5-day-old tobacco BY-2 WT and transgenic cells were treated with 150 mM of NaCl for 5 min before harvest. In case of $CaCl_2$ and $MgCl_2$, cells were treated for 5 days starting from subcultivation. Immediately after treatment, 31.5 ml cells was harvested through passing a single layer of filter paper lying in a Büchner funnel under vacuum of 500 Pa (Vacuubrand CVC2, Brand, Germany) (Babourina *et al.*, 2000). Right after removing the medium, cells was washed with 300 ml millipore water using the same approach to drain the water and then transferred at once into an incubator set at 80 °C for 3 days. Approximately 150 mg (the exact weight of the material was documented for calculation of ion concentration in per unit dry weight) dry cells were transferred into a 10 ml digestion tube (Gerhardt, UK) and 5 ml of 65 % nitric acid (Roth, Karlsruhe, Germany) was added. The digestion progressed at room temperature overnight followed by a 2 hour-long incubation in a boiling water bath (Ippolito & Barbarick, 2000). 4 ml of the digestion product after cooling was mixed with 21 ml of millipore water and subjected to AAS measurement. Na^+ and Ca^{2+} contents were measured by flame atomic absorption spectrometry (AAS) (AAnalyst 200, Perkin Elmer) in an air-acetylene flame (Institute of Mineralogy and Geochemistry, Karlsruhe Institute of Technology) respectively. And the intracellular Na^+ and Ca^{2+} contents were calculated according to the dry weight. Each data points represent the mean and standard

error from at least 3 independent experimental series. The results were tested for significance using Student's *t*-test at 95 % and 99 % confidence level.

2.9 Microscopy and image analysis

For morphological studies, cells were examined under an AxioImager Z.1 microscope (Zeiss, Jena, Germany) equipped with an ApoTome microscope slider for optical sectioning and a cooled digital CCD camera (AxioCam MRm; Zeiss). TRITC-/RFP- and GFP-/Alexa-Fluor® 488-fluorescence were observed through the filter sets 43 HE (excitation: 550 nm, beamsplitter: 570 nm, and emission: 605 nm) and 38 HE (excitation: 470 nm, beamsplitter: 495 nm, and emission: 525 nm) respectively (Zeiss). For cell mortality and cell size, samples were observed in the differential interference contrast (DIC) using a 20x objective (Plan-Apochromat 20x/0.75) and the MosaiX module of the imaging software (Zeiss). Images were processed and analyzed using the AxioVision (Rel. 4.8.2) software as described above.

For observation of individual cells in more details, the transgenic or stained cells were observed using the AxioObserver Z1 (Zeiss, Jena, Germany) inverted microscope equipped with a laser dual spinning disk scan head from Yokogawa (Yokogawa CSU-X1 Spinning Disk Unit, Yokogawa Electric Corporation, Tokyo, Japan), a cooled digital CCD camera (AxioCam MRm; Zeiss) and two laser lines (488 and 561 nm, Zeiss, Jena, Germany) attached to the spinning disk confocal scan head. Images were taken using a Plan-Apochromat 63x/1.44 DIC oil objective operated via the Zen 2012 (Blue edition) software platform.

Besides the above mentioned software, images acquired were processed with respect to size, contrast and brightness using the Photoshop software® (Adobe Systems, San Jose, CA, USA) for better presentation.

2.10 Determination of NtTPC1A and NtMCA2 transcripts by quantitative RT-PCR

The overexpression levels of the introduced calcium channel fusion proteins in the corresponding cell lines at transcription level were determined by quantitative RT-PCR. mRNA was extracted from 4-day-old non-transformed BY-2 WT cells as well as the two transgenic cell lines using the same approach as described in 2.4.1. The quality and integrity of RNA was controlled as described above using spectrophotometry and agarose gel electrophoresis. First-strand cDNA synthesis was carried out using 1 µg total RNA employing the DyNAmo^{TM} cDNA synthesis kit (Thermo Fisher Scientific Inc, Waltham, MA, USA) following the instructions of the manufacturer. For detection of the expression levels of NtTPC1A and NtMCA2 in comparison to tobacco BY-2 WT, two pairs of gene specific primers were designed (see Appendix 5.7, p.120). According to Schmidt and Delaney (2010) as well as pre-experiment, L25 and GAPDH were selected as internal standards. The specificity of the amplification was analyzed by melting curve analysis. qPCR analysis was carried out in 20 µl reactions containing in final concentration 200 nm of each primer, 200 nm of each dNTP, 1X GoTaq colourless buffer, 2.5 mm additional $MgCl_2$, 0.5 U GoTaq polymerase (Promega, Mannheim, Germany), 1x SYBR green I (Invitrogen, Darmstadt, Germany) and 1 µl of a 1:10 cDNA dilution according to Gutjahr *et al*. (2008). Three technical replicates were performed for each sample. The relative expression level of each gene was calculated with the delta delta C_t method (Livak & Schmittgen, 2001) using the L25 and GAPDH control for normalization. The experiment was repeated for four biological replicates and the mean fold changes were calculated and plotted along with corresponding standard errors. This protocol was adapted from (Svyatyna *et al.*, 2013).

3. Results

In this chapter, the results from this work will be presented in two main sections as established in the beginning. The first part deals with the role of the cytoskeleton in osmotic stress, namely if and how the plant cytoskeleton participates in modulating membrane dynamics and regulating volume increase when cells are subjected to osmotic stresses using expansion of protoplasts in distilled water as a system. Following that, the work focusing the characterization of the two putative calcium permeable channels will be illustrated which can be categorized into three sections. Firstly, the generation of stable transgenic cell lines and microscopic studies examining the two transgenic cell lines. Secondly, morphologic studies analyzing the effects of overexpressing NtTPC1A and NtMCA2 on cell growth and division as indicators for response to internal mechanical forces. Lastly, investigations about the overexpression cell lines' response to external mechanical forces simulated by osmotic stress. This chapter finally ends with a brief summary of the findings from this work.

3.1 The cytoskeleton, membrane dynamics and regulatory volume increase in plant cells

3.1.1 Osmotic water permeability depends on the cytoskeleton

To obtain quantitative data on the role of the cytoskeleton for osmoregulation, L_p values after treating with cytoskeletal agents (Fig. 3.1 A) were determined. Values for L_p were derived from time series, where protoplasts were transferred into a hypoosmotic medium (distilled water) at t = 0 and then recorded from t = 60 s at intervals of 30 s (Fig. 3.1 B). Since the protoplasts form ideal spheres, the volume could be easily deduced from the cross-sections. To validate this approach to estimate L_p, temporal changes of L_p were determined for 73 time series and were

found to be < 5 % (Fig. 3.1 C). Thus, protoplast swelling is approximately linear such that the obtained value of L_p is mostly independent of the time point used for its determination within the range tested. Using the same series a potential dependency of L_p and the surface calculated for the individual protoplasts is probed (Fig. 3.1 D), but no significant correlation was detected. Thus, L_p turned out to be a robust parameter which dependents neither on the time point of measurement nor on the individual differences in protoplast diameter.

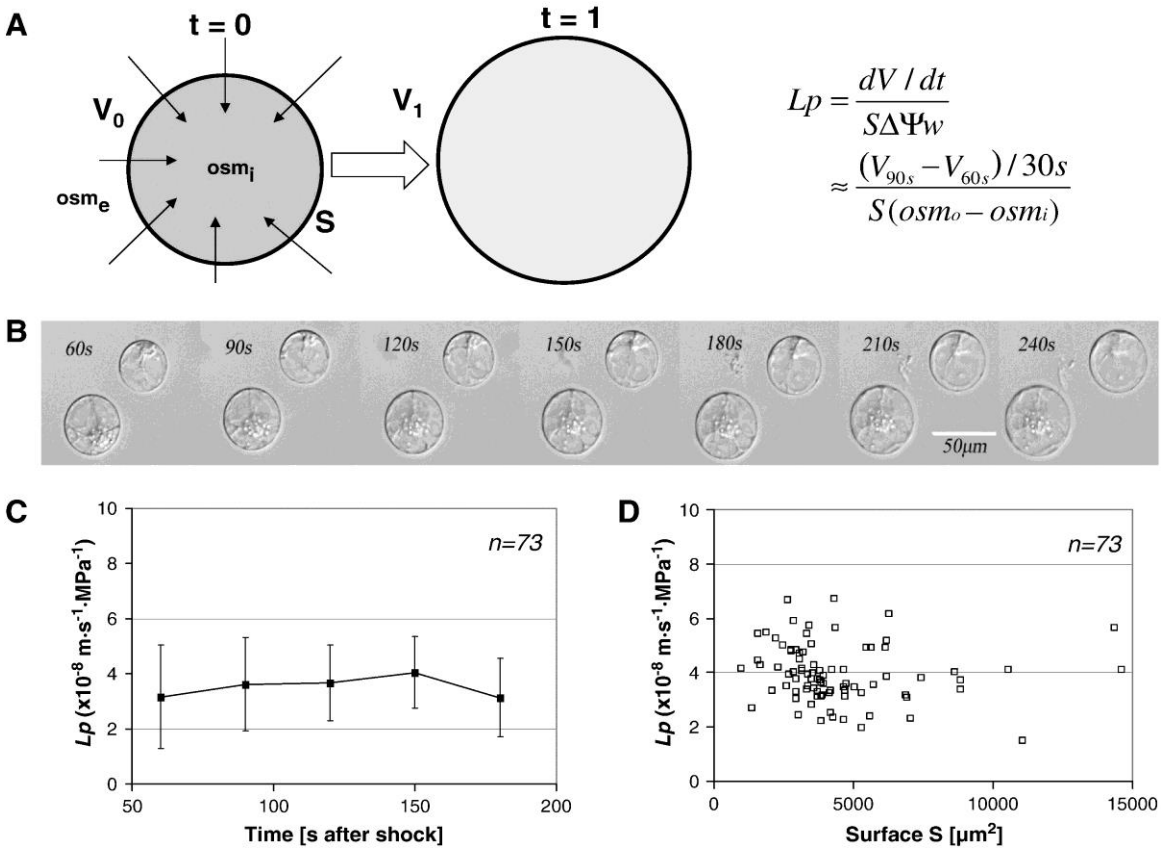

Fig. 3.1 Determination of osmotic water permeability (hydraulic conductivity) L_p. A. Set-up of experiment. At time 0 s, a protoplast is transferred into distilled water (osm_e = 0), and the increase in volume over the time was determined from photographic images of the protoplast based on the spherical geometry. B. Representative time series for two protoplasts of *V. rupestris* transferred at time 0 s into distilled water. C. Dependence of temporal changes of L_p on the time after transfer into distilled water calculated as mean and standard error from 73 individual time courses. Temporal changes of L_p remain < 5 %. D. Dependence of mean values L_p on the initial surface S based on 73 individual time courses. There is no correlation between initial surface S and time.

In the next step, L_p values after pharmacological manipulation of specific cellular targets were determined. When microtubules were eliminated by Oryzalin treatment (Fig. 3.2 A), L_p increased by 30 % in both cell lines, whereas stabilization of microtubules by Taxol decreased L_p by around 20 % (more pronounced in *V. rupestris* as compared to *V. riparia*). When actin filaments were eliminated by Latrunculin B, L_p increased by 20-25 % in both cell lines, treatment with Phalloidin did not produce significant changes in L_p. Since the response of *V. rupestris* and *V. riparia* followed the same pattern, just at different amplitude, the subsequent experiments were therefore focused on *V. rupestris*. To calibrate the amplitude of the changes in L_p after treatment with cytoskeletal drugs, the membrane was permeabilized by DMSO and an increase of L_p at 35 % for 1 % v/v DMSO was obtained (Fig. 3.2 B), which could not be raised further by higher concentration (2 % v/v). This means that the response obtained with Oryzalin almost sustained the level for unimpaired water influx, and Latrunculin B produced more than half of this level. Increasing the membrane fluidity by benzyl alcohol which increases the spacing between phospholipid chains, did not yield any significant effect on L_p even at 8 mM, a concentration that can completely compensate cold induced membrane rigidification in *Brassica napus* (Sangwan *et al.*, 2001). Likewise, neither chelating extracellular calcium by EGTA nor blocking calcium influx by gadolinium ions had any significant effect on L_p. However, treatment with the bacterial effector Harpin that causes massive bundling of actin in *V. rupestris* (Qiao *et al*., 2010) reduced L_p by about 10 %. To test a possible role of phospholipase D (Komis *et al.*, 2006), the influence of the phospholipase D activators *n*-butanol and *sec*-butanol (Munnik *et al.*, 1995) was tested. It was observed that both compounds increased L_p (Fig. 3.2 B) (compare Fig. 3.2 A and B).

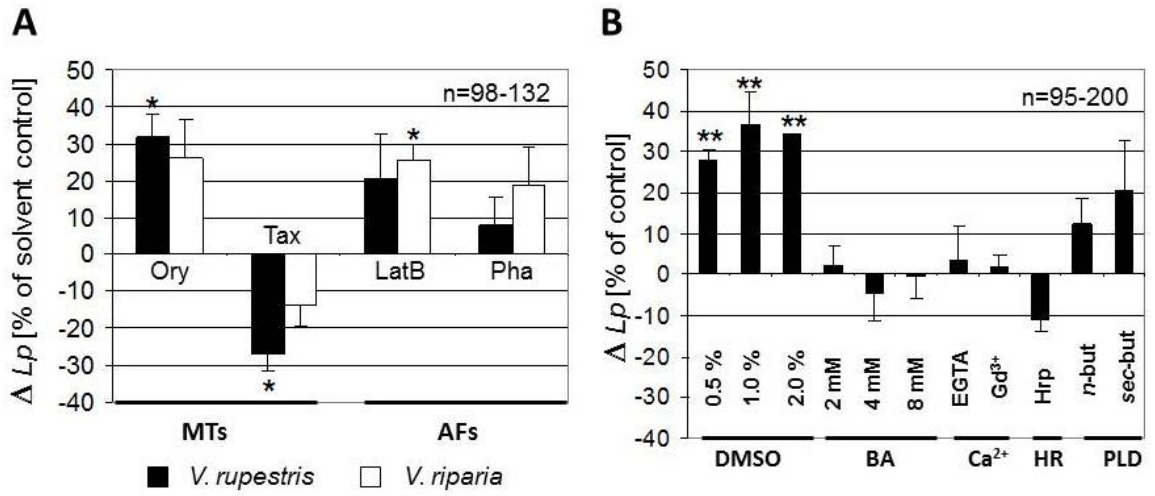

Fig. 3.2 Effect of pharmacological manipulation of cellular targets on L_p. A. Effect of drugs acting on microtubules (MTs) or actin filaments (AFs). Relative change of L_p plotted for *V. rupestris* (black bars) and *V. riparia* (white bars) after pretreatment with 10 µM Oryzalin (Ory), 10 µM Taxol (Tax), 1 µM Latrunculin B (LatB), and 1 µM Phalloidin (Pha), respectively, as compared to the solvent control. B. Effect of membrane permeabilization (DMSO), membrane fluidization (BA), calcium depletion (EGTA, 1 mM), block of calcium influx (Gd^{3+}, 80 µM), induction of a hypersensitive reaction (Hrp, 9 µg/ml), and activation of phospholipase D (PLD, 0.5 % of *n*-butanol or *sec*-butanol) in *V. rupestris*. All pretreatments started 30 min prior to the hypoosmotic shock. Data show mean values and standard errors from 98 to 132 (A) and 95-200 (B) individual time courses collected from 3 to 5 independent experimental series. *$P < 0.05$, **$P < 0.01$, Student's *t*-test.

At the same time, protoplasts generated from the tobacco BY-2 actin marker line GF-11 and the microtubule marker line *ß*-Tub6 were treated with cytoskeletal drugs at the presence of either hypo- or hyper- osmotic pressure to follow the cytoskeletal response to osmotic stress and cytoskeletal drugs *in vivo*. In control protoplasts (Fig. 3.3 GF-11 cell line, isotonic, control), actin showed the characteristic organization, with a fine network underneath the PM, and a radial array of actin cables tethering the nucleus (termed as perinuclear actin basket). In hypotonic solution, actin filaments were redistributed towards the membrane, whereas the perinuclear actin basket appeared depleted (Fig. 3.3 GF-11 cell line, hypotonic, control). In contrast, transfer into hypertonic solution partitioned actin towards the perinuclear actin basket, whereas the membrane associated actin

vanished (Fig. 3.3 GF-11 cell line, hypertonic, control). Treatment with Latrunculin B produced a general depletion of actin, whereby the membrane associated actin arrays were affected stronger than the perinuclear network consistent with a higher dynamics of the membrane-associated actin. Most prominently, the partitioning of actin towards the membrane under hypoosmotic conditions was suppressed by Latrunculin B. Treatment with Phalloidin, in contrast, caused a contraction of actin towards the nucleus. Microtubules form radial bundles emanating from the nucleus (Fig. 3.3 *ß*-Tub6 cell line, isotonic, control). These bundles were eliminated by Oryzalin treatment and widened by Taxol treatment (Fig. 3.3 *ß*-Tub6 cell line, isotonic, Ory and Tax). Hypoosmotic shock caused generally a depletion of the microtubular cytoskeleton. Oryzalin promoted, Taxol reduced this depletion (Fig. 3.3 *ß*-Tub6 cell line, hypotonic, Ory and Tax). For hyperosmotic shock, microtubules contracted towards the nucleus and appeared wider. This contraction was less pronounced in presence of Oryzalin, and promoted by Taxol (Fig. 3.3 *ß*-Tub6 cell line, hypertonic, Ory and Tax). Generally, during hyperosmotic shock, the protoplasts deviated from a spherical shape, most pronounced, when the microtubules were eliminated. These results showed that the cytoskeleton in protoplasts reorganized in response to hypo- and hyper-osmotic stress, and that cytoskeletal drugs modulate these responses.

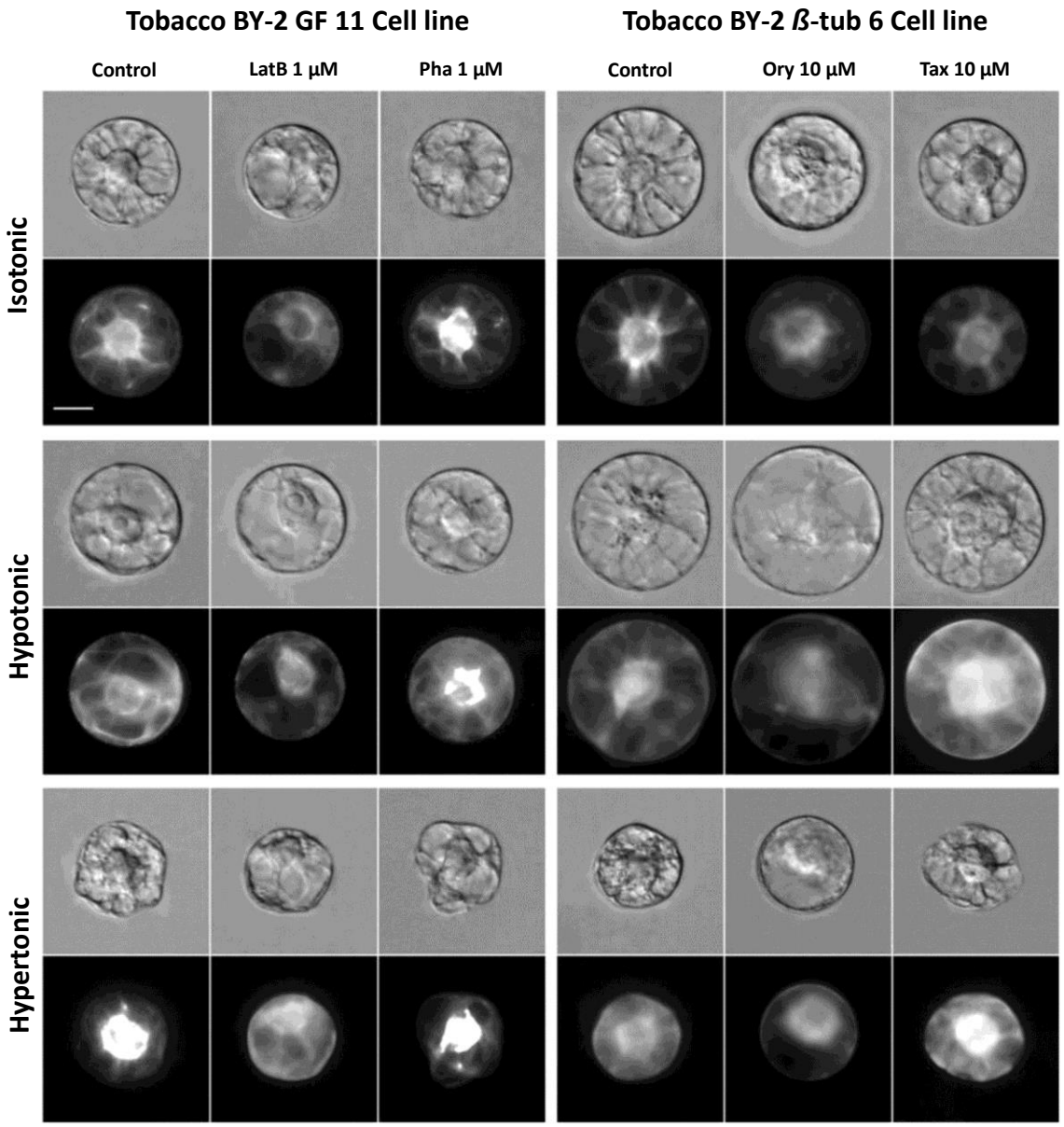

Fig. 3.3 Response of microtubules and actin filaments to cytoskeletal drugs in the tobacco cell line BY-2 expressing *Arabidopsis β*-tubulin TuB6 fused to GFP to visualize microtubules (right) and the GF-11 stably expressing the GFP-Fimbrin Actin Binding Domain (FABD) 2 construct allowing the visualization of actin microfilaments (left) *in vivo*. Protoplasts were treated for 30 min with either 1 µM Latrunculin B or 1 µM Phalloidin (left) or with 10 µM Oryzalin or 10 µM Taxol (right) and then either exposed to a hypoosmotic (0.15 M mannitol) or to hyperosmotic (0.40 M mannitol) medium (scale bar represents 20 µm).

3.1.2 Plasma membrane turnover responded to osmotic stress monitored by FM4-64 intensity

To gain insight into temporal changes of membrane turnover, the relative changes of average fluorescence intensity of FM4-64 during hypo- and hyper-osmotic stress were quantified (Fig. 3.4). Under isotonic control conditions, values were first constant for the first 10 s of observation (70 s after addition of the dye) suggesting that the binding of the dye was equilibrated at this time. Then, average intensity began to decrease slowly, which is expected from the bleaching in the course of fluorescence excitation. For hypotonic conditions, average fluorescence intensity transiently increased (consistent with the exposure of additional binding sites for the dye), but only slightly (by about 10 %) indicating that the concentration of free dye was limiting. Subsequently, the values decreased, but more rapidly than in the control, as to be expected from active integration of unlabelled membrane material diluting the stained PM. For protoplasts subjected to hyperosmotic pressure, the decrease of average intensity was much slower than in the control, consistent with the prediction that membrane material stained by the dye was contracted. Pretreatment of the protoplasts with *n*- or *sec*-butanol did not alter the fading pattern of fluorescent intensity compared to the control when exposed to hypotonic solution.

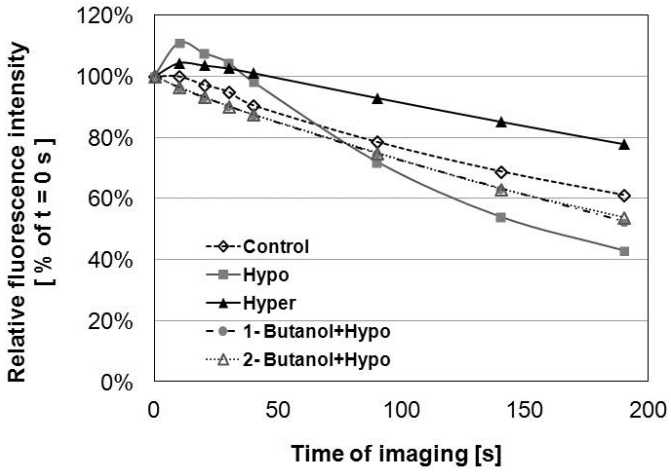

Fig. 3.4 Integrated fluorescence intensity of protoplasts labeled with FM4-64 as determined by Image J over time. Data are given as relative values with respect to the starting time point for the same protoplast and represent the average from at least 20 protoplasts pooled from more than three independent experimental series. Error bars are smaller than figure symbols.

3.1.3 Cytosolic calcium level is irrelevant to regulatory volume increase in BY-2 protoplasts

As it was shown above, neither chelating extracellular calcium by EGTA nor blocking calcium influx by gadolinium ions had any significant effect on L_p. However, external manipulation of calcium levels via calcium-chelating or calcium channel blocking agents especially when taking into account that the link between source and origin of the calcium ions and their signaling role, makes it imprudent to rule out the influence of intrinsic calcium level alteration on L_p. Therefore, relative L_p was determined for the two transgenic cells lines overexpressing these two putative calcium channels NtTPC1A and NtMCA2. The result shows that there is no significant difference between relative L_p of protoplasts generated from the two overexpression cell lines as compared to protoplasts of WT cells under the same experimental settings (see Fig. 3.5) which confirms the former findings and also suggests that potential calcium level change does not contribute to relative L_p during such a very rapid expansion process in protoplasts.

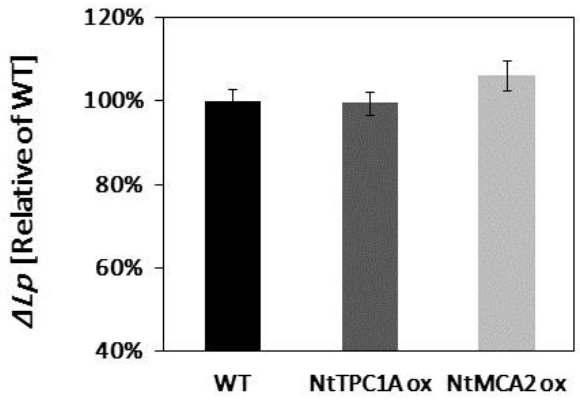

Fig. 3.5 Effects of overexpressing NtTPC1A and NtMCA2 on ΔL_p. Relative changes of L_p were plotted for BY-2 WT (black bar), NtTPC1A ox (dark grey bar) and NtMCA2 ox (light grey bar), respectively. Data show mean values and standard errors from 230 (WT), 161 (NtTPC1A ox) and 167 (NtMCA2 ox) individual protoplasts collected from 2-3 independent experimental series. There is no significant difference between the putative calcium channel overexpression cell lines and the WT pertaining to their L_p values according to the Student's *t*-test. $^{*}P < 0.05$, $^{**}P < 0.01$, Student's *t*-test.

3.2 Generation of transgenic cell lines and localization studies of NtTPC1A and NtMCA2 fusion proteins

3.2.1 Modification of the protocol for *Agrobacterium*-mediated transformation of tobacco BY-2 cells based on the Buschmann method

In order to understand the localization as well as the physiological functions of the NtTPC1A and NtMCA2 *in vivo*, generating cell lines overexpressing those two channel proteins was chosen as a strategy in this study. For that, the Gateway® cloning system was employed for its various advantages (see Appendix 5.8, p.121, for an overview of the Gateway® cloning technology). A C-terminal fusion construct of NtTPC1A and an N- terminal fusion construct of NtMCA2 were selected for generating stable transgenic tobacco suspension cell lines.

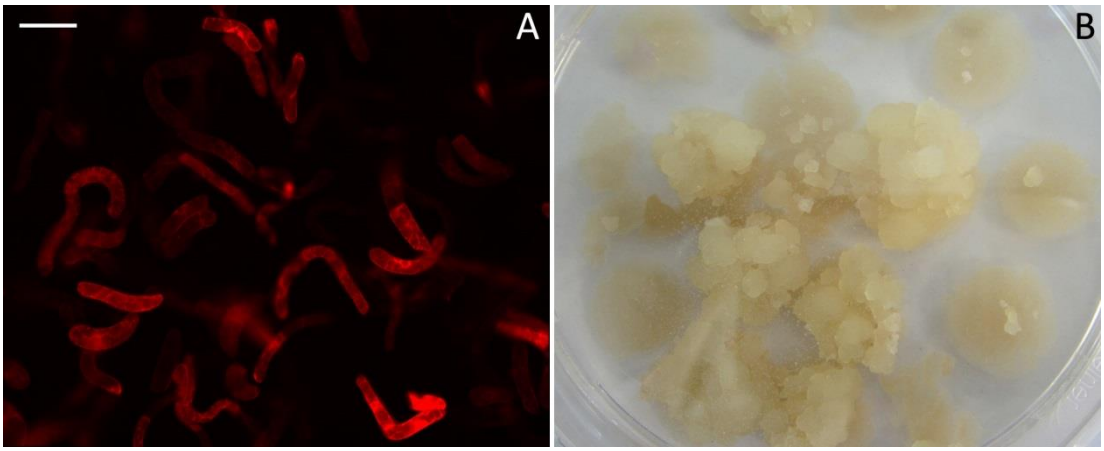

Fig. 3.6 A. Transient transformants of BY-2 cells 3 days after cocultivation on solid agar surface with *A. tumefaciens* strain LBA4404 transformed with binary pH7RWG2,0-NtTPC1A viewed with ApoTome microscope (bar represents 100 µm) B. Little calli appeared 3 weeks after incubation on MS agar medium supplied with 300 µg/ml cefotaxime and 60 µg/ml hygromycin.

The protocol for transient *Agrobacterium*-mediated transformation of BY-2 cells developed by Buschmann *et al*. (2010) was use for transforming BY-2 cells with a few modifications to improve the transient transformation efficiency. First and most importantly, the cocultivation temperature was decreased to 22 °C instead of

27 °C which produced higher transient transformation rate in BY-2 cells (see Fig. 3.6). This adjustment was made based on (Fullner & Nester, 1996; Dillen *et al.*, 1997) who suggested that there was a difference in temperature for optimal bacteria propagation and effective plant transformation. Second, mixture of cells and *Agrobacteria* were not directly placed on the MS Paul agar surface but on a layer of filter paper in between instead, which not only reduced the time consumption required for transferring the cells after cocultivation onto MS agar plates for selection, but also lowered the chance of mechanical wounding caused by transferring cells when using a sterile spatula. Another advantage of doing so is that the transformed cells/cell files will still stay close to each other and are therefore able to build up sizable calli more rapidly against the selection pressure. Last but not least, the progression of transformation should be monitored under the microscope starting from the second day on after dark incubation in order to determine when to transfer the cell onto MS agar for selection. However, the cocultivation should be no longer than 5 days which prone to lead to browning and high mortality after transferring the calli onto selection medium.

3.2.2 NtTPC1A-GFP fusion protein is targeted to the tonoplast

BY-2 cells stably overexpressing NtTPC1A-GFP fusion proteins in interphase presented mainly three different types of subcellular localization each accounted for different portions within the whole population (see Fig. 3.7). The great majority of cells within a 3-day-old suspension culture showed highly dynamic cytoplasmic strands. The NtTPC1A-GFP fusion proteins in these cells present patterns similar as shown in Fig. 3.7 A which appear to sectioned by the cytoplasm into small compartments. Most of the compartments seem to be isolated and have irregular surfaces. As the cell cycle progresses, more and more cells adopted patterns like the cell shown in Fig. 3.7 B with less numbers of visible subcellular compartments. However, the sizes of the compartments are becoming bigger. A very tiny portion of cells in the interphase have ceased cytoplasmic streaming in which only one

subcellular compartment labeled by the NtTPC1A-GFP fusion proteins was found and the nucleus was pushed to the side direct against the cell wall (Fig. 3.7 C). These GFP labeled compartments delineate the large transparent regions which are characterized for lytic vacuoles in well-developed plant cells shown by light microscopy.

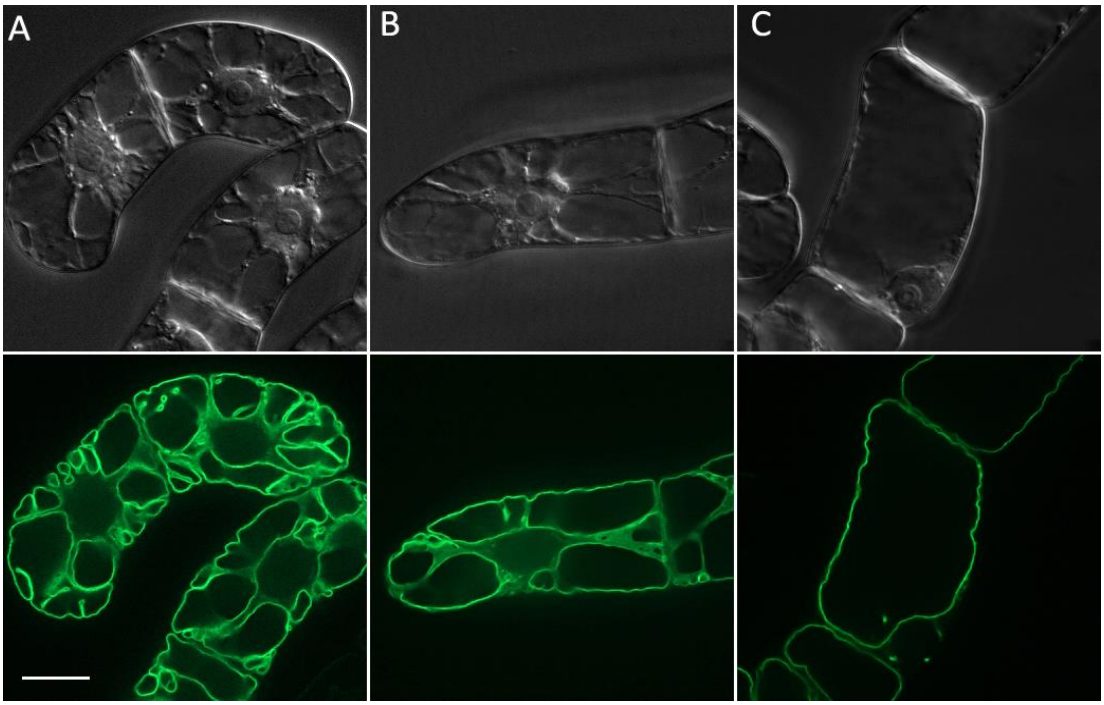

Fig. 3.7 Three different types of subcellular localization in tobacco BY-2 cells overexpressing NtTPC1A with its C- terminal fused to GFP. Upper panel: DIC; lower panel: GFP channel. A. BY-2 cells in interphase with very active cytoplasmic streaming. B. BY-2 cell in interphase with less active cytoplasmic streaming. C. BY-2 cell in interphase with ceased cytoplasmic streaming and a giant single subcellular compartment (scale bar represents 20 µm).

When the cells initiate mitosis, the localization patterns of NtTPC1A-GFP fusion proteins vary as the mitosis proceeds (Fig. 3.8). At the beginning of mitosis, small compartments merged together (Fig. 3.8 A). As the chromosomes aligned in the center of the cell where the future cell wall forms, only two giant compartments on each pole of the cell were observed with tubular protrusions emanating from the two facing ends of these two giant compartments embracing the chromosomes in the center (Fig. 3.8 B). When the chromosomes were pulled apart and the new

cell wall started to form again, the cytoplasmic streaming started to initiate at the same time (Fig. 3.8 C) which compartmentalize the two big sections. Subsequently, many small subcellular compartments were formed once again as the new nuclear envelop forms along with the establishment of organized cytoplasmic streaming (Fig. 3.8 D). All these localization patterns of NtTPC1A-GFP fusion proteins both during interphase as well as mitosis described here (Fig. 3.8 and 3.9) resemble that of plant vacuoles described in Oda *et al.* (2009) indicating the tonoplast localization of NtTPC1A in BY-2 cells. The tubular protrusions embracing the chromosomes were described as the tubular structure of vacuolar membrane (TVM) (Kutsuna & Hasezawa, 2002) and the cytoplasmic streams sectioning different vacuolar compartments were defined as transvacuolar strands (TVSs) (Ruthardt *et al.*, 2005).

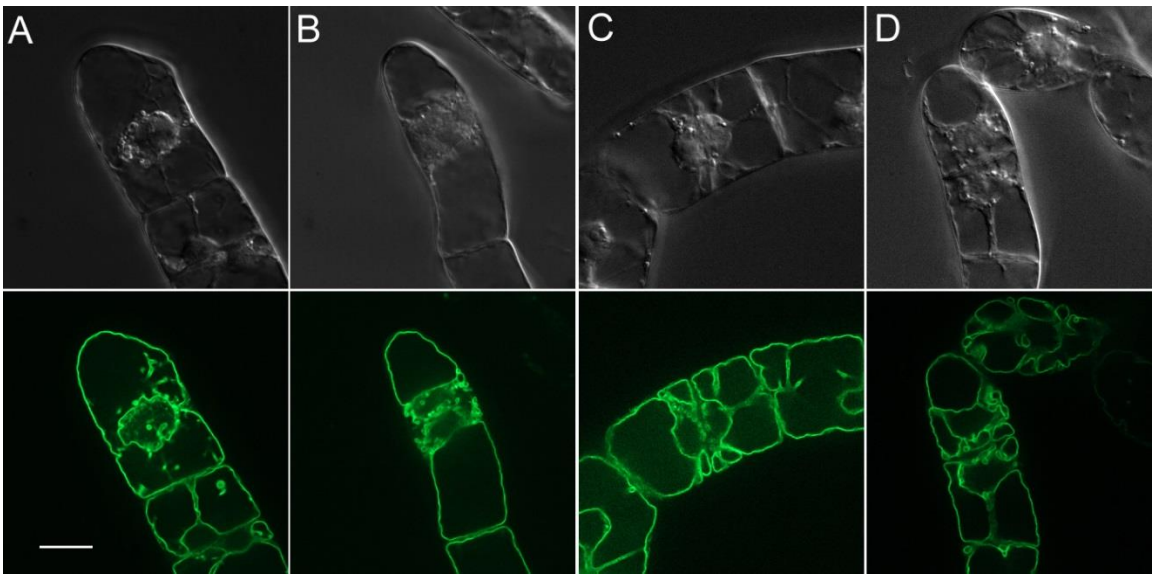

Fig. 3.8 Subcellular localization of NtTPC1A-GFP fusion proteins in tobacco BY-2 cells during mitosis. Upper panel: DIC; lower panel: GFP channel. A-D. BY-2 cells in different mitotic phases shown in chronological order (scale bar represents 20 µm).

Besides the above mentioned vacuolar structures revealed by NtTPC1A-GFP fusion proteins which have been very commonly observed, some other unusual organization forms of vacuoles were also observed in the NtTPC1A-GFP ox cell line (see Fig. 3.9) (Oda *et al.*, 2009). All these three unconventional types of

vacuolar structures were highly dynamic. In Fig. 3.9 A, the transvacuolar strands were moving from the nucleus towards the periphery of the cell with little vesicles attached along appeared to delineate new vacuolar compartments. Fast moving tubular structures of the vacuolar membrane look like worms meandering around in the cell was observed (Fig. 3.9 B). Vacuolar bulbs emitting very strong fluorescence moved continuously like bubbles (Fig. 3.9 C) probably formed from a double vacuole membrane (VM) that sandwiches a thin cytoplasm without any restrains from the cytoskeletons as indicated in literature (Saito *et al.*, 2002; Uemura *et al.*, 2002; Reisen *et al.*, 2005).

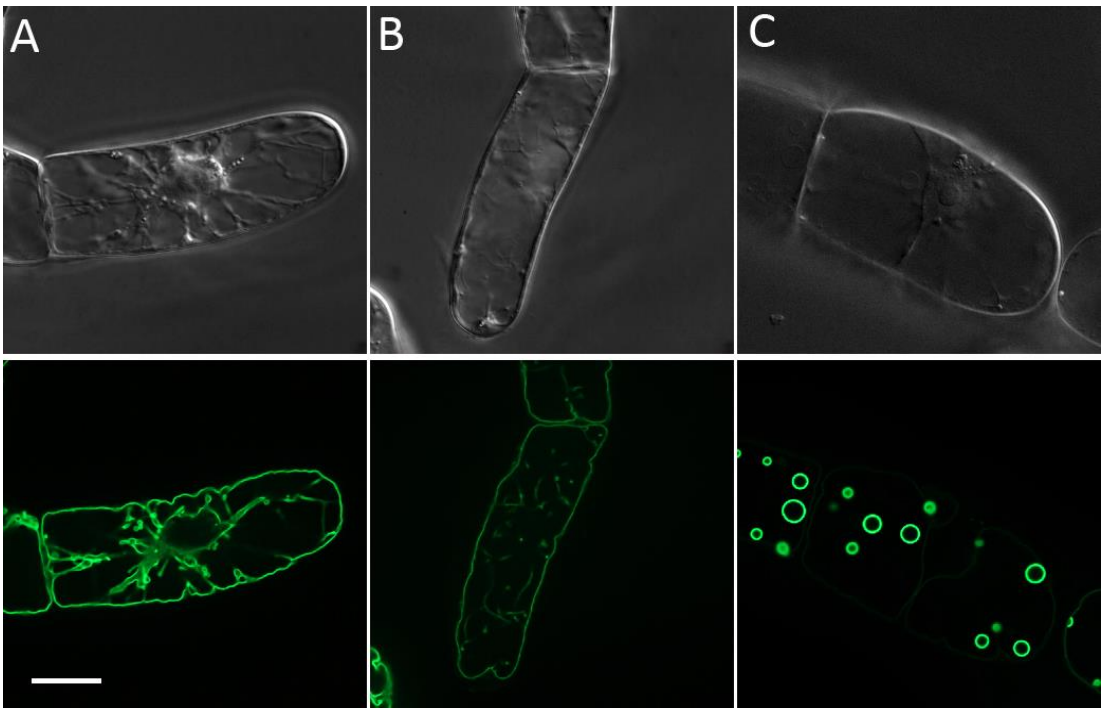

Fig. 3.9 Rare vacuolar structures in BY-2 revealed by overexpressing NtTPC1A fused with GFP. Upper panel: DIC; lower panel: GFP channel. A. Extremely active transvacuolar strands emanating from the nucleus. B. Highly dynamic tubular structure of the transvacuolar membrane (TVM) moving within the cell. C. Vacuolar bulbs moving constantly like bubbles (scale bar represents 20 µm).

3.2.3 GFP tagged NtMCA2 discloses its PM localization

BY-2 cells overexpressing GFP-NtMCA2 fusion proteins presented predominantly PM localization which is further confirmed via plasmolysis (Fig. 3.11). During

interphase, the PM was lightened by green fluorescence with the two connecting cell wall intensely highlighted. When the cell undergoes mitosis, the central plane where the future cell wall will be placed was marked with a green fluorescent signal precluding the formation of the nascent cell wall (Fig. 3.10 B). Along with the forming of the new cell wall, the GFP signal intensively accumulated at the cell plate simultaneously (see Fig. 3.10 C). Small GFP labeled vesicles near the nuclei are always presented which are probably vesicles used in the secretory pathway for proteins synthesis and PM targeting.

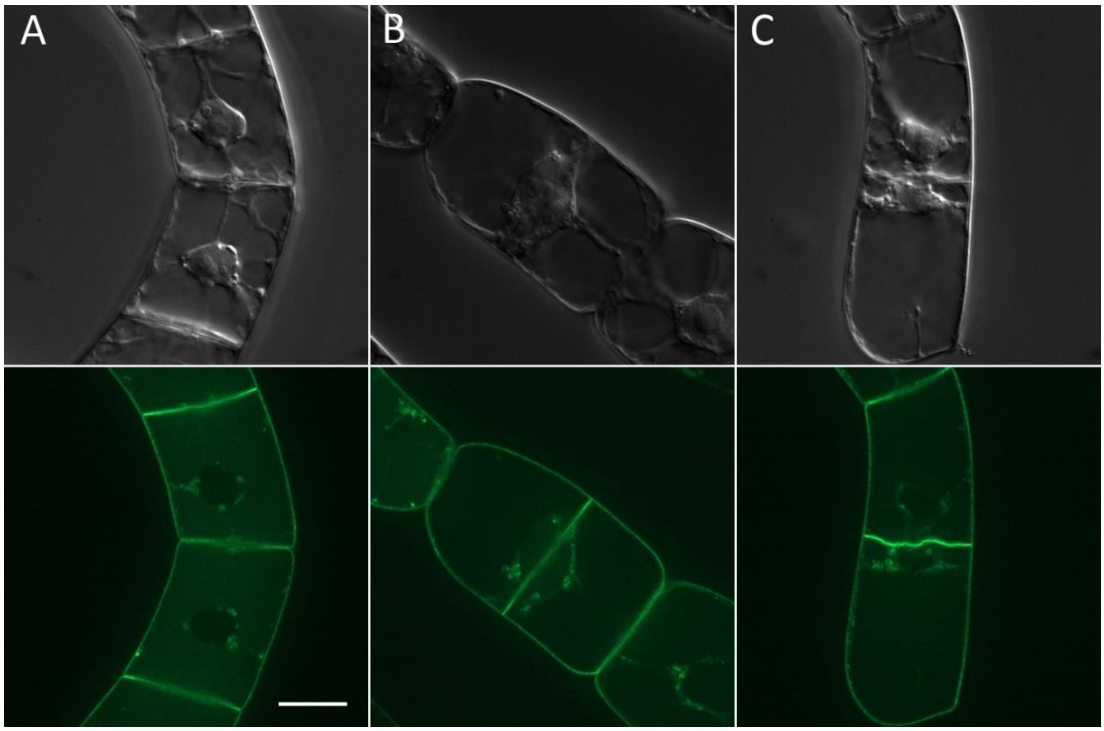

Fig. 3.10 BY-2 overexpressing NtMCA2 with its N- terminal fused to GFP during interphase (A) and mitosis (B, C). Upper panel: DIC; lower panel: GFP channel (scale bar represents 20 µm).

Plasmolysis was induced in this cells line by application of mannitol solution with low water potential. Pictures are taken at 10 s interval right after mannitol was added (Fig. 3.11). This treatment clearly showed that the GFP signal retracted simultaneously as the PM detached from the cell wall. The Hechtian strands (Buer *et al.*, 2000) which are stretched PM extending from the plasmolysed protoplast to the cell wall in plants were nicely revealed during this process.

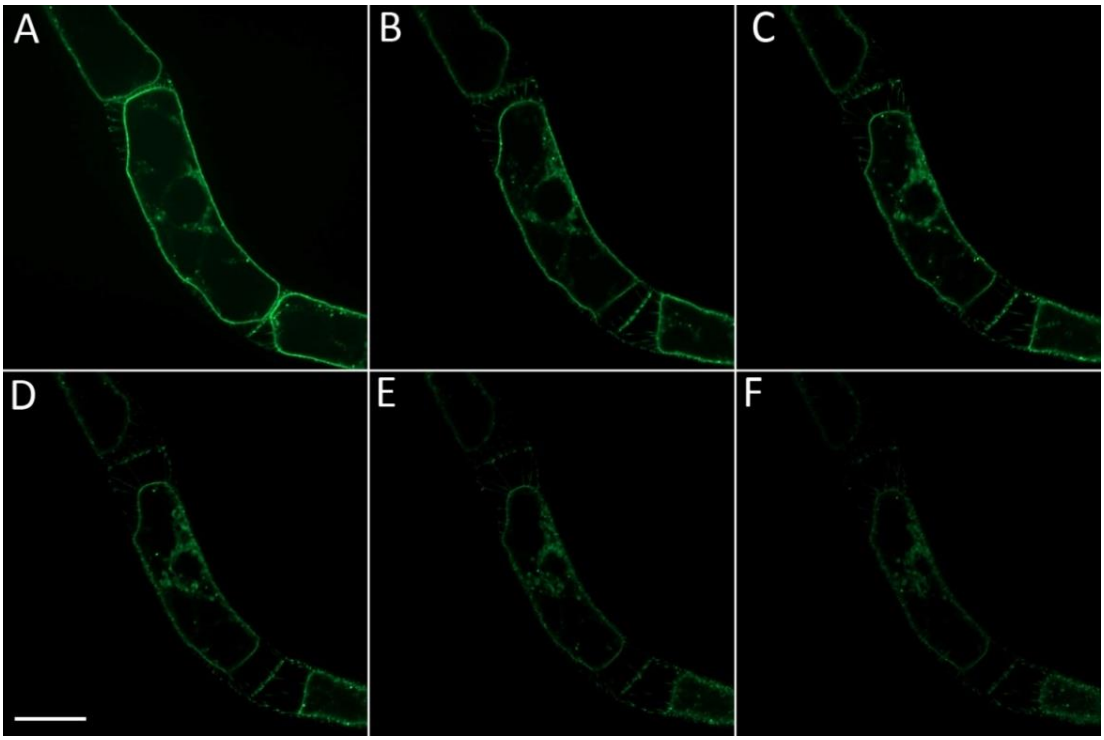

Fig. 3.11 BY-2 overexpressing NtMCA2 fused with GFP subjected to 0.5 M mannitol corroborated their PM localization as well as revealed Hechtian strands. A-F. Pictures taken at 10 s intervals immediately after mannitol treatment (scale bar represents 20 μm).

3.2.4 NtTPC1A and NtMCA2 fusion proteins under high resolution spinning disk microscopy

Combining the orthogonal projections and high resolution spinning disk microscopy, more detailed information about the localizations of these two fusion proteins under investigation are made available. The upper panel of Fig. 3.12 shows that the GFP-decorated vacuole structure appears like a single continuous compartment transected by tubular-like transvacuolar strands (TVSs) with large undulating membrane surface which enwraps the nucleus in the midst and fulfills the most majority part of the cellular space. This cell line is ideal to be used as a marker cell line for vacuolar structure and dynamic imaging of tonoplast *in vivo.* It can facilitate us to understand vacuolar responses to osmotic fluctuations, pathogen attack, programmed cells death (PCD), storage of proteins and so on.

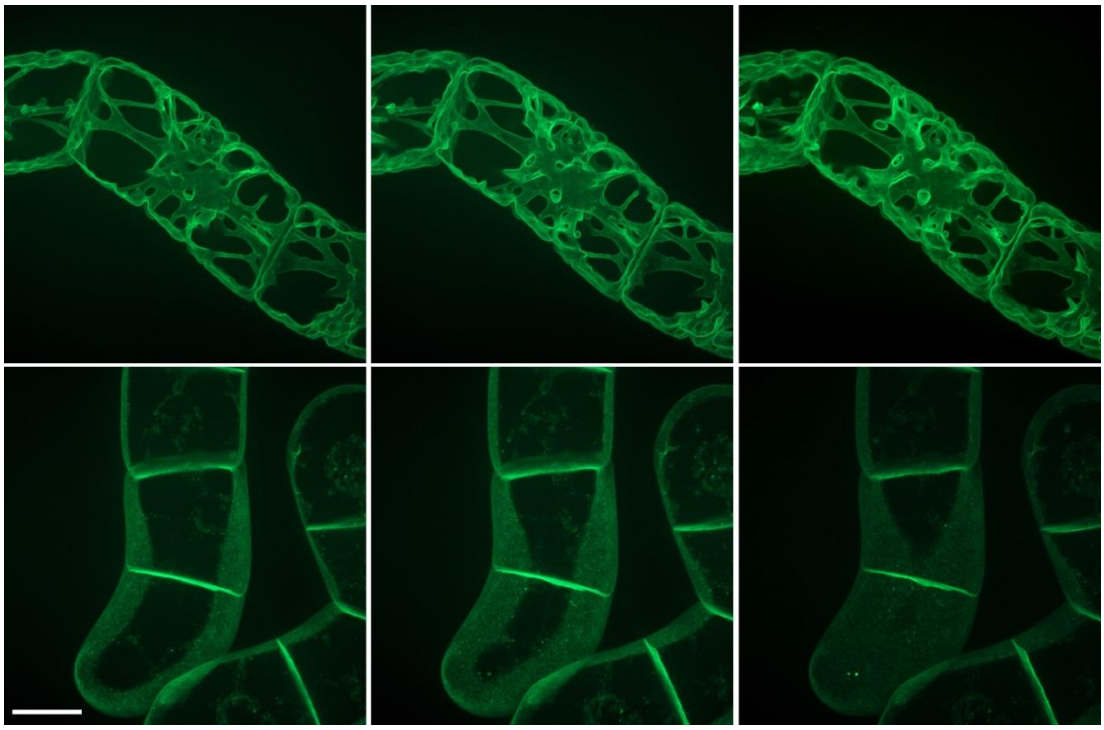

Fig. 3.12 BY-2 overexpressing NtTPC1A-GFP (upper panel) and GFP-NtMCA2 (lower panel). Left to right: increasing numbers of pictures in the z- axis projected together starting from the central plane of the cell (scale bar represents 20 µm).

In the lower panel, the PM highlighted by the GFP-NtMCA2 fusion proteins looks like a shell isolating the interior content of the cell from the extracellular space. These two putative channel proteins were also transiently coexpressed in BY-2 cells (see Fig. 3.13) in which the two different membrane systems can be well distinguished with the contour of the cell highlighted by the PM localized GFP-NtMCA2 fusion proteins encasing the vacuole structure delineated by the tonoplast localized NtTPC1A-RFP fusion proteins. What is worth mentioning here is that the distribution of GFP-NtMCA2 fusion proteins over the PM is not homogeneous. And instead, some spots were rather more concentrated than others suggesting the possibility of these channel proteins may form clusters and probably being a member of a bigger function complex.

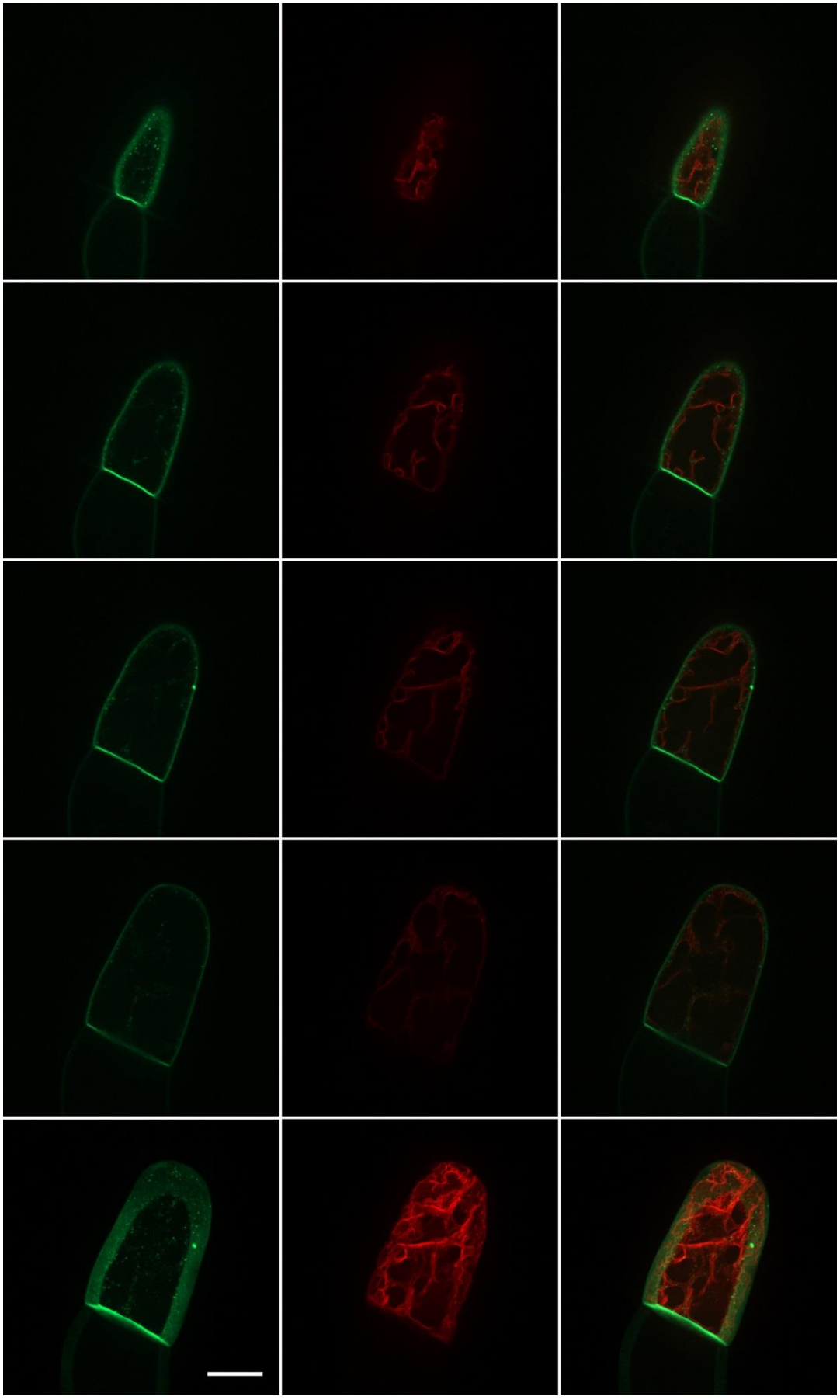

Fig. 3.13 Transient coexpression of NtTPC1-RFP and GFP-NtMCA2 fusion proteins in tobacco

BY-2 cells via modified *Agrobacteria* mediated transformation. Different panels represent individual cross sections from the peripheral to the central plane of the cell and the last panel shows the selected pictures in the z- axis projected together. Left: GFP channel; middle: RFP channel; right: merged GFP and RFP (scale bar represents 20 µm).

Due to the existence of the cell wall as well as turgor pressure, these two types of membranes are pressed very close together and only can be distinguished by fluorescent proteins of different color. It is very intriguing to find out how the vacuole organizes itself in the absence of the cell wall and whether it is able to retain its shape and structure. Therefore, cell wall free protoplasts of the NtTPC1A-GFP overexpression cell line were generated. It was shown in Fig. 3.14 that a protoplast overexpressing NtTPC1A-GFP floating in isotonic medium seems like a spherical shaped Swiss cheese with corrugated outer surface. It is clear that the outline of the membrane shown here was definitely not the PM which appears to be smooth when suspended in isotonic medium. All kinds of transvacuolar membrane protrusions emanating from the perinuclear region towards the periphery of the protoplast as many of them make it through and thus link the perinuclear space with the cytoplasm direct underneath the PM which composes the arteries for intracellular transportation.

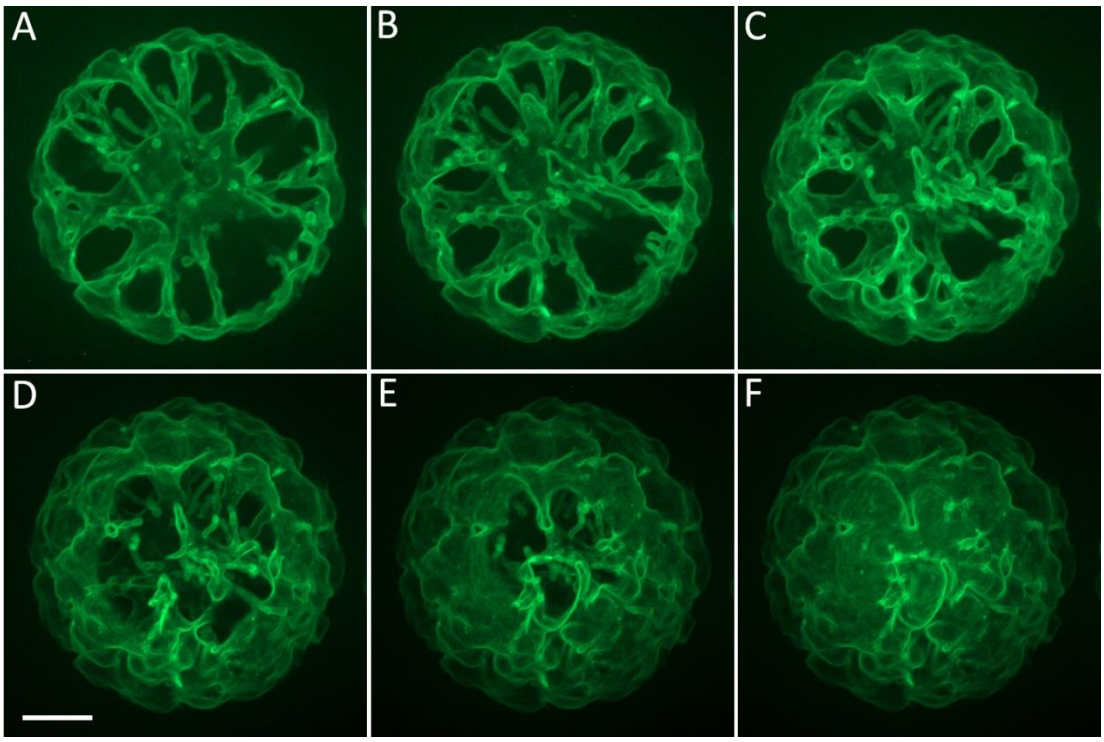

Fig. 3.14 Protoplast generated from BY-2 stably overexpressing NtTPC1A its C- terminal fused to GFP. A-F. Increasing numbers of pictures in the z- axis projected together starting from the central plane of the protoplast (scale bar represents 10 µm).

Considering the importance of actin filaments in organizing transvacuolar strands which has only been suggested by various pharmacological experiments (Uemura *et al.*, 2002; Kutsuna *et al.*, 2003; Mathur *et al.*, 2003; Ovecka *et al.*, 2005; Lovy-Wheeler *et al.*, 2007) as well as one *in vivo* dual labeling using fluorescent dyes (Higaki *et al.*, 2006). Here, an actin marker, actin-binding domain 2 of plant fimbrin (FABD2) fused to RFP was transiently expressed in the NtTPC1A-GFP stable cell line via biolistic to visualize both AFs and VMs for the first time *in vivo* free of staining of any kind. The perinuclear basket formed by actin filaments (Kandasamy *et al.*, 1999) as well as the cortical AFs were visualized by RFP (see Fig. 3.15 RFP channel). Through the merged picture, it can be seen that actin filaments stretching along the transvacuolar strands and shaping the vacuole. At positions where the vacuole forms irregular grooves or turns, thick actin bundles were also presented surrounding them (indicated by white arrows).

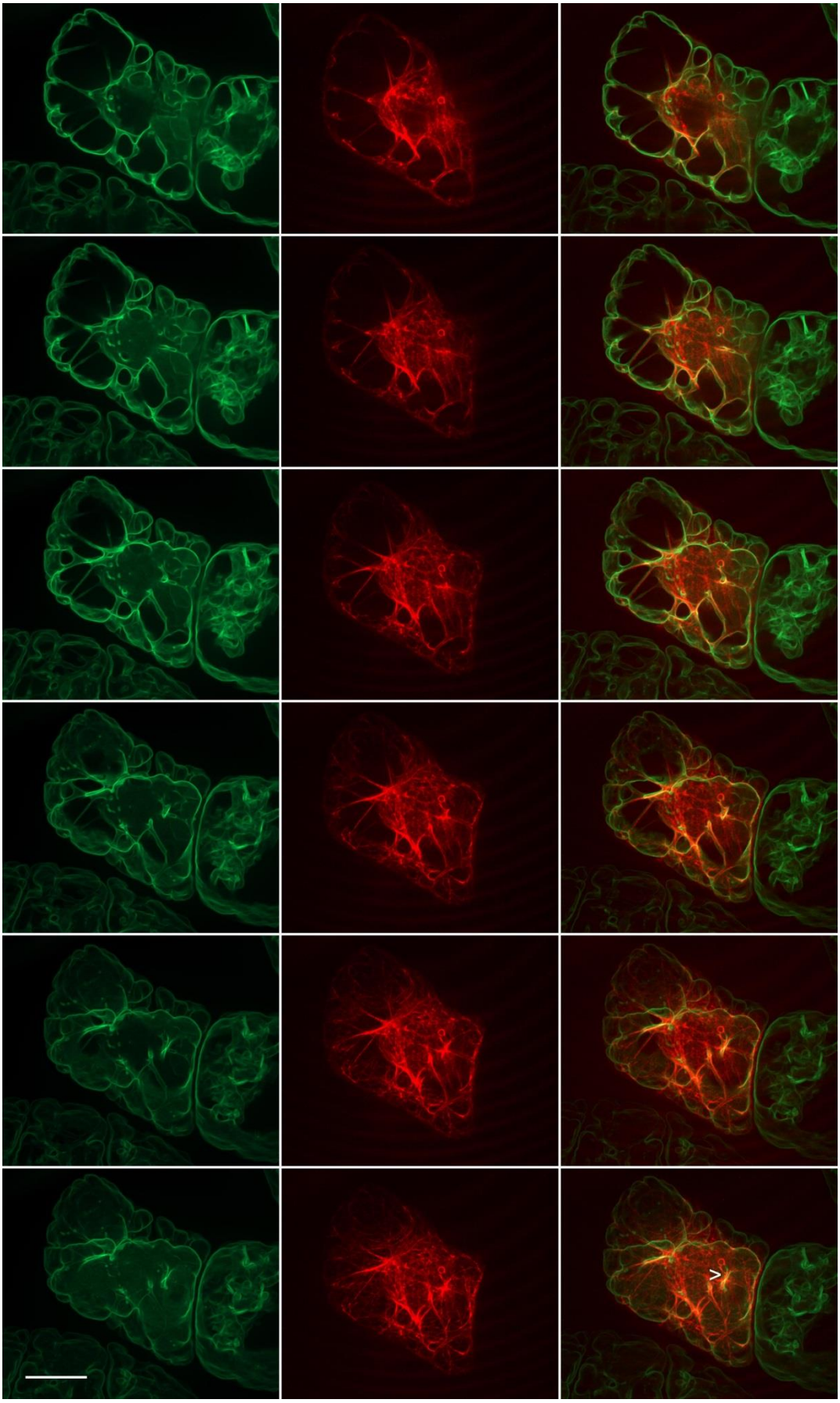

Fig. 3.15 A BY-2 cell stably overexpressing NtTPC1A fused with GFP transiently coexpresses an

FABD2-RFP (Fimbrin Actin Binding Domain) fusion construct which marks the actin filaments in red. Left to right: GFP channel, RFP channel, merged GFP and RFP; top to bottom: increasing numbers of pictures in the z- axis projected together starting from the near central cross sections of the cell (scale bar represents 20 µm).

3.2.5 Dependency of the localization of NtTPC1A fusion proteins on actin

As it has been shown that actin filaments are closely related to the shape of vacuoles and considering the role of cytoskeleton in intracellular trafficking, the chemical agents affecting the stability of the cytoskeletons were applied to the transgenic cell lines to find out if and to what extent they did affect the localization of the fusion proteins *in vivo*. Fig. 3.16 A and B showing cells overexpressing NtTPC1A during interphase and mitosis after being treated with Latrunculin B which eliminates the actin filaments by inhibition of actin polymerization through forming complexes with G-actin monomers (Coue *et al.*, 1987; Spector *et al.*, 1989). In Fig. 3.16 A and B, the typical structures of transvacuolar strands like shown in Fig. 3.7 A (see p.47) were severely disrupted by Latrunculin B treatment which left the cells with enormous single vacuolar compartment pushing the nucleus against the cell wall (Fig. 3.16 A). The newly formed small transvacuolar strands right after mitosis were also severely disturbed by Latrunculin B treatment (Fig. 3.16 B). In contrast, the cells treated with Phalloidin (Fig. 3.16 C and D) did not show obvious alteration in localization patterns when compared to cells without Phalloidin treatment (see Fig. 3.7, p.47 and Fig. 3.8, p.48).

The MT-depolymerizing agent Oryzalin had little influence on the localization of NtTPC1A-GFP fusion proteins in cells in interphase (Fig. 3.17 A). In contrast, cells undergoing mitosis appeared to be more affected (Fig. 3.17 B), which was in accordance with the important role of MTs in mitosis. Stabilizing MTs by Taxol did not evidently alter the patterns of NtTPC1A-GFP fusion proteins at all (Fig. 3.17 C and D).

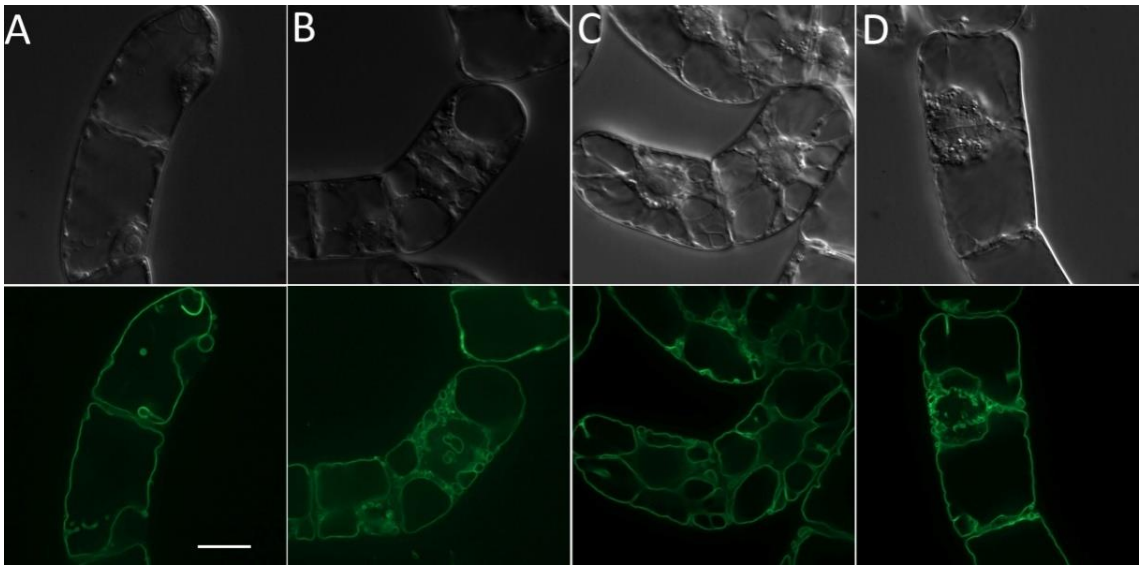

Fig. 3.16 Localization of NtTPC1A-GFP fusion proteins in BY-2 was altered by 30 min of 2 µM Latrunculin B treatment which eliminates AFs and remained unchanged after 30 min of 2 µM Phalloidin incubation which stabilizes AFs. Upper panel: DIC; lower panel: GFP channel. A, B. Cells in interphase and mitosis treated with Latrunculin B. C, D. Cells in interphase and mitosis treated with Phalloidin (scale bar represents 20 µm).

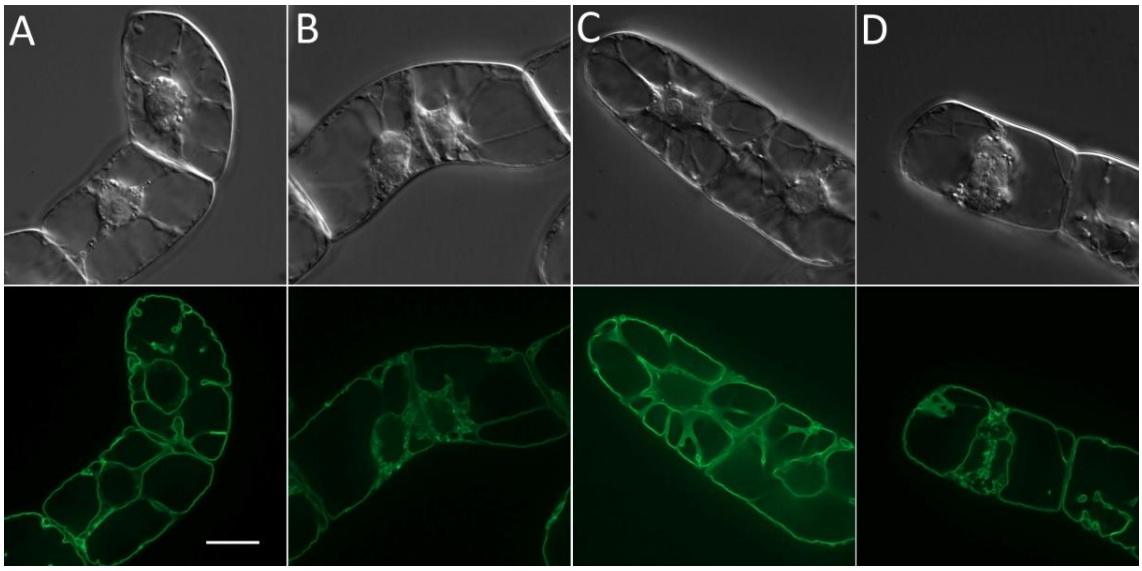

Fig. 3.17 Localization of NtTPC1A-GFP fusion proteins in BY-2 cells was altered by 30 min of 20 µM Oryzalin treatment which disrupts MTs and remained unchanged by 30 min of 20 µM Taxol incubation which is known to stabilize MTs. Upper panel: DIC; lower panel: GFP channel. A, B. Cells in interphase and mitosis treated with Oryzalin. C, D. Cells in interphase and mitosis treated with Taxol (scale bar represents 20 µm).

3.2.6 NtMCA2 and its hidden actin link

The cytoskeletons are intensively involved in intracellular trafficking through guiding trafficking vesicles towards their destinations (Petrasek & Schwarzerova, 2009). For this reason, the dependency of the membrane-localized NtMCA2 fusion proteins on the cytoskeletons is subjected to investigation. As the actin filaments disrupted by Latrunculin B treatment, sizable vesicles accumulated around the nuclei (Fig. 3.18 A), which was less significant in cells undergoing mitosis (Fig. 3.18 B). Stabilizing actin filaments caused the vesicles which use to be near the nuclei to diffuse in the cytoplasmic strands probably due to the deceleration of actin-dependent transport (Fig. 3.18 C and D). In contrast, pharmacological manipulation of microtubule network (Fig. 3.19) did not cause detectable alteration with regard to the localization of NtMCA2 fusion proteins (compare with Fig. 3.10, p.50).

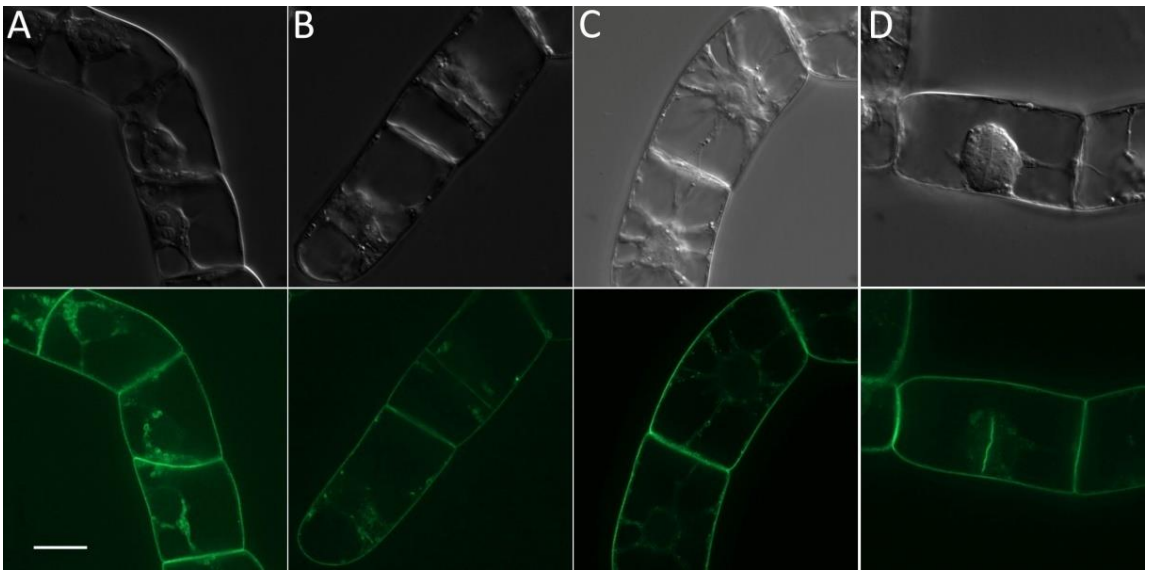

Fig. 3.18 Localization of GFP-NtMCA2 fusion proteins in tobacco BY-2 cells after 30 min of 2 µM Latrunculin B or 2 µM Phalloidin treatment. Upper panel: DIC; lower panel: GFP channel. A, B. Cells in interphase and mitosis treated with Latrunculin B which wipes out AFs. Cells in interphase showed relocation of the fusion protein after Latrunculin B treatment (A). C, D. Cells in interphase and mitosis treated with Phalloidin which stabilize AFs. Decelerated transport of NtMCA2 fusion proteins caused by Phalloidin treatment was observed (C) (scale bar represents 20 µm).

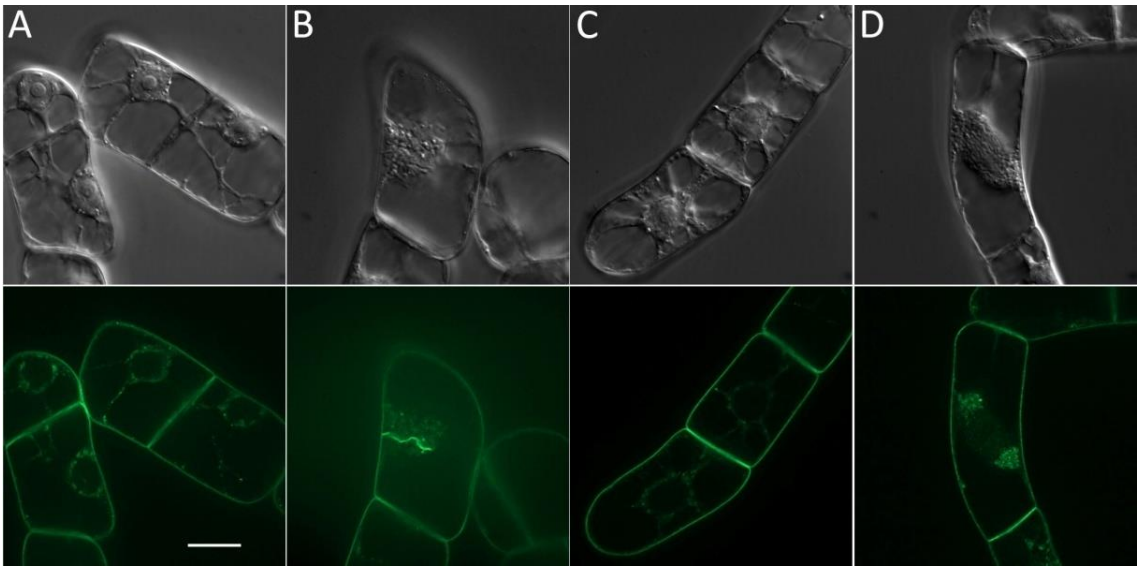

Fig. 3.19 Localization of GFP-NtMCA2 fusion proteins in BY-2 was not obviously altered by 30 min of 20 μM Oryzalin treatment which removes MTs and remained unchanged by 30 min of 20 μM Taxol incubation which prevents MT from depolymerization. Upper panel: DIC; lower panel: GFP channel. A, B. Cells in interphase and mitosis treated with Oryzalin. C, D. Cells in interphase and mitosis treated with Taxol (scale bar represents 20 μm).

3.2.7 NtMCA2 cycles constitutively between intracellular compartments and the PM

Constitutive cycling has been shown to be a widely adopted regulatory mechanism for many PM proteins (Royle & Murrell-Lagnado, 2003) and among which the molecular players involved as well as the mechanism of constitutive cycling for the auxin efflux carrier PIN proteins has been intensively studied (Grunewald & Friml, 2010). BFA is able to block trafficking from recycling endosomes to the PM and causes an aggregation of endosomes. It is therefore used as an approach to determine whether a PM protein undergoes constitutive cycling. And this treatment is employed to exam if NtMCA2 is undergoing constitutive cycling since eliminating AFs causes relocation of the fusion proteins which is also observed for the PIN proteins (Chang *et al.*, 2011) that are known to cycle between the PM and the recycling endosomes. It can be seen from Fig. 3.20 A that small vesicles accumulated around the nucleus in a cell file from a 3-day-old cell culture after 60 min of BFA treatment. Similar effect was also

observed in this cell line when actin filaments were eliminated by LatB treatment (see Fig. 3.18 A, p.59). In Fig. 3.20 B, giant BFA compartments were formed adjacent to the nuclei after being treated with 100 µM of BFA for 60 min in a cell file from a 7-day-old suspension culture. The accumulation of small vesicles and the formation of BFA bodies in the same cell line could be due to the relative rates at which the constitutive cycling is taking place which is probably related to the growth phase of the cell culture. The results indicated that firstly NtMCA2 is undergoing constitutive cycling like many other PM proteins and secondly this process is most likely cell cycle dependent.

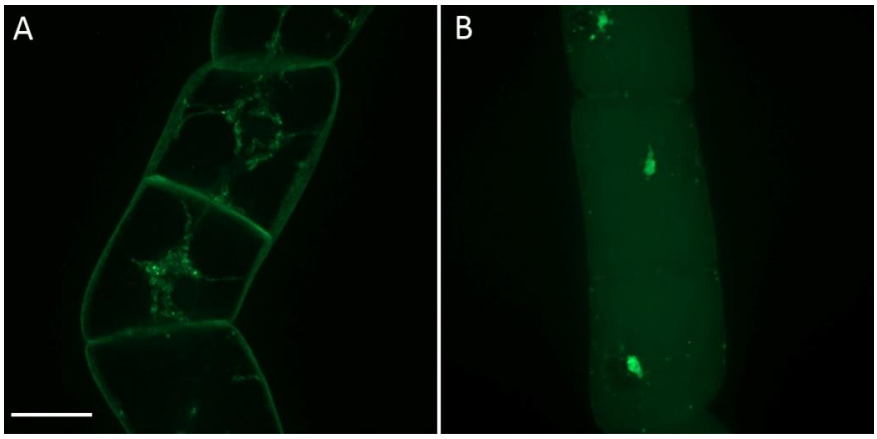

Fig. 3.20 Localization of GFP-NtMCA2 fusion proteins in tobacco BY-2 after treating with 100 µM of BFA for 60 min. A. Small vesicles probably recycling endosomes accumulated around the nuclei in cells from a 3-day-old BY-2 suspension culture. B. BFA-induced NtMCA2 accumulation in BFA compartments in cells from a 7-day-old suspension culture (scale bar represents 20 µm).

3.3 How do NtTPC1A and NtMCA2 ox cell lines respond to internal forces - revealed by cell growth and division?

3.3.1 Quantitative PCR revealed 5 times more transcripts in NtTPC1A and NtMCA2 ox cell lines in comparison to the WT

Quantitative analysis via qPCR showed that the transcripts of NtTPC1A and NtMCA2 in the overexpression cell lines were 5.7 and 5.5 times more abundant in comparison with the WT respectively (see Fig. 3.21).

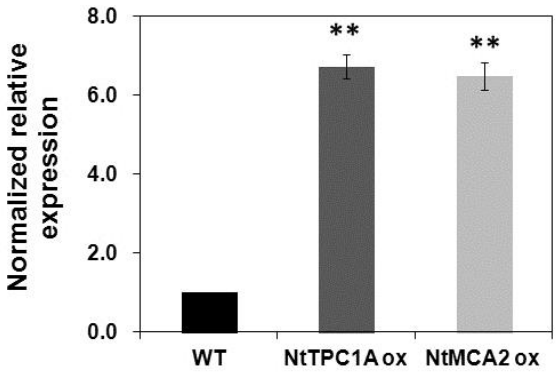

Fig. 3.21 Transcription levels of the genes NtTPC1A and NtMCA2 were quantified relative to the WT control after normalization with the two selected housekeeping genes: L25 and GAPDH. BY-2 WT (black bar), NtTPC1A ox (dark grey bar) and NtMCA2 ox (light grey bar). Data were collected from four biological repeats. *$P < 0.05$, **$P < 0.01$, Student's *t*-test.

So far, both microscopic studies as well as qPCR analysis had demonstrated that both NtTPC1A and NtMCA2 had been successfully overexpressed in tobacco BY-2 suspension cultures. These transgenic suspension cell lines are therefore suitable to be used in functional analyses.

Calcium has been well established as a very important regulator for cell growth, especially in polarized tip growth (Cheung & Wu, 2008). An extracellular influx of calcium has been detected using Ca^{2+} ion-selective vibrating probe (Kuhtreiber & Jaffe, 1990) in root hair cells (Gilroy & Jones, 2000) and pollen tubes (Holdaway-Clarke *et al.*, 1997). It has been suggested to be important for maintaining the stability of the newly formed cell wall probably by affecting the activity of ATPase and proton influx carriers (Choi *et al.*, 2011). Therefore, the growth of cell lines overexpressing NtTPC1A and NtMCA2 was subjected to investigation. Two parameters, cell size as well as division synchrony were chosen as indicators for cell expansion and division which cover the main aspects of growth in BY-2 cell suspension culture.

3.3.2 Cell elongation is significantly inhibited in BY-2 cells overexpressing NtTPC1A and NtMCA2

Data of cell width and cell length collected from at least 1500 individual cells originated from three independent experimental series together with the ratio of cell length and cell width were plotted in Fig. 3.22. It was shown that

overexpressing NtTPC1A and NtMCA2 imposed no influence on cell expansion under normal cultivation condition (Fig. 3.22 A control). However, the elongation growth was significantly inhibited in both overexpression cell lines (Fig. 3.22 B control) hinting interaction with cortical microtubules (Dixit & Cyr, 2004). Due to the inhibitory effect on elongation growth, the ratio of cell length and cell width was significantly reduced in comparison to that of the WT cell (Fig. 3.22 C control).

3.3.3 NtTPC1A ox cell line responds to IAA in the same way as the WT

IAA, as a polar transported phytohormone, significantly stimulated cell expansion in the NtTPC1A ox cell line (Fig. 3.22 A 2 µM IAA) and meanwhile inhibited elongation growth (Fig. 3.22 B 2 µM IAA) compared to the WT cells subjected to the same treatment and this led to a sharply decreased ratio of cell length to cell width (Fig. 3.22 C 2 µM IAA). Again, when comparing the ratio of cell length and cell width of NtTPC1A ox cell line with and without IAA treatment, a significant decrease in the ratio of cell length and cell width was observed after IAA treatment (Fig. 3.22 D NtTPC1A ox) which resembles when BY-2 WT cells that were treated with 2 µM of IAA (Fig. 3.22 D WT). This indicates that overexpressing NtTPC1A does not compromise BY-2 cells' response to IAA.

3.3.4 NtMCA2 ox cell line exhibits altered IAA response in comparison to the WT

For the NtMCA2 ox cell line, both cell expansion and cell elongation growth were inhibited by IAA treatment in comparison to the WT (Fig. 3.22 A and B 2 µM IAA). However, the ratio of cell length and cell width in this cell line is not significantly different form the WT after IAA treatment (Fig. 3.22 C 2 µM IAA) as expected from the inhibitory effect on both cell width and cell length. Furthermore, IAA treatment did not alter the ratio of cell length and cell width in the NtMCA2 ox when

compared with the untreated cells overexpressing NtMCA2 (Fig. 3.22 D NtMCA2) which was quite different from the WT's response to IAA (Fig. 3.22 D WT). This difference suggests that BY-2 cells' response to the phytohormone IAA is interfered by overexpressing NtMCA2.

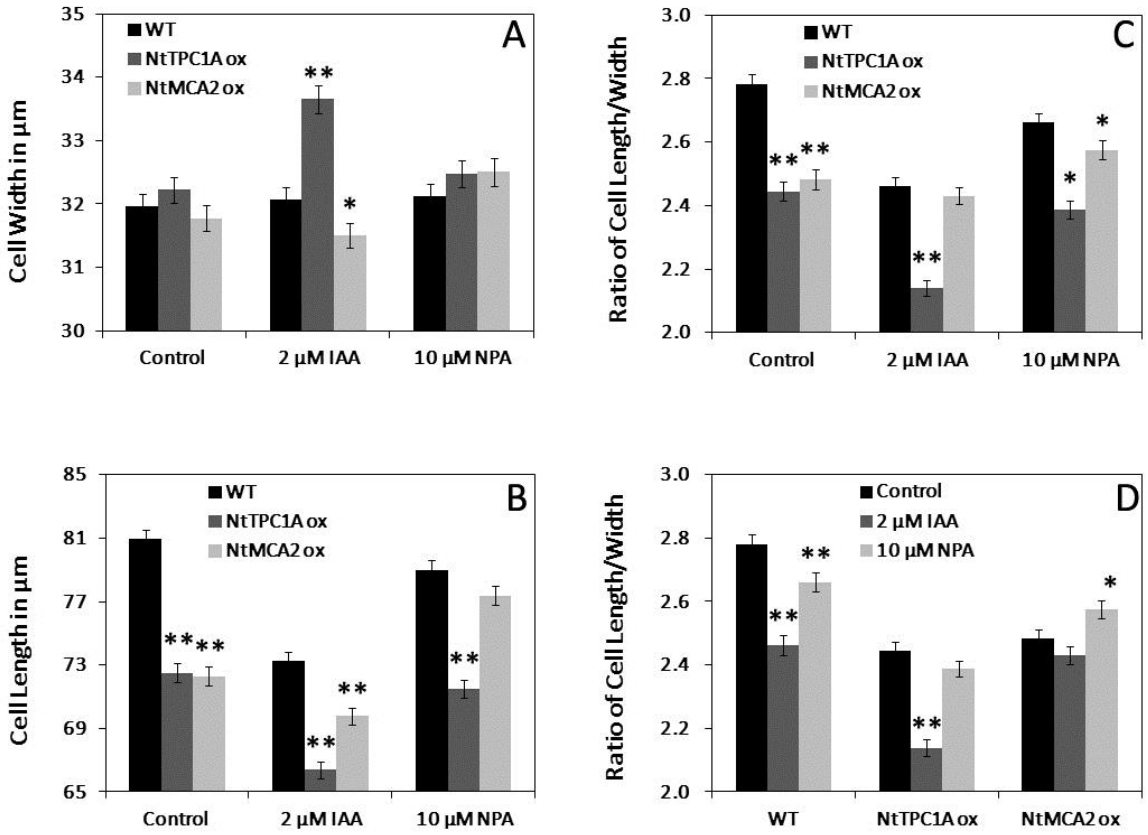

Fig. 3.22 Effects of overexpressing NtTPC1A-GFP and GFP-NtMCA2 on cell growth as well as their response to auxin and polar auxin-transport inhibitor NPA. Cell width and cell length were plotted for BY-2 WT (black bar), NtTPC1A ox (dark grey bar) and NtMCA2 ox (light grey bar), respectively (A-C). In Fig. 3.22 D, the color codes were assigned to different treatments as indicated in the figure legend. Data show mean values and standard errors from 1841 (WT), 1573 (NtTPC1A ox) and 1539 (NtMCA2 ox) individual cells collected from 3 independent experimental series. Differences in cell width, cell length and ratio of cell length to cell width between the overexpression cell lines and the WT under each experimental condition as well as each individual cell line under various experimental conditions were tested for significance. *$P < 0.05$, **$P < 0.01$, Student's *t*-test.

3.3.5 NPA impedes cell elongation in the NtTPC1A ox cell line however not in the NtMCA2 ox cell line

NPA, which blocks polar auxin transport, suppresses cell elongation significantly in the NtTPC1A ox cell line (Fig. 3.22 A 10 µM NPA). However, it only causes a less significant decrease in the ratio of cell length and cell width compared to the WT cells subjected to the same treatment (Fig. 3.22 C 10 µM NPA). This is probably due to the fact that the WT respond to the NPA treatment with slightly decreased cell length to cell width ratio as well and that's what made the difference less significant. When compare the cells treated with NPA and the untreated ones of the NtTPC1A ox cell line, the difference had vanished (Fig. 3.22 D NtTPC1A ox). In other words, overexpressing NtTPC1A jeopardizes the sensitivity of cell elongation to NPA in BY-2 cells.

Surprisingly, cell elongation growth in the NtMCA2 ox cell line was stimulated by NPA treatment because the significant reduction in the cell length due to the effect of overexpressing NtMCA2 was partially compensated by NPA treatment (Fig. 3.22 B control and 10 µM NPA). Even though the ratio of cell length and cell width was still decreased compared to the WT experienced the same treatment (Fig. 3.22 C 10 µM NPA), when compared to the untreated cells of the overexpression cell line, the cell length to cell width ratio was actually significantly increased (Fig. 3.22 D NtMCA2).

In summary, overexpressing NtTPC1A and NtMCA2 significantly inhibited cell elongation in BY-2 cells. The NtTPC1A ox cell line exposed to both IAA and NPA treatments had reduced cell length to cell width ratio compared to the WT cells. However, no significant difference was observed in cell length to cell width ratio in the NtTPC1A ox cell line with and without NPA treatment which is different from the WT cells indicating that overexpressing NtTPC1A impairs response to NPA in BY-2 cells. The NtMCA2 ox cell line presents reduced sensitivity to IAA treatment.

NPA treatment stimulates cell elongation in the NtMCA2 ox cell line which is a completely opposite effect in comparison with the WT. This stimulating effect of NPA on cell elongation partially compensates the inhibitory effect on cell elongation caused by overexpression of NtMCA2 in BY-2 cells.

3.3.6 Cell division synchrony remains unchanged in both overexpression cell lines

Cell divisions in BY-2 cells are synchronized by a polarized flow of auxin through the cell file (Campanoni *et al.*, 2003). This pattern has been shown to be highly sensitive to perturbations of actin (Maisch & Nick, 2007). Considering the role of calcium in signaling as well as in cell wall construction, the division synchrony is investigated in these two overexpression cell lines. The frequency distributions of cell files with certain cell numbers are plotted in Fig. 3. 26. The characteristic oscillatory behavior of clear peaks at files with even cell numbers is presented in all three cell lines investigated (Fig. 3. 23). However, no significant difference of the frequency of hexa-cellular files, diagnostic for directional synchrony, (Campanoni *et al.*, 2003) was observed between the WT and either of the overexpression cell lines.

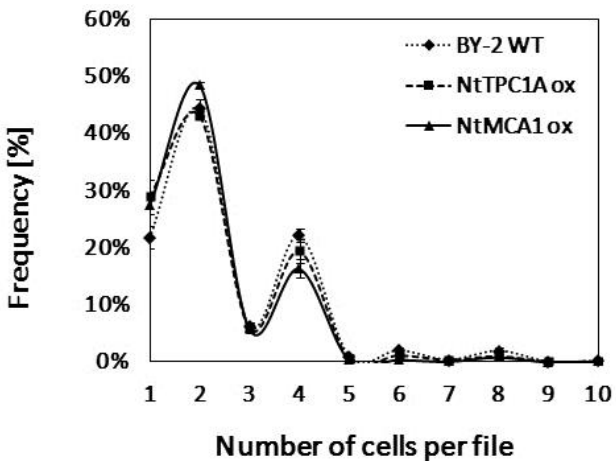

Fig. 3.23 Effects of overexpressing NtTPC1A and NtMCA2 on cell division synchrony. Relative frequency of cell files with certain numbers of cells was plotted for BY-2 WT (dotted line with diamond), NtMCA2 ox (dotted line with square) and NtTPC1A ox (straight line with triangle), respectively. Data show mean values and standard errors from 1500 (WT), 1771 (NtTPC1A ox) and 1826 (NtMCA2 ox) individual cell files collected from 3 independent experimental series. Differences in relative frequency between the overexpression cell lines and the WT were tested for significance. *$P < 0.05$, **$P < 0.01$, Student's *t*-test.

3.4 How do NtTPC1A and NtMCA2 ox cell lines respond to external forces - simulated by osmotic stress?

3.4.1 NtTPC1A and NtMCA2 ox cell lines are more tolerant to mild salt stress

Calcium has been recognized as a central regulator of almost every stress signaling pathway including mechanical stimuli and salt stress. In the meantime, the potential role of NtMCA2 as mechanosensor for sensing osmotic alterations during salt stress as well as NtTPC1A for functioning downstream of the signaling pathway made the investigation of the performance of these two calcium channel overexpression cell lines under salt stress a necessity. Therefore, the following experiments are concentrated on the cell lines response to salt stress as well as intracellular calcium content to understand the functions of these two calcium channels in mechanosensing and calcium signaling.

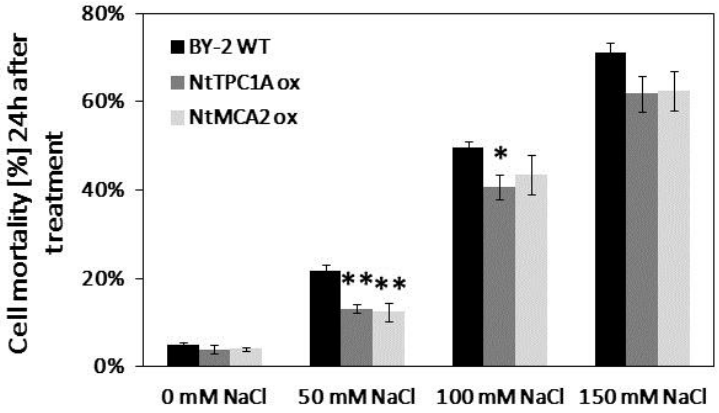

Fig. 3.24 Effects of overexpressing NtTPC1A and NtMCA2 on cell mortality under salt stress. Cell mortalities 24h after NaCl treatments (concentrations as indicated) were plotted for BY-2 WT (black bar), NtMCA2 ox (dark grey bar) and NtTPC1A ox (light grey bar), respectively. Data show mean values and standard errors from 5 independent experimental series. Differences in cell mortality between the overexpression cell lines and the WT were tested for significance. *$P < 0.05$, **$P < 0.01$, Student's *t*-test.

Cell mortalities determined 24 h after subcultivation/NaCl treatments of various concentrations were plotted in Fig. 3.24. The results showed that the mortalities in both overexpression cell lines were significantly lower than the WT when treated

with 50 mM NaCl. Increasing the NaCl concentration to 100 mM made the difference less significant and further increase made the difference between the overexpression cell lines and the WT vanished entirely. For examining the long term effects, the packed cell volume (PCV) was determined 4 days after subcultivation/NaCl treatments of various concentrations. Fig. 3.25 shows that after 4 days cultivation, there were no difference between the two overexpression cell lines and the WT when treated with NaCl no higher than 100 mM even though a significant difference in cell mortalities were detectable 24 h after treatment (Fig. 3.24). This is probably due to the fast cell dividing rate which compensates the increased cell mortality in 4 days. Very severe growth inhibition were observed in all three cell lines after treating with 150 mM NaCl for 4 days.

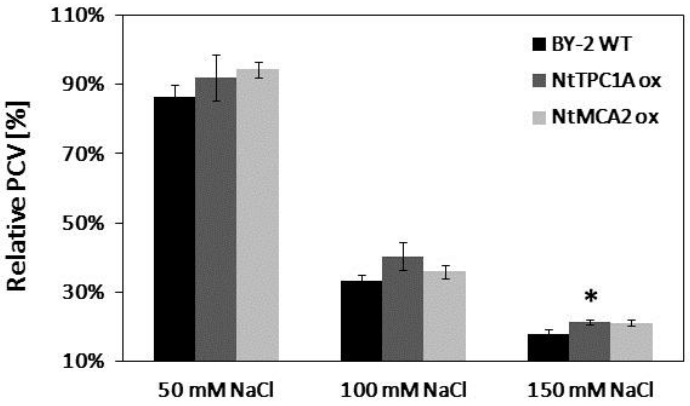

Fig. 3.25 Effects of overexpressing NtTPC1A and NtMCA2 on packed cell volume. Relative PCVs measured 4 days after NaCl treatments were plotted for BY-2 WT (black bar), NtTPC1A ox (dark grey bar) and NtMCA2 ox (light grey bar), respectively (concentrations as indicated). Data show mean values and standard errors from 5 independent experimental series. Differences in PCV between the overexpression cell lines and WT were tested for significance. *$P < 0.05$, **$P < 0.01$, Student's *t*-test.

3.4.2 Both overexpression cell lines are more tolerant to selected calcium channel blockers

Both inorganic and organic compounds have been reported to inhibit Ca^{2+} fluxes and therefore, Al^{3+} (Ding *et al.*, 1993; Pickard & Ding, 1993), Gd^{3+} (Allen & Sanders, 1994; Klusener *et al.*, 1995) and verapamil (Spedding & Paoletti, 1992) were chosen to test the sensitivity of the overexpression cell lines to these

selected calcium channel blockers using PCV as an indicator. As shown in Fig. 3.26 A, overexpressing NtTPC1A and NtMCA2 increases the tolerance of BY-2 to $AlCl_3$ especially at higher concentrations. NtMCA2 ox cell line could survive 800 µM of $GdCl_3$ which leads to the elimination of all cells in the WT suspension (Fig. 3.26 B). However, the NtTPC1A overexpression cell line showed no difference compared to the WT when treated with verapamil and even the WT cells suffered no growth inhibition at 200 µM (data not shown).

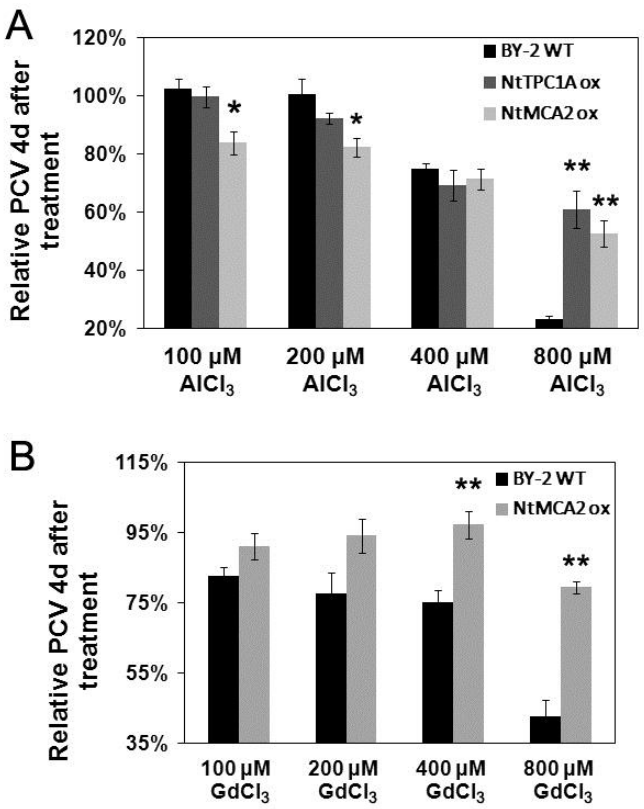

Fig. 3.26 Effects of overexpressing NtTPC1A and NtMCA2 on tolerance to selected calcium channel blockers. Relative PCVs measured 4 days after treatment (concentrations and types of calcium channel blockers are indicated in figure legends) were plotted for BY-2 WT (black bar), NtTPC1A ox (dark grey bar) and NtMCA2 ox (grey bar). Data show mean values and standard errors from 3-5 independent experimental series. Differences in PCV between the overexpression cell lines and the WT were tested for significance. *P < 0.05, **P < 0.01, Student's t-test.

3.4.3 More channel proteins yet less intercellular calcium content

The intracellular Ca^{2+} levels measured via atomic absorption spectrometry (AAS) were plotted in Fig. 3.27. When compare the intracellular Ca^{2+} levels of the two overexpression cell lines with the WT, significant decreases in intracellular Ca^{2+} level at the 0.05 level were presented in both NtTPC1A and NtMCA2 overexpression cell lines.

3.4.4 NtMCA2 ox cell line is salt tolerant probably by retaining Ca^{2+} and excluding Na^{+}

The significant difference in intracellular calcium content between the WT and the two overexpression cell lines vanished after NaCl treatment. However, when compared the intracellular Ca^{2+} levels in each cell line before and after NaCl treatment, the intracellular Ca^{2+} levels experienced a very significant decrease after 150 mM of NaCl treatment in both the WT and the NtTPC1A ox cell line. In contrast, this drop in intracellular Ca^{2+} level caused by NaCl treatment was absent in the NtMCA2 ox cell line.

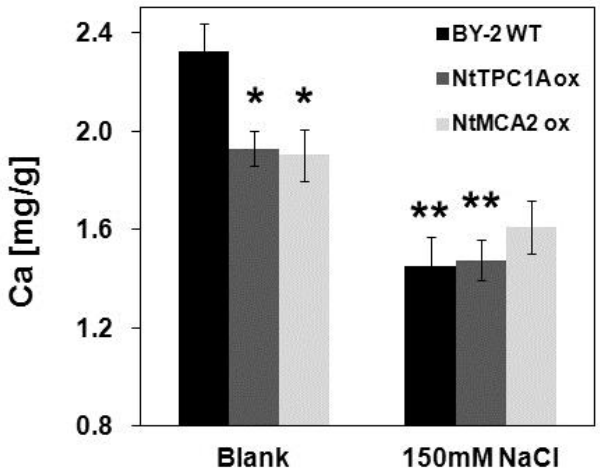

Fig. 3.27 Effects of overexpressing NtTPC1A and NtMCA2 on intracellular calcium content. Intracellular calcium contents were plotted for BY-2 WT (black bar), NtTPC1A ox (dark grey bar) and NtMCA2 ox (light grey bar) respectively. Data show mean values and standard errors from 5-6 independent experimental series. Differences in intracellular calcium contents between the overexpression cell lines and the WT as well as each individual cell line before and after NaCl treatment were tested for significance. *$P < 0.05$, **$P < 0.01$, Student's *t*-test.

In the meantime, the intracellular Na^{+} levels after NaCl treatment were also determined. Fig. 3.28 shows that there is no significant difference between the WT and the two overexpression cell lines in intracellular Na^{+} levels before NaCl treatment. However, the intracellular Na^{+} level in the NtMCA2 ox cell line after 150 mM NaCl treatment was significantly lower than the other two cell lines. This ability to retain Ca^{2+} ions as well as excluding the toxic Na^{+} is featured for salt tolerance in plants. And the results indicate that NtMCA2 is involved in salt stress probably through influencing calcium homeostasis as well as signaling.

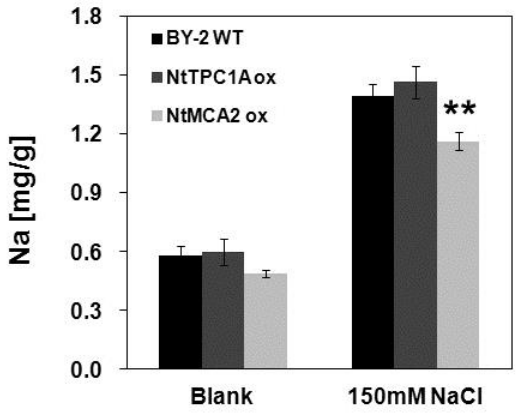

Fig. 3.28 Effects of overexpressing NtTPC1A and NtMCA2 on intracellular Na^+ content when exposed to NaCl. Na^+ concentrations were plotted for BY-2 WT (black bar), NtTPC1A ox (dark grey bar) and NtMCA2 ox (light grey bar) respectively. Data show mean values and standard errors from 5 independent experimental series. Differences in intracellular sodium contents between the overexpression cell lines and the WT as well as each individual cell line both before and after NaCl treatment were tested for significance. *P < 0.05, **P < 0.01, Student's t-test.

3.4.5 Intracellular calcium content reduction in both ox cell lines can be restored by calcium supplement

Since the intracellular Ca^{2+} levels in both overexpression cell lines are lower than the WT, the intracellular Ca^{2+} levels after calcium supplements were determined to find out whether the Ca^{2+} uptake abilities were completely compromised by overexpression. Fig. 3.29 illustrates that additional Ca^{2+} in the medium did not alter the uptake in the WT cells significantly. However, the presence of additional Ca^{2+} at 2 mM could compensate the decreased intracellular Ca^{2+} in both overexpression cell lines to the WT level. Further increase of the extracellular Ca^{2+} to 5 mM level did not yield significant improve in the amount of uptake.

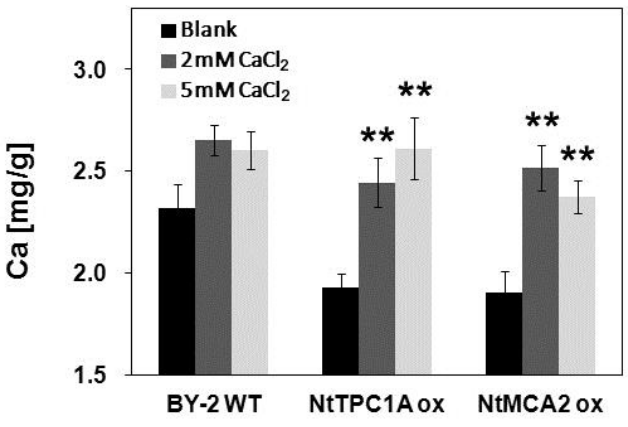

Fig. 3.29 Calcium supplements were able to compensate for the decreased intracellular calcium contents caused by overexpressing NtTPC1A and NtMCA2. Ca^{2+} contents were plotted for BY-2 WT (black bar), NtTPC1A ox (dark grey bar) and NtMCA2 ox (light grey bar) respectively without and with 2 or 5 mM $CaCl_2$. Data show mean values and standard errors from 3 independent experimental series and differences in intracellular calcium levels without or with calcium supplements were tested for significance. *P < 0.05, **P < 0.01, Student's t-test.

3.4.6 NtTPC1A and NtMCA2 are not exclusively calcium permeable

Intracellular Ca^{2+} levels of all cell lines were determined at the present of Mg^{2+} to see how exclusive those putative calcium channels were (see Fig. 3.30). The results demonstrate that Mg^{2+} supplements lead to a very significant drop in intracellular Ca^{2+} levels in the WT and a less significant drop in both overexpression cell lines probably because of the initially low calcium level in the overexpression cell lines. And there was no significant difference in intracellular Ca^{2+} levels between the WT and the overexpression cell lines after additional Mg^{2+} was given to the cultivation medium.

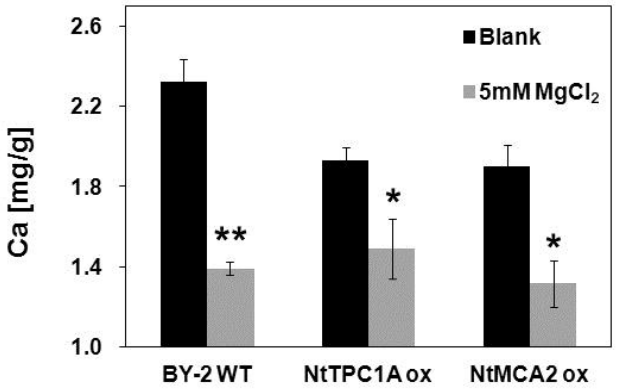

Fig. 3.30 Magnesium supplements given to cell lines overexpressing NtTPC1A and NtMCA2 cause intracellular calcium concentration decrease. Ca^{2+} contents are plotted for BY-2 WT, NtTPC1A ox and NtMCA2 respectively without and with 5 mM $MgCl_2$. Data show mean values and standard errors from 3 independent experimental series and differences in intracellular calcium levels without or with magnesium supplements was tested for significance. *P < 0.05, **P < 0.01, Student's t-test.

3. 5 Summary

The emerging concept of the CW-PM-CTK continuum in plant cells prompts researchers to identify the molecular players involved in establishing this continuum as both a physically and chemically interconnected entity. Meanwhile, to understand how does this CW-PM-CTK continuum in plants are involved in mediating multiple cellular functions, such as mechanosensing, growth regulation, defence response and various other signaling events. Based on this general background, the role of the plant cytoskeletons in mechanosensing specified during cell volume control in response to osmotic stress as well as the

possibilities of two putative calcium channels participating in mechanosensing were investigated in this study. Using cell wall free protoplasts and a quantitative method to approximate hydraulic conductivity L_p, a role of the plant cytoskeleton in plant protoplast volume control in response to hypotonic shock through regulating the insertion of the intracellular store of membrane material has been demonstrated. This finding supports that submembraneous actin modulate the mechanical properties of the PM as well as the formation and dynamicity of tubulovesicular membrane folds or invaginations, which are both involved in mechanosensing. By monitoring the PM dynamic using the fluorescent dye FM4-64 and a localized debundling of actin filaments via photoactivation of caged auxin (see Appendix 5.9, p.122) as well as *in vivo* visualization of actin and microtubule organization in response to both hypo- and hyper- osmotic pressure in the GF-11 and *β*-tub 6 marker lines, the link between osmotic stresses, membrane dynamics and the cytoskeletal networks was manifested.

NtTPC1A and NtMCA2 encoding respectively putative calcium channels in BY-2 cells (Kadota *et al.*, 2004; Kurusu *et al.*, 2012b) have been individually studied. However, a completed understanding about their function *in vivo* is still far from being accomplished. Two of them were chosen as potential candidates participating in mechanosensing in plant based on previous reports. In order to perform microscopic as well as functional studies, two cell lines overexpressing these two putative calcium channels with GFP tags were established as the prerequisite for subsequent works. And during the process of establishing stable transgenic cell lines, the transformation procedure based on the Buschmann method (Buschmann *et al.*, 2010) was also modified which showed an improved performance in transforming tobacco BY-2 cells.

L_p determination of protoplasts generated from the NtTPC1A and NtMCA2 ox cell line excluded the role of these two channels in protoplast volume regulation under the described experimental settings which is in agreement with externally manipulating calcium channel activities. Microscopic studies demonstrated the

tonoplast localization of the NtTPC1A and confirmed the PM localization of the NtMCA2 in tobacco BY-2 cells. For the first time, both vacuolar structure and actin filaments were simultaneously marked *in vivo* free of staining of any kind in plant cells. This approach revealed that actin filaments play a critical role in shaping as well as organizing the plant vacuoles. The localization of NtMCA2 is found to be sensitive to the BFA, an endocytosis inhibitor, suggesting that constitutive recycling might be a way for the cell to regulate the function of NtMCA2 proteins.

Quantitative PCR showed a more than 6 times ratio when comparing the transcripts of NtTPC1A and NtMCA2 in the overexpression cell line with the WT. The elongation growth was significantly inhibited by overexpression of these two channel proteins and they also showed altered response to either IAA or NPA. Intracellular calcium content measurements through AAS revealed reduced intracellular calcium contents in both NtTPC1A and NtMCA2 ox cell lines in comparison with the WT. The intracellular calcium content decrease in response to NaCl treatment was absent only in the NtMCA2 overexpression cell line indicating distinct roles of these two channels in osmotic stress sensing and/or signaling. The presence of calcium supplement in the cultivation medium was able to restore the decreased intracellular calcium contents in NtTPC1A and NtMCA2 overexpression cell lines to the level of the WT. Additional magnesium in the cultivation medium lead to significant decrease in intracellular calcium content suggesting that these two channels are not exclusively calcium permeable.

Overexpression of these two selected putative calcium channels in BY-2 cells causes altered responses to internal mechanical forces indicated by cellular growth as well as external stimuli suggested by salt stress. These observed alterations in intact cells are in contrast with the independency of L_p on manipulation of calcium homeostasis concluded from experiments performed with protoplasts. This contract emphasizes that the presence of the cell wall as part of the integral CW-PM-CTK continuum is indispensable for the function of calcium channels in mechanosensing.

4. Discussion

4.1 Controlling regulatory volume change is one way for the cytoskeleton to participate in mechanosensing

Different mechanisms have been proposed for the role of the cytoskeleton in volume control (Maurel, 1997; Komis *et al.*, 2001): (1) the cortical cytoskeleton might regulate (osmosensory) ion-channel activity and thus limit water uptake, or it might regulate (downstream) mass transport across the membrane. (2) Transvacuolar bundles of actin might impede protoplast swelling by mechanic tethering (for microtubules that do not harbor tensile resistance, but only compressive resistance, such a mechanism would not work). (3) The dynamic cortical cytoskeleton might adhere to the PM and controls the mobilization of material into the expanding membrane. In the following, the experimental results about the role of the cytoskeleton in volume control will be discussed in the conceptual framework of these three mechanisms.

Protoplast swelling is based on osmotic water influx and requires the incorporation of additional material into the expanding membrane (Meckel *et al.*, 2005). The initial stimulus is the osmotically generated force upon the membrane resulting from water influx, which might be sensed by MS ion channels (Kung, 2005). In plants, the molecular base of MS channel activities remains to be elucidated, but is thought to involve calcium influx (Jaffe *et al.*, 2002). However, neither Gd^{3+} ions, inhibitors of MS calcium channels, nor the calcium chelator EGTA, had any significant effect on the L_p values (Fig. 3.2 B, p.40), consistent with previous work on guard cell protoplasts, where changes of PM surface (monitored via membrane capacitance) in response to osmotic stimuli were also found to be independent of calcium (Homann, 1998). The cytoskeletal regulation of L_p is therefore unlikely to be caused by cytoskeletal gating of the sensory

calcium channels. Since L_p records a combination of net water influx and plasma membrane incorporation, the cytoskeletal effect on swelling might be caused by a modulation of mass flux, for instance of net water influx. Therefore the organization of actin is manipulated by optochemical engineering in isotonic conditions and could by this treatment induce a symmetry break with a local bulging at the illuminated side (please refer to Appendix 5.9, p.122). Since pressure is non-directional, the amplitude of this bulging is limited, but clearly the effect on actin is not global, but locally confined (consistent with published evidence on walled cells; (Kusaka *et al.*, 2009). Under these conditions, net influx of water should be zero. Therefore, it is concluded that the cytoskeletal effect on volume increase is independent of ion channel and water channel activities.

Intensive expansion ability of PMs is confined to ~2 % (Wolfe *et al.*, 1985) and occurred only during the first few seconds after being transferred into hypoosmotic medium. It is therefore tested, whether L_p can be modulated by altering the extensive properties of the membrane. Treatment with benzyl alcohol (BA) which increases the fluidity of lipid bilayers (Sangwan *et al.*, 2001) did not cause any significant change of L_p (Fig. 3.2 B, p.40). Since the membrane fluidizer BA did not alter L_p, a potential activity of both butanols used in our experiments as membrane fluidizers is obviously not helpful to explain, why they promote L_p. This promotion is more probably linked with their enzymatic activities. In contrast, DMSO, which has been used as membrane stabilizer in a study on cold adaptation of plant cells (Sangwan *et al.*, 2001), increased L_p values. However, DMSO is not only stabilizing membranes, but also causes membrane permeabilization, which in the context of our experiment increases the water permeability of the membrane (Gurtovenko & Anwar, 2007). It is therefore not surprising that increased L_p values were observed after treatment with DMSO. Thus, our data do not support a model, where intensive changes of the membrane play any role for the observed swelling response.

Thus, the volume increase must be supported by incorporation of additional membrane material or unfolding of membrane invaginations. Direct tracking of endocytosis is limited by the small size of the vesicles that are smaller than the resolution limit for light microscopy. Therefore, the relative changes in the intensity of the membrane dye FM4-64 were quantified to monitor membrane dynamics during hypo- and hypertonic stress. The data indicated that new membrane material was inserted into the expanding PM during hypotonic stress, whereas membrane material contracted during hypertonic stress. The role of the cytoskeleton in this process might be twofold: either mere mechanic stabilization of the membrane leads to a resisting tension. Alternatively, the cytoskeleton might control the mobilization of membrane resources during swelling. In this functional context, the cytoskeleton might either convey the transport of membrane material to the membrane (stimulating function), or constrain the release of the material during the integration itself (impeding function). When osmotic tension exceeds the resistance tension, and if no more resources of membrane material can be mobilized, this would lead to protoplast lysis. The situation for microtubules seems to be straightforward. L_p values increase was observed after treatment with the microtubule-eliminating agent Oryzalin, and decrease after stabilization of microtubules by Taxol (Fig. 3.2 A, p.40). Activation of phospholipase D by *n*-butanol increases L_p, as to be expected from microtubule detachment from the membrane (Fig. 3.2 B, p.40). This activity seems to be independent of PA synthesis by phospholipase D, since *sec*-butanol is as effective as *n*-butanol. The *V. riparia* cell line was somewhat less responsive to the microtubule drugs Oryzalin and Taxol with respect to L_p (Fig. 3.2 A, p.40). Since the effect of both drugs depends on the innate turnover of microtubules, this indicates that microtubules are less dynamic in *V. riparia* as compared to *V. rupestris*, which is supported by previous findings of a higher degree of tyrosinylated α-tubulin, a marker for cycling tubulin (Qiao *et al.*, 2010). Microtubules might therefore simply impede membrane material from being inserted into the expanding membrane.

The role of actin seems to be more complex. Here, elimination of actin by Latrunculin B caused an increase of L_p values. However, a mild treatment with Phalloidin, a drug suppressing disassembly of F-actin does not cause a decrease, but an increase of L_p as well, which although not statistically significant, worth paying attention. This might be linked with differences in the cellular target sites of the two drugs seems to differ (Fig. 3.3 GF-11 cell line): Latrunculin B depleted membrane associated actin and suppressed the repartitioning of actin towards the membrane observed in hypoosmotic conditions. Phalloidin, however mainly targeted to the perinuclear actin cables. A stimulating role of actin stability is consistent with previous findings, where the same concentration of Phalloidin (Berghofer *et al.*, 2009) or inducible expression of an actin-binding domain (Hohenberger *et al.*, 2011) stabilized the membrane against electric permeabilization. In *V. riparia*, L_p values were more responsive to actin drugs as compared to *V. rupestris*, indicating a higher innate turnover of submembraneous actin in *V. riparia* over *V. rupestris*. These observations suggest a positive role of actin stability for swelling, which might involve actin-driven transport of membrane resources towards the insertion sites.

Here the roles of actin filaments and microtubules for regulatory volume increases were dissected by monitoring apparent water permeability values after pharmacological manipulation of different cellular targets. The roles of calcium channel activity or extensive changes of membrane extensibility for the swelling response were excluded. It is concluded that a dynamic population of microtubules impedes the integration of membrane material into the expanding membrane. This microtubule population can be controlled by activation of phospholipase D independently of PA synthesis. In contrast, a dynamic population of actin acts as positive regulator of protoplast swelling. Bundling of transvacuolar actin cables by the Harpin elicitor can block expansion, probably by merely mechanic tethering. Actin dynamicity can be upregulated by the plant hormone auxin (Wang & Nick, 1998). Using this phenomenon, it is demonstrated

that a localized protoplast expansion can be triggered even under isotonic conditions using optochemical engineering with caged auxin consistent with a model, where actin dynamicity supports the delivery of membrane resources into expanding membrane during hypotonic challenge (Fig. 4.1).

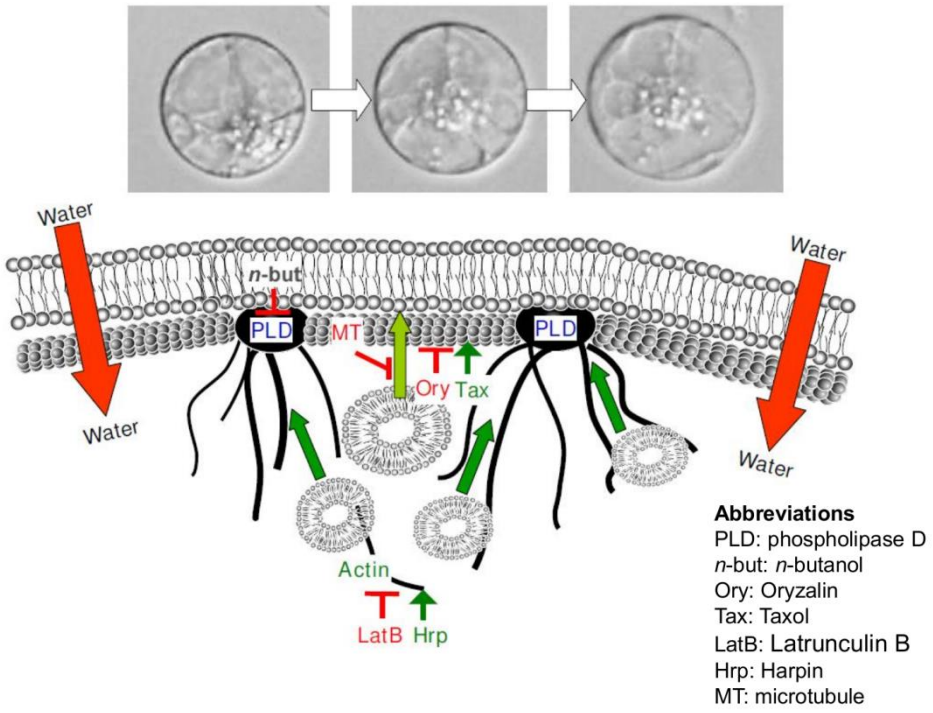

Fig. 4.1 Schematic illustration of how submembraneous cytoskeleton controls the release of intracellular membrane stores during regulatory volume change.

4.2 Could NtTPC1A and NtMCA2 function as MS ion channels?

The most important feature of an MS channel is its ability to mediate ion flux upon force triggered switch to an opened state. Two (probably simplistic) two-state models for MS ion channels gating in plants have been proposed and reviewed by Monshausen & Haswell (2013). The first one is the so called ‘intrinsic’ model, proposing that the mechanical force is transmitted to the channel directly through the lipid bilayer in which the MS channel resides and operate in a similar way as the bacteria MS ion channels. Increased membrane tension leads to an increased pulling force exerted upon the channel by the lipid bilayers and

because of their limited intensive expansion property, these alterations induce a conformational change in the channel and leads to the switch of the channel to the opening state (Fig. 4.2 A 1). Alternatively is the 'trapdoor' model, which suggests that the mechanical force is transmitted to the channel via links to other subcellular structures such as the cell wall or the cytoskeletons. Opening of the trapdoor allows ions to gain access to the channel pore (Fig. 4.2 A 2). As soon as the MS channel opened, the release of osmolytes, or the influx of the ions including secondary messenger Ca^{2+}, or the depolarization of the PM can be induced which can trigger downstream signaling events (Monshausen & Haswell, 2013). In both cases, the gating has a rapid time-course of channel activation. When compare the models from Brierley (2010) with these from Monshausen & Haswell (2013), another two scenarios seemed worth mentioning as well. The first one is the indirect gating of MS ion channels via adjacent MS proteins that are not directly connected to the putative channel (Fig. 4.2 B 1) which hints for a sensing complex. In the other scenario, mechanical force triggers the release of diffusible second messenger molecules allowing channel activation and ionic in flux (Fig. 4.2 B 2). Except in the 'intrinsic' model, the ion channels in all other three hypothetic mechanisms only being counted as MS channels are because they are capable of responding to mechanical stimuli indirectly but not *per se* mechano-gated ion channels which is different from the MS ion channels found in *E. coli* (Christensen & Corey, 2007).

The well-studied bacterial MS channels from *E. coli* (Booth *et al.*, 2007) has for a long time served as a dogma of MS channels as what criteria should a channel protein meet and how it should behave in response to mechanical stimuli in order to qualify as genuine MS ion channel (Arnadottir & Chalfie, 2010). Many candidates for MS channels have been identified across a wide range of organisms and yet few of them really meet all the criteria set for MS channels in *E. coli* (Arnadottir & Chalfie, 2010), not in mammalians, not even their homologs in plants. *Arabidopsis* plants, in which all root expressed *MSLs* (msl4/5/6/9/10) were

simultaneously knocked out showed no evident phenotype. The physiological responses to osmotic as well as mechanical stresses remained intact in this quintuple knockout mutant as well (Haswell *et al.*, 2008). MSL9 and MSL10 have higher permeability to Cl^- than Ca^{2+}, and therefore the likelihood of MSL9 and MSL10 contributing to mechanical stress- or gravistimulation-induced $[Ca^{2+}]_{cyt}$ increases is small (Haswell *et al.*, 2008). Neither conclusive roles in osmoregulation nor contribution to calcium homeostasis has been verified for plant MSLs based on information available so far. And this leads to the speculation that perhaps organisms composed of a large number of differentiated cells which are structurally significant different from *E. coli* indeed abandoned such simple membrane tension gated channels and evolved new mechanisms with 'upgraded' MS channels for sensing mechanical forces. With these four hypotheses for the gating mechanisms of putative MS ion channels in mind, the possibility of NtMCA2 and NtTPC1A investigated in this study being MS channels will be discussed.

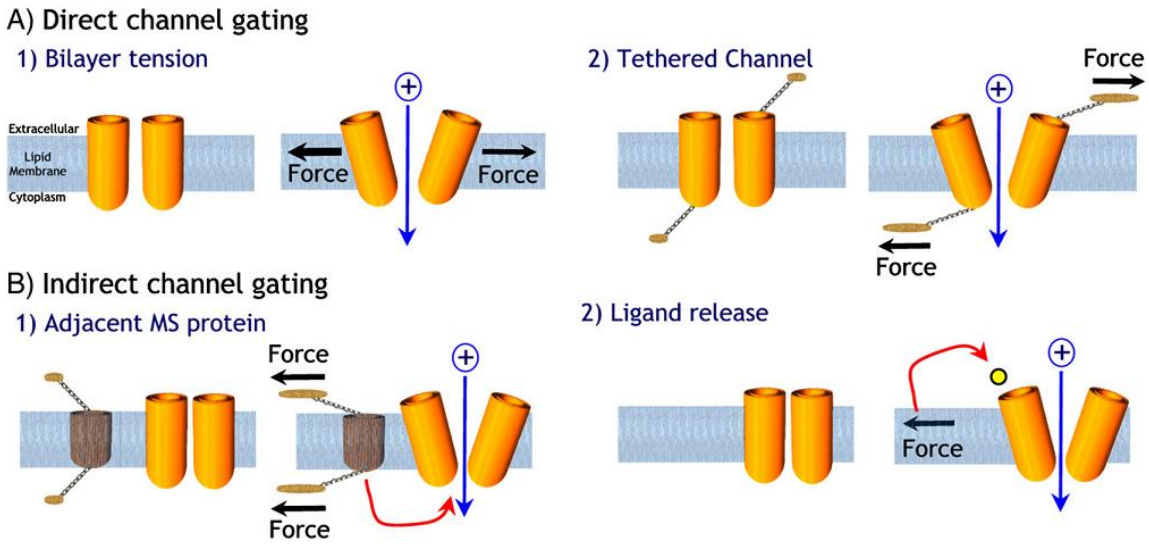

Fig. 4.2 Proposed models by which a putative mechanotransduction channel is gated by mechanical stimuli. Putative mechanotransduction channels can be activated either directly (A) or indirectly (B) by mechanical force (black arrows) cited from (Brierley, 2010).

4.2.1 What are the indications from the supra-molecular structural aspect?

In this study, the N-terminal fusion proteins of NtMCA2 have been shown to reside predominantly at the PM in tobacco BY-2 suspension cells and punctuated remains were also found in Hechtian Strands after plasmolysis which was similar as reported by Kurusu *et al.* (2012c). Spinning disk microscopy showed that GFP-NtMCA2 fusion proteins often form concentrated dots on the PM indicating the existence of a bigger complex for mechanosensing like the focal adhesions in mammalian cells (Geiger *et al.*, 2009) and its counterparts in plants, the plasmalemmal reticulum (Gens *et al.*, 2000; Pickard, 2008). What also has been found is that NtMCA2 undergoes constitutive cycling and that this process is probably cell cycle dependent. Although specific cellular function can be achieved through regulating the expression level of certain membrane protein encoding genes, this type of regulation is rather slow and normally involves either the *de novo* synthesis of proteins or changes of degradation rate of existing proteins. This specialized trafficking becomes a more efficient way of modulation for membrane proteins. The constitutive cycling of a variety of transmembrane proteins such as receptors, channels and transporters has recently been directly demonstrated in a wide range of cell types (Royle & Murrell-Lagnado, 2003), among which the molecular mechanism for constitutive cycling of auxin efflux carrier PIN proteins is well understood (Grunewald & Friml, 2010). Actin has been suggested to be implicated in the constitutive cycling of PINs (Geldner *et al.*, 2001; Kleine-Vehn *et al.*, 2008) which holds true for NtMCA2 as well. The coiled-coil segment predicted for NtMCAs has been suggested to be used for protein-protein interactions by Kurusu *et al.* (2012c). Two N-glycosylation sites have also been predicted flanking the coiled-coil segment using Proscan (see Appendix 5.2.2, p.117, for predicted N-glycosylation sites which are shaded in grey background). The N-glycosylation sites is a commonly used post-translational modification which plays important roles in cell adhesion (Varki, 1993). The probability of being a part of a mechanical force sensing complex, constitutive cycling as well as

potential interaction with the cell wall matrix indicated by microscopic studies and *in silico* analysis all hints an MCA included sensing device which is highly dynamic and would be very useful for plant cells whose positions are fixed within the plant tissue and have to deal with forces of various intensity and directionality. Actually, the constant assembly, disassembly and movement of molecular components for mechanosensing, such as the PM, cell-adhesion complexes and the CTK, even when ostensibly stable, are important for mechanosensing in mammalian cells. And the dynamics of these cellular mechanotransducers can help to understand the timescale of various mechanoresponses (Hoffman *et al.*, 2011).

It is clearly shown in this study that NtTPC1A-GFP fusion proteins located at the VM and various types of vacuole structures in BY-2 cells which are probably linked to designated biological functions were revealed (Oda *et al.*, 2009). And this finding settles the question about the localization of NtTPC1A in tobacco cells. The vacuole structure has been shown to depend heavily on actin filaments for it organization as well as dynamicity. The *AtTPC1* is firstly cloned because their structural similarities to the rat *TPC1* which forms of the α_1 subunit of the L-type voltage-gated calcium channels in mammalian cells. The α_1 subunit of the L-type voltage-gated calcium channels in mammalian cells is the pore-forming subunit (Catterall, 2000) with 24 transmembrane segments. In contrast, the TPCs from plant have only 12 transmembrane segments. The result from this study showing decreased intracellular calcium level in the NtTPC1A overexpression cell line leads to the speculation that TPC1s in plants function as at least dimers *in vivo*. The transmembrane segment 6 forms the binding site for the pore-blocking Ca^{2+} antagonists, such as dihydropyridine (DHP), phenylalkylamine (PAA) and benzothiazepine in mammalians. By using fluorescent labeled DHP, it was found that this conventional L-type calcium channel blocker is not colocalized with the NtTPC1A-RFP fusion proteins (data not show) indicating that NtTPC1A is somehow different from the pore-forming α_1 subunit in mammalian cells with

respect to the binding of DHP despite the overall structural similarities predicted.

Another more concerned issue here is if such a VM localized putative voltage-gated putative calcium permeable channel could play a role in mechanosensing. When it comes to MS ion channels, it is often linked with PM embedded ion channels because of their advantages in being at the interphase where forces from both internal and external converge. However, this does not contradict the fact the endomembranes are also subjected to mechanical forces due to the heterogeneity of subcellular organelles, the flow of ions and osmolytes between organelles and cytoplasm as well as the various intracellular transportation processes, and are consequently also in need of mechanosensitivity. The vacuole accounts for over 80-90 % of the cell volume in mature somatic cells in plant and participates in storage of proteins, ions, and secondary metabolites, protein degradation, autophagy, defense responses, programmed cell death, the adjustment of osmotic pressure, as well as maintenance of turgor pressure (Oda *et al.*, 2009). Among these, many processes requires the sensing of mechanical forces. In fact, *YVC1P*, a TRP-like channel gene, encodes a distant member of the TRP superfamily is located at the limiting membrane of intracellular vacuoles in yeast (Palmer *et al.*, 2001; Denis & Cyert, 2002). The YVC1P channel is activated not only by increased cytoplasmic Ca^{2+} but also by increasing hydrostatic pressure across the vacuolar membrane (Zhou *et al.*, 2003) which in other words is mechanosensitive. Meanwhile, the MS channels reside on the endoplasmic reticulum membrane are also suggested to mediate gravity-sensing in *Arabidopsis* columella cells (Leitz *et al.*, 2009). Other than that, what prompts the role of NtTPC1A as an MS ion channel is the finding that native L-type calcium current in dissociated human smooth muscle cells can be modulated by mechanical perturbation (Farrugia *et al.*, 1999; Holm *et al.*, 2000). Heterologous expressed α_{1c} subunit of this L-type calcium channel exhibits MS behavior similar to the native channel and the mechanosensitivity resides within the pore forming α_{1c} subunit (Lyford *et al.*, 2002). Due to the general

structural resemblance as well as the functional requirements, it is reasonable to infer that NtTPC1A may also able to respond to mechanical stimuli besides membrane potential. And this inference has been supported by (Lyford *et al.*, 2002) who suggested that L-type voltage-gated calcium channel is also MS. The authors proposed that the initial increase in calcium flux of the L-type calcium channel via mechanoactivation will stimulates its own activity and/or other signaling components and resulting in a more effective signal transduction.

4.2.2 What are the evidences from the functional perspective?

So far, the possibilities of the two channels being MS from the supra-molecular structural point of view have been discussed. In the following, the functional links of these two channels to mechanosensitivity will be attempted. Both overexpression of GFP-NtMCA2 and NtTPC1A-GFP led to decreased total intracellular calcium contents in comparison to the WT under normal cultivation condition determined by AAS. This decrease can be rescued by adding calcium supplement to the cultivation medium or further reduced by addition of magnesium. An explanation that accounts for the decreased intracellular calcium contents in both overexpression cell lines is that both NtMCA2 and NtTPC1A probably form multimeric complexes either homogeneously or heterogeneously to comprise functional channels *in vivo* which is quite common for channel proteins. For example, the well characterized MS channel protein of *E. coli*, the MscL forms a homohexamer complex (Blount *et al.*, 1996). Not even a single known mammalian MS channel candidates functions as monomer (Martinac, 2014). A very recent publication from Shigematsu *et al.* (2014) showed that purified AtMCA2 formed a tetramer in a detergent-solubilized state which supports the speculation that NtMCA2 functions as multimers *in vivo*. The voltage-gated calcium channels which NtTPC1s bear structural similarity to are oligomeric complexes composed of four different subunits (Hofmann *et al.*, 1994). Due to the high probability of multimerization, dominant negative effect caused by

overexpression could lead to decreased uptake in the NtMCA2 ox cell line. Excessive release of calcium in to the cytosol could be caused in NtTPC1A ox cell line due to the overexpression of a pore-forming α_1- subunit together with the necessity to maintain the required low cytosolic calcium level (Reddy, 2001) leading to the loss of intracellular calcium in this overexpression cell line. However, homologously overexpressing GFP-NtMCA2 fusion has been reported to enhance calcium uptake in BY-2 cells analyzed via calcium isotope (Kurusu *et al.*, 2012c). This discrepancy is likely due to the results of a short term accumulation (up to 30 min) (Kurusu *et al.*, 2012c) and a long term one (5 day long) in this study. It needs to be noticed that both the increase as well as the decrease in intracellular calcium contents were not very distinct, which speaks for a robust and intricate system which plants use to maintain their intracellular calcium level (Reddy & Reddy, 2004).

Mechanical forces come from external have often been described as disturbances or stresses and to which the plants have to respond by adjusting their growth and development as well as modulate the mechanical properties of the load-bearing tissues or organs. The mechanical force generated internally is intrinsic to plants which is experienced by each living cell at all levels and has deeply influenced plant architecture (Bastien *et al.*, 2013), organogenesis (Potocka *et al.*, 2011; Lucas *et al.*, 2013), cell division (Lynch & Lintilhac, 1997), organization of the MT network (Wymer *et al.*, 1996; Hejnowicz *et al.*, 2000; Uyttewaal *et al.*, 2012) and so on. The most primary and fundamental internal mechanical stress experienced by all living plant cells is turgor pressure which is an important contributor to the structural stability of the plant and the primal driving force for cellular growth and expansion. Together with regulated cell-wall extensibility, they play a critical role in determining plant cell size and shape. For this reason, the cell sizes are carefully examined in both overexpression cell lines. The results revealed inhibition in cell elongation in both overexpression cell lines which is indicative of an interaction between components involving in calcium

signaling and sensing internal mechanical force being manifested in cell elongation growth. The collective effort between SA ion channels, calcium signaling and cell wall mechanics in modulating cell growth has been intensively studied in tip growth systems. Activation of SA ion channels caused by increased membrane tension due to increased turgor pressure, followed by a transient spike in cytosolic calcium level which further activates proton influx carriers and cell wall alkalinization and help to stabilize the newly formed cell wall was proposed as a model for how these components are contributing to the modulation of tip growth (Choi *et al.*, 2011). The increased cytosolic calcium level also promotes ROS production which not only raises the rigidity of the cell wall but also triggers ROS-dependent signaling transduction when enters the cytosol via aquaporins (Choi *et al.*, 2011). Whether this delicately maintained balance between driving force from turgor and inhibitory force from the cell wall for cell growth through the above mentioned molecular players is universal for all cell types in plants needs further investigation. There is evidence indicating that cytosolic calcium level (Hardham *et al.*, 2008; Monshausen *et al.*, 2009), pH and ROS (Yahraus *et al.*, 1995; Gus-Mayer *et al.*, 1998; Monshausen *et al.*, 2009) are probably common elements which are found both in mediating turgor-driven expansion as well as response of cells to mechanical agitation. This conserved functional cassette capable of converting membrane tension into Ca^{2+}, pH and ROS has been suggested to be evolved originally for responding to membrane tension driven by turgor expansion to coordinate growth with cell wall properties are also implicated in tip growth (Choi *et al.*, 2011) as well as hinted in stress response (Torres & Dangl, 2005). Both overexpression of the PM localized NtMCA2 as well as the VM localized NtTPC1A lead to significant inhibited elongation growth in BY-2 cells under normal growth conditions indicating that the operation of the above mentioned functional cassette is applicable in BY-2 suspension cells which are non-specialized somatic cells and the interaction between these molecular players is probably compromised by overexpression. Cortical microtubules, a plant-specific cytoskeletal array which is responsible for the directional expansion

of plant cell by providing molecular rails for cellulose synthases to move along, is probably deeply implicated in this process. The capability of the NtMCA2 overexpression cell line to maintain it intracellular calcium level and at the same time exclude sodium ions outside of the cells under NaCl stress indicates the duality of this channel protein. It also supports that calcium channels are common element shared by both growth regulation and salt stress. Whether the overexpressed channels are functioning as primary mechanosensors or downstream components of the mechanotransduction pathway is however not clear.

4.3 A dynamic tensegrial-based model for mechanosensing in plants

Bacterial MS channels from *E. coli* has been taken as examples of MS channels which are later shown to be used commonly in prokaryotes for maintaining intracellular composition in response to osmotic stresses (Martinac, 2001). They act more like safety valves instead of sensors considering that MscL only becomes stretch sensitive until the membrane tension becomes near-lytic (Batiza *et al.*, 1999). The threat of cellular lysis in response to hypotonic stress does not exist in mammalian cells or walled plants *in vivo*. Animals rely on mechanosensitive processes for a wide array of regulatory and sensory tasks, such as hearing, touch, balance, blood flow regulation, and cardiac function (Sachs & Morris, 1998) and plants depend on them for morphogenesis, growth, organogenesis, gravitropism, proprioception and so on (Sachs & Morris, 1998; Mirabet *et al.*, 2011; Bastien *et al.*, 2013). It is therefore not hard to imagine that mechanoperception relies on more complicate and diverse types of transducer molecules and various mechanisms in multicellular organisms due to more complex structural and functional demands. And this is supported by the study of more complicated organism *C. elegans* (Chalfie, 1997; Tavernarakis & Driscoll, 1997). The available molecular data from human studies also suggest a

multiplicity of structural designs and mechanisms of mechanoperception (Tsunozaki & Bautista, 2009; Brierley, 2010; Del Valle *et al.*, 2012).

Other than the demands for more diverse and precisely regulated mechanosensory device, the simplicity of the gating mechanism of bacterial MS channels makes such kind of channels along mechanotransducers in multicellular organisms questionable. The direct interaction between the transmembrane domain of the channel and the lipid bilayer required by MS channels characterized in prokaryotes has been argued to be an unavoidable consequence of inserting a channel into the membrane which is suggested to be common to all membrane-spanning, pore-forming proteins (Gu *et al.*, 2001). The authors also suggest that being inherently susceptible to lipid bilayer tension is common for multiconformational membrane proteins, which is not a carefully designed property rather an inevitable concomitant. What's more, the turgor pressure pushing the PM against the CW in plants under normal growth condition imposes extra challenges for lateral tension on the membrane to be delivered to the SA channels, which hardly supports the sensing of minute changes in membrane geometry.

Meanwhile, the role of the cell wall as an indispensable component of the plant cell with its resemblance to the mammalian ECM in mechanosensing should definitely be taken into consideration. Mapping the viscoelasticity and elasticity in living meristems using atomic force microscopy (AFM) revealed pectin demethylesterification at the site of incipient organs prior to the formation of new organs in shoot primordia (Peaucelle *et al.*, 2011) which indicates that biochemistry and mechanics of cell walls is involved in organogenesis. Organization of crystalline cellulose studied in poplar wood revealed that the formation of tension wood which increases mechanical resistance of the stem is associated with increased lattice spacing of cellulose (Clair *et al.*, 2011).

Additionally, accumulating evidences showed that the plant cytoskeletons respond to both biotic as well as abiotic stresses. The assembly and disassembly of the actin network is critical to the formation of membrane protrusions, such as filopodia, ruffles and lamellipodia as well as cell motility in animals (Shlomovitz & Gov, 2008; Mogilner & Keren, 2009). Likewise, previous work of (Hohenberger *et al.*, 2011) also suggested that tubulovesicular membrane folds or invaginations increase membrane surface and might be structurally maintained by actin filaments in plant cells. This hints the involvement of actin filaments in membrane topology and thereby influencing the mechanical properties of the PM. Cortical microtubules (MTs) and cell division planes of tobacco protoplasts embedded in agarose were found to be aligned perpendicular to the force generated by centrifugation and this phenomenon is eliminated by anti-microtubule drugs which led Wymer *et al.* (1996) to propose the role of MTs as mechanosensor. Various evidences also suggested the role of MTs in gravity sensing (Schwuchow *et al.*, 1990; Himmelspach & Nick, 2001). Nick *et al*. (1990) use auxin-mediated movement of cMTs from the longitudinal to the transverse direction to explain phototropic curvature as well as gravitropic bending of maize coleoptiles. Besides that, a rapid, but transient partial disassembly of MTs in cold-tolerant wheat cultivars was observed to precede the formation of cold-stable microtubules and the recovery of growth rate (Abdrakhamanova *et al.*, 2003). The roles of MTs in mechano-, gravi- and cold- sensing were summarized in Nick (2008). The discovery of kinesins with calponin-homology (CH) domain which can bind both cytoskeleton elements (Preuss *et al.*, 2004; Frey *et al.*, 2009; Xu *et al.*, 2009; Klotz & Nick, 2012) provide physical entity which connects the rigid network of microtubules with the tensile actin filaments and support the formation of a dynamic sensory tensegrity in plants.

Due to the considerations about the limitations of the bacteria MS channel based ‘intrinsic’ model mentioned above, the tensegrial nature of the plant CW and CTKs as well as evidences suggesting their roles in mechanosensing, a model in

which a dynamic tensegrial-based entity employing CTK tethered ion channels together with various associated proteins as a mechanism of mechanosensing in plants is proposed. The ion channels in this model do not necessarily need to be mechano-gated *per se*, like the MscL from *E. coli*, because the sensory function is undertaken by this sensory tensegrity. The advantages of such a mechanism in plant mechanoperception include: (1) first and foremost, a tensegrial structure guarantees the effective convergence as well as amplification of mechanical stimuli which help to conquer the obstacles faced by plants in sensing mechanical stimuli (2) The tensegrial structure ensures the rapid transmission of mechanical stimuli over a long distance on the tissue level, and meanwhile supports direct influence on gene expression on the single cell level. (3) The sensory CTK tensegrity could function as a central integrator (Nick, 2011) of various stimuli for an integrated response under complicated circumstances in order to yield maximum benefits for the whole plant. (4) Ion channels linked to the tensegrial structure provide diverse mechanisms for activation, such as directly tethered to the CTK/CW or via CTK/CW associated proteins or indirect activation via adjacent MS proteins within the mechanosensing complex. (5) Submembraneous CTK modulating the constraining forces on the lipid bilayer affects how mechanical stimuli are perceive by the membrane embedded proteins which add another layer of regulation in mechanosensing. (6) The tensegrial cell wall matrix could provide more possibilities of distinguishing mechanical stimuli of distinct features due to the large amount of wall associated sensory proteins (Ringli, 2010). (7) The dynamic link between different components maximizes the flexibility of this sensory tensegrity which can be rapidly reset to a new balanced state after mechanical disturbance. A schematic illustration of this dynamic tensegrial network based-mechanosensing entity can be seen in Fig. 4.4 in which the current views as well as molecular players known are integrated.

Fig. 4.3 A schematic illustration of a tensegrial-based entity for mechanosensing in plants. The cell wall tensegrial matrix (CWM) is mainly composed of cellulose microfibril (CM), the main load-bearing elements, cross-linked to a matrix consisting of hemicellulose (HC) and pectin,

dispersed with structural proteins such as extensins as well as other soluble proteins (SP). The CTK sensory tensegrity made of AFs and MTs interconnected via linker proteins, such as KCHs (Nick, 2011). For clarity, cAFs, cMTs and CTKs are only illustrated on the left side of the figure. Cell wall associated sensory proteins speculated to be implicated in mechanosensing including members of the WAKs (wall-associated kinases) subfamily of the RLKs family (receptor-like kinases), LecRK (L-type lectin RLKs with ability to bind to RGD (arginine-glycine-aspartic acid) tripeptides) from the RLKs family and THE1 (THESEUS 1, a member of the subfamily of *Catharanthus roseus* Protein Kinase1-Like receptor kinases) (Ringli, 2010). Membrane embedded MS ion channels with known molecular identities include PM located MSLs (MscS-like) and MCAs (MID1-Complementing Activity 1), VM localized TPC1s (Two Pore Channel 1). Other MS proteins or channels tether to the CTKs and/or CWM forming bigger signaling complexes speculated to be involved in mechanosensing (Monshausen & Gilroy, 2009) are also demonstrated (MS complex).

This tensegrial-based mechanosensing entity in plants operates in multiple levels including: 1) the cortical cytoskeletons modulate the PM topology as well as mechanics and are involved in cell volume control during osmotic changes. 2) Transmission and convergence of mechanical stimuli through the cell wall tensegrity and initiation of mechanical signal transduction through various cell wall associated sensory proteins likely use the kinase-dependent signaling pathway. 3) The CTK tensegrity senses and transmits mechanical stimuli directly to the nucleus through a nuclear envelop (NE) anchor (KASH-SUN combinations in mammalians) and impacts gene expression (Wang *et al.*, 2009; Starr & Fridolfsson, 2010). 4) The CTK tensegrity triggers mechanical signal transduction via direct tether to or indirect link with ion channels, probably calcium permeable channels, embedded in the PM, VM or other endomembranes. Actually, connections between the cytoskeletons and ion channels have been proposed to be a mechanism which contribute to mechanosensory transduction in animal cells in a very recent review (Martinac, 2014)

A distinct feature of this tensegrial-based mechanosensing entity is its dynamicity. The dynamic composition of the cell wall matrix is tightly regulated over time down to the subcellular cell wall microdomains within a single cell. It depends on various informations gathered by different types of cell wall monitoring proteins

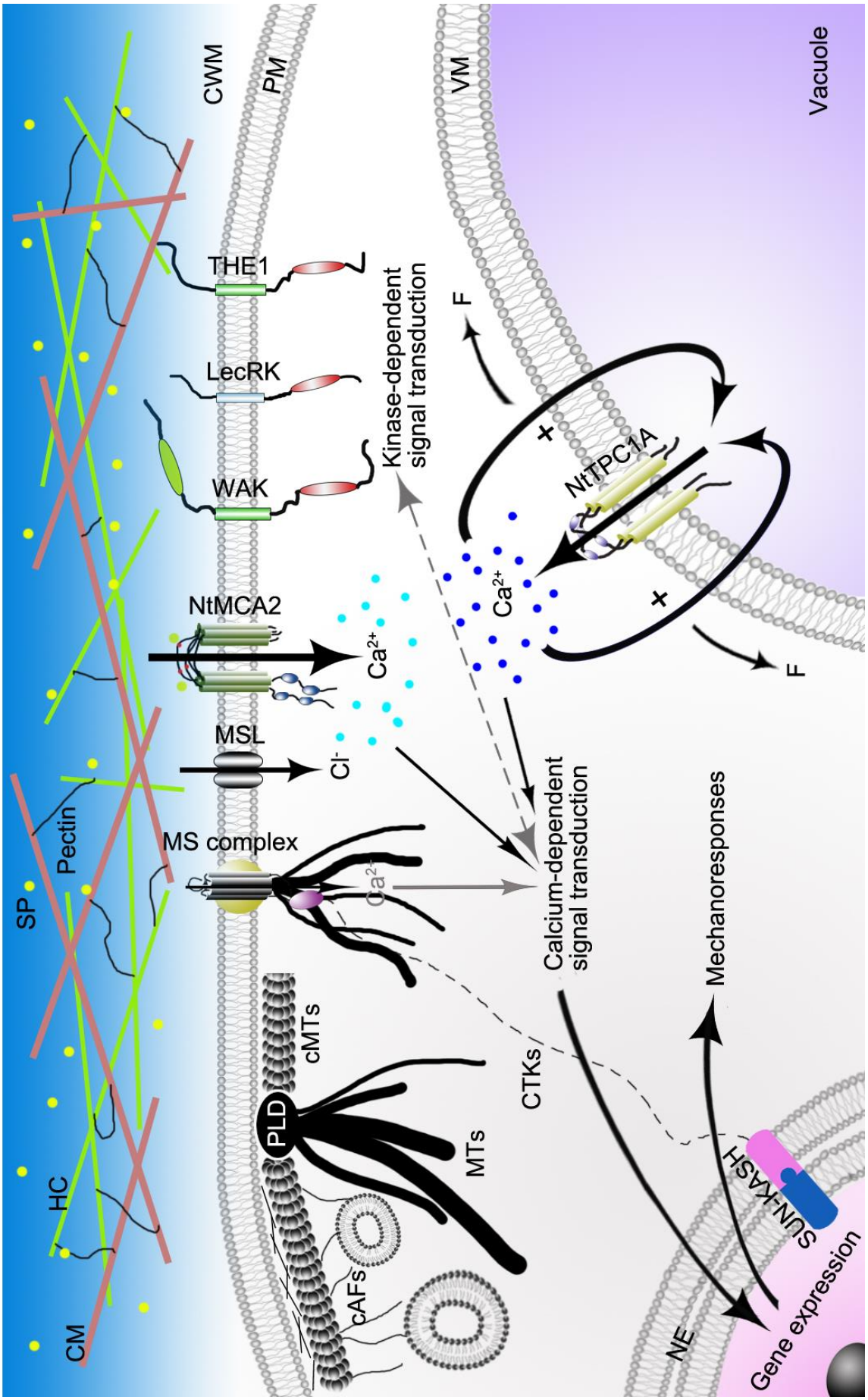
CWM
PM
VM
Vacuole
THE1
LecRK
WAK
Kinase-dependent signal transduction
F
NtTPC1A
+
+
F
NtMCA2
Ca2+
Ca2+
MSL
Cl-
MS complex
Ca2+
Pectin
SP
Calcium-dependent signal transduction
Mechanoresponses
cMTs
PLD
CTKs
MTs
HC
CM
cAFs
SUN-KASH
NE
Gene expression

and affects the mechanical properties of the cell wall. The intrinsic remodeling of the CTK allows a highly dynamic tensegrity and rapid reset of a new balanced state of the tensegrity after disturbance. These two dynamic tensegrial structures provide the foundation for dynamic mechanotransduction. The dynamic recruiting of linker proteins which connects the AFs and MTs as well as CTKs with various ion channels provide the possibility for differentiate spatiotemporal responses to the same mechanical stimulus even within the same cell and becomes the cornerstone of dynamic mechanotransduction. In combination with various downstream signaling pathways, such as the kinase- and calcium- dependent signaling pathways, are capable of mediating diverse mechanoresponses. Hoffmann *et al.* (2011) also proposed the cellular mechanotransduction in mammalian cells is taking place under a dynamic context considering that all the potential molecular players involved are undergoing assembly, disassembly and movement constantly, even when apparently stable. This dynamic tensegrial-based mechanosensing entity not only accomplishes mechanoresponses to stimuli of different time scale, amplitude, duration with precision, but also allows an integrated response considering the emerging role of the CTKs as a central integrator (Nick, 2011).

4.4 Conclusion

The results from this study support the above proposed model from the following aspects: first of all, the role of the cortical cytoskeletons, mainly AFs, the core elements of the sensory tensegrity, in modulating PM mechanics by stabilizing as well as controlled releasing of submembraneous material which is demonstrated by quantifying protoplast expansion velocity. Secondly, overexpression of two selected putative calcium channels NtTPC1A and NtMCA2 in BY-2 cells causes altered responses to internal mechanical forces indicated by cellular growth as well as external stimuli suggested by salt stress which support that these two calcium channels are deeply involved in mechanosensing. Thirdly, the contrast

between the independency of expansion velocity on various approaches manipulating calcium content in the cell wall free protoplasts and the clear influence of overexpressing calcium channels on growth and osmotic stress in intact walled cells indicates the significant role of the cell wall as an indispensable component of the sensory tensegrity entity. The presence of the cell wall is important for the MS ion channel activity considering the potential link between NtMCA2 and the cell wall matrix. Lastly, the constitutive recycling of NtMCA2 supports its dynamic regulation mechanism and supports diverse ways of transducing mechanical stimuli. Finally, the probability of NtTPC1s functioning as a VM localized mechanosensitive voltage-gated channel added another aspect of mechanosensing in plants.

4.5 Outlook

The most convincing evidence demonstrating the intrinsic mechanosensitivity of MS channels is to use liposomal reconstitution of the purified MS channel candidates (Martinac *et al.*, 2010), which has been done for several MS channel proteins (Kloda *et al.*, 2007; Nomura *et al.*, 2012). However, this is only applicable when the mechanosensitivity of the channels does not rely on the involvement of CTK and/or CWM elements as well as the PM microdomains, which has been argued not to be the case for MS ion channels in multicellular eukaryotes. Consequently, the future researches shall concentrate on resolving how the MS channels are tethered to CWM and/or CTK as well as unraveling how the membrane and cell wall microdomains contribute to the mechanosensitivity of potential channels and linker proteins.

The verification of such a MS complex is a very huge project involving in the complete revelation of various molecular players involved and establishing their interacting relationships as well as assigning physiological function to these interactions. It will definitely face tremendous difficulties in practice due to the

large numbers of proteins involved as well as technological challenges. However, it should be dealt with one step at a time. Approaches are proposed in the following which could be used to verify the involvements of these two channels investigated in this study. The most important point which needs to be clarified is whether these overexpressed fluorescent protein-tagged NtMCA2 channels are still functionally unimpaired *in vivo.* This would help to: Firstly, resolve the discrepancy with regards to calcium uptake activity *in vivo* when NtMCA2 is overexpressed with and EGFP fused to its N-terminal. Secondly, understand whether a more complex and inherent environment is needed for the regulation of the mechanosensitivity of NtMCA2 since it is indicated to be partially functional when expressed in yeast. Ca^{2+} imaging relying on spinning disk fluorescence microscopy would help to answer these questions. Tetramerization had been show for AtMCA2 *in vitro* (Shigematsu *et al.*, 2014). Whether multimerization is required *in vivo* to form functional NtMCA2 channels has been suggested in this study and if so, heterogeneously or homogeneously. This can be resolved by fusing NtMCAs with fluorescent proteins of different colors and coexpress them *in vivo*. A very long helix has been predicted close to the N-terminal of this protein according to Predictprotein (58 AAs, shaded in grey background, see Appendix 5.2.2, p.117), which makes the role of this long helix very intriguing and a coiled-coil region was also predicted for protein interaction close to the N-terminal (Kurusu *et al.*, 2013). Whether these secondary structures are used for protein-protein interactions and the identities of the interacting proteins are very important for understanding the mechanisms of mechanosensitivity of this ion channel protein.

Electrophysiological studies using transgenic BY-2 cells and the non-transgenic cells can be used to determine the conductance of this channel and it could also tell if the N-terminal fusion version is functional. The idea of the VM-localized NtTPC1A being a mechanosensitive voltage-gated channels is an audacious one, however, not entirely groundless. The necessity of a VM located MS ion channel

as well as the possibility of voltage-gated ion channels being MS at the same time as elaborated above make this idea worth testing. Electrophysiological approach should be used to characterize NtTPC1A as a MS channel. Moreover, similar methods can be used to determine the oligomeric state of NtTPC1s.

Other than electrophysiological characterization, attention should also be concentrated on revealing the interaction between the ion channels and the CTKs. However, it should be aware that this interaction might be achieved via AFs or MTs associated proteins rather than directly. The linker between the components of this tensegrity should also be investigated under various types of stresses to understand the spatiotemporal regulation of mechanosensing. The possibility that these two channels function as downstream players of the mechanical signal transduction pathway instead of primary sensors cannot be excluded based on evidences available so far. Being able to show the role of ion channels as genuine mechanotransducers will be a huge step forward towards understanding the mechanisms of mechanoperception in plants. Many evidences suggest that to establish the link between ion channels, other MS proteins candidates and the CTK/CWM seems like a promising direction to go.

References

Abdrakhamanova A, Wang QY, Khokhlova L, Nick P. **2003.** Is microtubule disassembly a trigger for cold acclimation? *Plant Cell Physiol* **44:** 676-686.

Abramoff MD, Magalhaes PJ, Ram SJ. **2004.** Image processing with Image J. *Biophotonics International* **11:** 36-42.

Allen GJ, Sanders D. **1994.** Two voltage-gated, calcium release channels coreside in the vacuolar membrane of broad bean guard cells. *Plant Cell* **6:** 685-694.

Arnadottir J, Chalfie M. **2010.** Eukaryotic mechanosensitive channels. *Annu.Rev.Biophys.* **39:** 111-137.

Babourina O, Leonova T, Shabala S, Newman I. **2000.** Effect of sudden salt stress on ion fluxes in intact wheat suspension cells. *Annals of Botany* **85:** 759-767.

Baldwin KL, Strohm AK, Masson PH. **2013.** Gravity sensing and signal transduction in vascular plant primary roots. *Am.J.Bot.* **100:** 126-142.

Baluska F, Samaj J, Wojtaszek P, Volkmann D, Menzel D. **2003.** Cytoskeleton-plasma membrane-cell wall continuum in plants. Emerging links revisited. *Plant Physiol* **133:** 482-491.

Baluska F, Volkmann D, Menzel D. **2005.** Plant synapses: actin-based domains for cell-to-cell communication. *Trends Plant Sci.* **10:** 106-111.

Barritt G, Rychkov G. **2005.** TRPs as mechanosensitive channels. *Nat.Cell Biol.* **7:** 105-107.

Bastien R, Bohr T, Moulia B, Douady S. **2013.** Unifying model of shoot gravitropism reveals proprioception as a central feature of posture control in plants. *Proc.Natl.Acad.Sci.U.S.A* **110:** 755-760.

Batiza AF, Rayment I, Kung C. **1999.** Channel gate! Tension, leak and disclosure. *Structure.* **7:** R99-103.

Behrens HM, Gradmann D, Sievers A. **1985.** Membrane-potential responses following gravistimulation in roots of *Lepidium sativum L*. *Planta* **163:** 463-472.

Berger F, Taylor A, Brownlee C. **1994.** Cell fate determination by the cell wall in early *Fucus* development. *Science* **263:** 1421-1423.

Berghofer T, Eing C, Flickinger B, Hohenberger P, Wegner LH, Frey W, Nick P. **2009.** Nanosecond electric pulses trigger actin responses in plant cells. *Biochem.Biophys.Res.Commun.* **387:** 590-595.

Berrier C, Besnard M, Ajouz B, Coulombe A, Ghazi A. **1996.** Multiple mechanosensitive ion channels from *Escherichia coli*, activated at different thresholds of applied pressure. *J.Membr.Biol.* **151:** 175-187.

Bershadsky AD, Balaban NQ, Geiger B. **2003.** Adhesion-dependent cell mechanosensitivity. *Annu.Rev.Cell*

Dev.Biol. **19:** 677-695.

Blount P, Sukharev SI, Moe PC, Schroeder MJ, Guy HR, Kung C. **1996.** Membrane topology and multimeric structure of a mechanosensitive channel protein of *Escherichia coli*. *EMBO J.* **15:** 4798-4805.

Boonsirichai K, Guan C, Chen R, Masson PH. **2002.** Root gravitropism: an experimental tool to investigate basic cellular and molecular processes underlying mechanosensing and signal transmission in plants. *Annu.Rev.Plant Biol.* **53:** 421-447.

Booth IR, Edwards MD, Black S, Schumann U, Miller S. **2007.** Mechanosensitive channels in bacteria: signs of closure? *Nat.Rev.Microbiol.* **5:** 431-440.

Braam J. **2005.** In touch: plant responses to mechanical stimuli. *New Phytol.* **165:** 373-389.

Braam J, Davis RW. **1990.** Rain-, wind-, and touch-induced expression of calmodulin and calmodulin-related genes in *Arabidopsis*. *Cell* **60:** 357-364.

Brierley SM. **2010.** Molecular basis of mechanosensitivity. *Auton.Neurosci.* **153:** 58-68.

Brownlee C. **2002.** Role of the extracellular matrix in cell-cell signalling: paracrine paradigms. *Curr.Opin.Plant Biol* **5:** 396-401.

Buer CS, Weathers PJ, Swartzlander GA, Jr. 2000. Changes in Hechtian strands in cold-hardened cells measured by optical microsurgery. *Plant Physiol* **122:** 1365-1377.

Bukoreshtliev NV, Haase K, Pelling AE. **2013.** Mechanical cues in cellular signalling and communication. *Cell Tissue Res.* **352:** 77-94.

Buschmann H, Green P, Sambade A, Doonan JH, Lloyd CW. **2010.** Cytoskeletal dynamics in interphase, mitosis and cytokinesis analysed through *Agrobacterium*-mediated transient transformation of tobacco BY-2 cells. *New Phytol.*

Bushman W, Thompson JF, Vargas L, Landy A. **1985.** Control of directionality in lambda site specific recombination. *Science* **230:** 906-911.

Campanoni P, Blasius B, Nick P. **2003.** Auxin transport synchronizes the pattern of cell division in a tobacco cell line. *Plant Physiol* **133:** 1251-1260.

Canut H, Carrasco A, Galaud JP, Cassan C, Bouyssou H, Vita N, Ferrara P, Pont-Lezica R. **1998.** High affinity RGD-binding sites at the plasma membrane of *Arabidopsis thaliana* links the cell wall. *Plant J.* **16:** 63-71.

Carpaneto A, Ivashikina N, Levchenko V, Krol E, Jeworutzki E, Zhu JK, Hedrich R. **2007.** Cold transiently activates calcium-permeable channels in *Arabidopsis* mesophyll cells. *Plant Physiol* **143:** 487-494.

Carter C, Pan S, Zouhar J, Avila EL, Girke T, Raikhel NV. **2004.** The vegetative vacuole proteome of *Arabidopsis thaliana* reveals predicted and unexpected proteins. *Plant Cell* **16:** 3285-3303.

Catterall WA. **2000.** Structure and regulation of voltage-gated Ca^{2+} channels. *Annu.Rev.Cell Dev.Biol* **16:**

521-555.

Chalfie M. **1997.** A molecular model for mechanosensation in *Caenorhabditis elegans*. *Biological Bulletin, Vol.192 (1997) Key: citeulike:3278724* **192:** 130.

Chang X, Heene E, Qiao F, Nick P. **2011.** The phytoalexin resveratrol regulates the initiation of hypersensitive cell death in *Vitis* cell. *PLoS.One.* **6:** e26405.

Chehab EW, Eich E, Braam J. **2009.** Thigmomorphogenesis: a complex plant response to mechano-stimulation. *J.Exp.Bot.* **60:** 43-56.

Chen CS, Tan J, Tien J. **2004.** Mechanotransduction at cell-matrix and cell-cell contacts. *Annu.Rev.Biomed.Eng* **6:** 275-302.

Cheung AY, Wu HM. **2008.** Structural and signaling networks for the polar cell growth machinery in pollen tubes. *Annu.Rev.Plant Biol* **59:** 547-572.

Choi W-G, Swanson SJ, Gilroy S. **2011.** Calcium, mechanical signaling, and tip growth. In: Luan S, ed. *Coding and Decoding of Calcium Signals in Plants*. Springer Berlin Heidelberg, 41-61.

Christensen AP, Corey DP. **2007.** TRP channels in mechanosensation: direct or indirect activation? *Nat.Rev.Neurosci.* **8:** 510-521.

Clair B, Almeras T, Pilate G, Jullien D, Sugiyama J, Riekel C. **2011.** Maturation stress generation in poplar tension wood studied by synchrotron radiation microdiffraction. *Plant Physiol* **155:** 562-570.

Clark GB, Thompson G, Jr., Roux SJ. **2001.** Signal transduction mechanisms in plants: an overview. *Curr.Sci.* **80:** 170-177.

Corry B, Martinac B. **2008.** Bacterial mechanosensitive channels: experiment and theory. *Biochim.Biophys.Acta* **1778:** 1859-1870.

Cosgrove DJ. **2005.** Growth of the plant cell wall. *Nat.Rev.Mol.Cell Biol.* **6:** 850-861.

Coue M, Brenner SL, Spector I, Korn ED. **1987.** Inhibition of actin polymerization by latrunculin A. *FEBS Lett.* **213:** 316-318.

Cvrckova F. **2000.** Are plant formins integral membrane proteins? *Genome Biol* **1:** RESEARCH001.

Cvrckova F, Novotny M, Pickova D, Zarsky V. **2004.** Formin homology 2 domains occur in multiple contexts in angiosperms. *BMC.Genomics* **5:** 44.

Darwin C, Darwin F. **1880.** The Power of Movement in Plants. In: London, England: Murray, John.

Deeks MJ, Cvrckova F, Machesky LM, Mikitova V, Ketelaar T, Zarsky V, Davies B, Hussey PJ. **2005.** *Arabidopsis* group Ie formins localize to specific cell membrane domains, interact with actin-binding proteins and cause defects in cell expansion upon aberrant expression. *New Phytol.* **168:** 529-540.

Del Valle ME, Cobo T, Cobo JL, Vega JA. **2012.** Mechanosensory neurons, cutaneous mechanoreceptors, and putative mechanoproteins. *Microsc.Res.Tech.* **75:** 1033-1043.

Denis V, Cyert MS. **2002.** Internal Ca^{2+} release in yeast is triggered by hypertonic shock and mediated by a TRP channel homologue. *J.Cell Biol.* **156:** 29-34.

Derbyshire P, Findlay K, McCann MC, Roberts K. **2007.** Cell elongation in *Arabidopsis* hypocotyls involves dynamic changes in cell wall thickness. *J.Exp.Bot.* **58:** 2079-2089.

Dillen W, De Clercq J, Kapila J, Zambre M, Van Montagu M, Angenon G. **1997.** The effect of temperature on *Agrobacterium tumefaciens*-mediated gene transfer to plants. *The Plant Journal* **12:** 1459-1463.

Ding JP, Badot P-M, Pickard BG. **1993.** Aluminium and hydrogen ions inhibit a mechanosensory calcium-selective cation channel. *Aust.J Plant Physiol* **20:** 771-778.

Discher DE, Janmey P, Wang YL. **2005.** Tissue cells feel and respond to the stiffness of their substrate. *Science* **310:** 1139-1143.

Ditengou FA, Teale WD, Kochersperger P, Flittner KA, Kneuper I, van der Graaff E, Nziengui H, Pinosa F, Li X, Nitschke R, Laux T, Palme K. **2008.** Mechanical induction of lateral root initiation in *Arabidopsis thaliana*. *Proc.Natl.Acad.Sci.U.S.A* **105:** 18818-18823.

Dixit R, Cyr R. **2004.** The cortical microtubule array: from dynamics to organization. *Plant Cell* **16:** 2546-2552.

Ebihara L, Hall JE, MacDonald RC, McIntosh TJ, Simon SA. **1979.** Effect of benzyl alcohol on lipid bilayers. A comparisons of bilayer systems. *Biophys.J.* **28:** 185-196.

Engler AJ, Griffin MA, Sen S, Bonnemann CG, Sweeney HL, Discher DE. **2004.** Myotubes differentiate optimally on substrates with tissue-like stiffness: pathological implications for soft or stiff microenvironments. *J.Cell Biol.* **166:** 877-887.

Farrugia G, Holm AN, Rich A, Sarr MG, Szurszewski JH, Rae JL. **1999.** A mechanosensitive calcium channel in human intestinal smooth muscle cells. *Gastroenterology* **117:** 900-905.

Fasano JM, Massa GD, Gilroy S. **2002.** Ionic signaling in plant responses to gravity and touch. *J.Plant Growth Regul.* **21:** 71-88.

Finer J.J., Vain P., Jones M.W., McMullen M.D. 1992. Development of the particle inflow gun for DNA delivery to plant cells. *Plant Cell Reports* **11:** 323-328.

Forterre Y, Skotheim JM, Dumais J, Mahadevan L. **2005.** How the Venus flytrap snaps. *Nature* **433:** 421-425.

Freshour G, Clay RP, Fuller MS, Albersheim P, Darvill AG, Hahn MG. **1996.** Developmental and tissue-specific structural alterations of the cell-wall polysaccharides of *Arabidopsis thaliana* roots. *Plant Physiol* **110:** 1413-1429.

Frey N, Klotz J, Nick P. **2009.** Dynamic bridges-a calponin-domain kinesin from rice links actin filaments and microtubules in both cycling and non-cycling cells. *Plant Cell Physiol* **50:** 1493-1506.

Fuller BR. **1961.** Tensegrity. *Portfolio Artnews Annual* **4:** 112-127.

Fullner KJ, Nester EW. **1996.** Temperature affects the T-DNA transfer machinery of *Agrobacterium tumefaciens*. *J Bacteriol.* **178:** 1498-1504.

Furuichi T, Cunningham KW, Muto S. **2001.** A putative two pore channel AtTPC1 mediates Ca^{2+} flux in *Arabidopsis* leaf cells. *Plant Cell Physiol* **42:** 900-905.

Geiger B, Bershadsky A. **2001.** Assembly and mechanosensory function of focal contacts. *Curr.Opin.Cell Biol.* **13:** 584-592.

Geiger B, Spatz JP, Bershadsky AD. **2009.** Environmental sensing through focal adhesions. *Nat.Rev.Mol.Cell Biol.* **10:** 21-33.

Geldner N, Friml J, Stierhof YD, Jurgens G, Palme K. **2001.** Auxin transport inhibitors block PIN1 cycling and vesicle trafficking. *Nature* **413:** 425-428.

Gens JS, Fujiki M, Pickard BG. **2000.** Arabinogalactan protein and wall-associated kinase in a plasmalemmal reticulum with specialized vertices. *Protoplasma* **212:** 115-134.

Gentzbittel L, Abbott A, Galaud JP, Georgi L, Fabre F, Liboz T, Alibert G. **2002.** A bacterial artificial chromosome (BAC) library for sunflower, and identification of clones containing genes for putative transmembrane receptors. *Mol.Genet.Genomics* **266:** 979-987.

Gillespie PG, Walker RG. **2001.** Molecular basis of mechanosensory transduction. *Nature* **413:** 194-202.

Gilroy S, Jones DL. **2000.** Through form to function: root hair development and nutrient uptake. *Trends Plant Sci.* **5:** 56-60.

Goldmann WH. **2012a.** Mechanotransduction and focal adhesions. *Cell Biol.Int.* **36:** 649-652.

Goldmann WH. **2012b.** Mechanotransduction in cells. *Cell Biol.Int.* **36:** 567-570.

Gross P, Julius C, Schmelzer E, Hahlbrock K. **1993.** Translocation of cytoplasm and nucleus to fungal penetration sites is associated with depolymerization of microtubules and defence gene activation in infected, cultured parsley cells. *EMBO J.* **12:** 1735-1744.

Grossmann G, Opekarova M, Malinsky J, Weig-Meckl I, Tanner W. **2007.** Membrane potential governs lateral segregation of plasma membrane proteins and lipids in yeast. *EMBO J.* **26:** 1-8.

Grunewald W, Friml J. **2010.** The march of the PINs: developmental plasticity by dynamic polar targeting in plant cells. *EMBO J* **29:** 2700-2714.

Gu CX, Juranka PF, Morris CE. **2001.** Stretch-activation and stretch-inactivation of Shaker-IR, a voltage-gated K^+ channel. *Biophys.J.* **80:** 2678-2693.

Guan X, Buchholz G, Nick P. **2013.** The cytoskeleton is disrupted by the bacterial effector HrpZ, but not by the bacterial PAMP flg22, in tobacco BY-2 cells. *J Exp.Bot.*

Gurtovenko AA, Anwar J. **2007.** Modulating the structure and properties of cell membranes: the molecular mechanism of action of dimethyl sulfoxide. *J Phys.Chem.B* **111:** 10453-10460.

Gus-Mayer S, Naton B, Hahlbrock K, Schmelzer E. **1998.** Local mechanical stimulation induces components of the pathogen defense response in parsley. *Proc.Natl.Acad.Sci.U.S.A* **95:** 8398-8403.

Gutjahr C, Banba M, Croset V, An K, Miyao A, An G, Hirochika H, Imaizumi-Anraku H, Paszkowski U. **2008.** Arbuscular mycorrhiza-specific signaling in rice transcends the common symbiosis signaling pathway. *Plant Cell* **20:** 2989-3005.

Haley A, Russell AJ, Wood N, Allan AC, Knight M, Campbell AK, Trewavas AJ. **1995.** Effects of mechanical signaling on plant cell cytosolic calcium. *Proc.Natl.Acad.Sci.U.S.A* **92:** 4124-4128.

Hamada H, Kurusu T, Okuma E, Nokajima H, Kiyoduka M, Koyano T, Sugiyama Y, Okada K, Koga J, Saji H, Miyao A, Hirochika H, Yamane H, Murata Y, Kuchitsu K. **2012.** Regulation of a proteinaceous elicitor-induced Ca^{2+} influx and production of phytoalexins by a putative voltage-gated cation channel, OsTPC1, in cultured rice cells. *J.Biol.Chem.* **287:** 9931-9939.

Hamant O. **2013.** Widespread mechanosensing controls the structure behind the architecture in plants. *Curr.Opin.Plant Biol.* **16:** 654-660.

Hamant O, Heisler MG, Jonsson H, Krupinski P, Uyttewaal M, Bokov P, Corson F, Sahlin P, Boudaoud A, Meyerowitz EM, Couder Y, Traas J. **2008.** Developmental patterning by mechanical signals in *Arabidopsis*. *Science* **322:** 1650-1655.

Hamant O, Traas J. **2010.** The mechanics behind plant development. *New Phytol.* **185:** 369-385.

Hamill OP, Martinac B. **2001.** Molecular basis of mechanotransduction in living cells. *Physiol Rev.* **81:** 685-740.

Hardham AR, Takemoto D, White RG. **2008.** Rapid and dynamic subcellular reorganization following mechanical stimulation of *Arabidopsis* epidermal cells mimics responses to fungal and oomycete attack. *BMC.Plant Biol.* **8:** 63.

Hartley JL, Temple GF, Brasch MA. **2000.** DNA cloning using in vitro site-specific recombination. *Genome Res.* **10:** 1788-1795.

Hashiguchi Y, Tasaka M, Morita MT. **2013.** Mechanism of higher plant gravity sensing. *Am.J.Bot.* **100:** 91-100.

Hashimoto K., Saito M., Lida H., Matsuoka H. 2005. Evidence for the plasma membrane localization of a putative voltage-dependent Ca^{2+} channel, OsTPC1, in rice. *Plant Biotechnol* **22:** 235-239.

Haswell ES, Meyerowitz EM. **2006.** MscS-like proteins control plastid size and shape in *Arabidopsis thaliana*. *Curr.Biol.* **16:** 1-11.

Haswell ES, Peyronnet R, Barbier-Brygoo H, Meyerowitz EM, Frachisse JM. **2008.** Two MscS homologs provide mechanosensitive channel activities in the *Arabidopsis* root. *Curr.Biol.* **18:** 730-734.

Hejnowicz Z, Rusin A, Rusin T. **2000.** Tensile tissue stress affects the orientation of cortical microtubules in the wpidermis of sunflower hypocotyl. *J.Plant Growth Regul.* **19:** 31-44.

Henson JH. **1999.** Relationships between the actin cytoskeleton and cell volume regulation. *Microsc.Res.Tech.* **47:** 155-162.

Higaki T, Kutsuna N, Okubo E, Sano T, Hasezawa S. **2006.** Actin microfilaments regulate vacuolar structures and dynamics: dual observation of actin microfilaments and vacuolar membrane in living tobacco BY-2 Cells. *Plant Cell Physiol* **47:** 839-852.

Himmelspach R, Nick P. **2001.** Gravitropic microtubule reorientation can be uncoupled from growth. *Planta* **212:** 184-189.

Hoffman BD, Grashoff C, Schwartz MA. **2011.** Dynamic molecular processes mediate cellular mechanotransduction. *Nature* **475:** 316-323.

Hofmann F, Biel M, Flockerzi V. **1994.** Molecular basis for Ca^{2+} channel diversity. *Annu.Rev.Neurosci.* **17:** 399-418.

Hohenberger P, Eing C, Straessner R, Durst S, Frey W, Nick P. **2011.** Plant actin controls membrane permeability. *Biochim.Biophys.Acta* **1808:** 2304-2312.

Holdaway-Clarke TL, Feijo JA, Hackett GR, Kunkel JG, Hepler PK. **1997.** Pollen tube growth and the intracellular cytosolic calcium gradient oscillate in phase while extracellular calcium influx is delayed. *Plant Cell* **9:** 1999-2010.

Holm AN, Rich A, Sarr MG, Farrugia G. **2000.** Whole cell current and membrane potential regulation by a human smooth muscle mechanosensitive calcium channel. *Am.J.Physiol Gastrointest.Liver Physiol* **279:** G1155-G1161.

Homann U. **1998.** Fusion and fission of plasma-membrane material accommodates for osmotically induced changes in the surface area of guard-cell protoplasts. *Planta* **206:** 329-333.

Hussey PJ, Allwood EG, Smertenko AP. **2002.** Actin-binding proteins in the *Arabidopsis* genome database: properties of functionally distinct plant actin-depolymerizing factors/cofilins. *Philos.Trans.R.Soc.Lond B Biol Sci.* **357:** 791-798.

Ingber DE. **1993.** Cellular tensegrity: defining new rules of biological design that govern the cytoskeleton. *J.Cell Sci.* **104 Pt 3:** 613-627.

Ingber DE. **2003a.** Tensegrity I. Cell structure and hierarchical systems biology. *J.Cell Sci.* **116:** 1157-1173.

Ingber DE. **2003b.** Tensegrity II. How structural networks influence cellular information processing networks. *J.Cell Sci.* **116:** 1397-1408.

Ingber DE. **2006.** Mechanical control of tissue morphogenesis during embryological development. *Int.J.Dev.Biol.* **50:** 255-266.

Ingber DE. **2008.** Tensegrity and mechanotransduction. *J.Bodyw.Mov Ther.* **12:** 198-200.

Ippolito JA, Barbarick KA. **2000.** Modified nitric acid plant tissue digest method. *Communications In Soil Science and Plant Analysis* **31:** 2473-2482.

Ishibashi K, Suzuki M, Imai M. **2000.** Molecular cloning of a novel form (two-repeat) protein related to voltage-gated sodium and calcium channels. *Biochem.Biophys.Res.Commun.* **270:** 370-376.

Ismail A, Riemann M, Nick P. **2012.** The jasmonate pathway mediates salt tolerance in grapevines. *J.Exp.Bot.* **63:** 2127-2139.

Jaffe MJ, Leopold AC, Staples RC. **2002.** Thigmo responses in plants and fungi. *Am.J Bot.* **89:** 375-382.

Jovanovic AM, Durst S, Nick P. **2010.** Plant cell division is specifically affected by nitrotyrosine. *J.Exp.Bot.* **61:** 901-909.

Kachar B, Parakkal M, Fex J. **1990.** Structural basis for mechanical transduction in the frog vestibular sensory apparatus: I. The otolithic membrane. *Hear.Res.* **45:** 179-190.

Kadota Y, Furuichi T, Ogasawara Y, Goh T, Higashi K, Muto S, Kuchitsu K. **2004.** Identification of putative voltage-dependent Ca^{2+}-permeable channels involved in cryptogein-induced Ca^{2+} transients and defense responses in tobacco BY-2 cells. *Biochem.Biophys.Res.Commun.* **317:** 823-830.

Kandasamy MK, McKinney EC, Meagher RB. **1999.** The late pollen-specific actins in angiosperms. *Plant J.* **18:** 681-691.

Kanzaki M, Nagasawa M, Kojima I, Sato C, Naruse K, Sokabe M, Iida H. **1999.** Molecular identification of a eukaryotic, stretch-activated nonselective cation channel. *Science* **285:** 882-886.

Karimi M, Inze D, Depicker A. **2002.** GATEWAY vectors for *Agrobacterium*-mediated plant transformation. *Trends Plant Sci.* **7:** 193-195.

Kawano T, Kadono T, Fumoto K, Lapeyrie F, Kuse M, Isobe M, Furuichi T, Muto S. **2004.** Aluminum as a specific inhibitor of plant TPC1 Ca^{2+} channels. *Biochem.Biophys.Res.Commun.* **324:** 40-45.

Kleine-Vehn J, Langowski L, Wisniewska J, Dhonukshe P, Brewer PB, Friml J. **2008.** Cellular and molecular requirements for polar PIN targeting and transcytosis in plants. *Mol.Plant* **1:** 1056-1066.

Kloda A, Lua L, Hall R, Adams DJ, Martinac B. **2007.** Liposome reconstitution and modulation of recombinant N-methyl-D-aspartate receptor channels by membrane stretch. *Proc.Natl.Acad.Sci.U.S.A* **104:** 1540-1545.

Klotz J, Nick P. **2012.** A novel actin-microtubule cross-linking kinesin, NtKCH, functions in cell expansion and division. *New Phytol.* **193:** 576-589.

Klusener B, Boheim G, Liss H, Engelberth J, Weiler EW. **1995.** Gadolinium-sensitive, voltage-dependent calcium release channels in the endoplasmic reticulum of a higher plant mechanoreceptor organ. *EMBO J* **14:** 2708-2714.

Knepper C, Savory EA, Day B. **2011.** *Arabidopsis* NDR1 is an integrin-like protein with a role in fluid loss and plasma membrane-cell wall adhesion. *Plant Physiol* **156:** 286-300.

Knight TA. **1806.** On the direction of the radicle and germen during the vegetation of seeds. *Philosophical transactions of the royal society of london* **96:** 99-108.

Kobayashi Y, Yamada M, Kobayashi I, Kunoh H. **1997.** Actin microfilaments are required for the expression of nonhost resistance in higher plants. *Plant and cell physiology.* **38:** 725-733.

Koivusalo M, Kapus A, Grinstein S. **2009.** Sensors, transducers, and effectors that regulate cell size and shape. *J Biol Chem.* **284:** 6595-6599.

Komis G, Apostolakos, Galatis B. **2001.** Altered patterns of tubulin polymerization in dividing leaf cells of *Chlorophyton comosum* after a hyperosmotic treatment. *New Phytologist* **149:** 193-207.

Komis G, Apostolakos P, Galatis B. **2002a.** Hyperosmotic stress induces formation of tubulin macrotubules in root-tip cells of *Triticum turgidum*: their probable involvement in protoplast volume control. *Plant Cell Physiol* **43:** 911-922.

Komis G, Apostolakos P, Galatis B. **2002b.** Hyperosmotic stress-induced actin filament reorganization in leaf cells of *Chlorophyton comosum*. *J Exp.Bot.* **53:** 1699-1710.

Komis G, Quader H, Galatis B, Apostolakos P. **2006.** Macrotubule-dependent protoplast volume regulation in plasmolysed root-tip cells of *Triticum turgidum*: involvement of phospholipase D. *New Phytol.* **171:** 737-750.

Krol E, Plachno BJ, Adamec L, Stolarz M, Dziubinska H, Trebacz K. **2012.** Quite a few reasons for calling carnivores 'the most wonderful plants in the world'. *Ann.Bot.* **109:** 47-64.

Kubitscheck U, Homann U, Thiel G. **2000.** Osmotically evoked shrinking of guard-cell protoplasts causes vesicular retrieval of plasma membrane into the cytoplasm. *Planta* **210:** 423-431.

Kuhtreiber WM, Jaffe LF. **1990.** Detection of extracellular calcium gradients with a calcium-specific vibrating electrode. *J Cell Biol* **110:** 1565-1573.

Kung C. **2005.** A possible unifying principle for mechanosensation. *Nature* **436:** 647-654.

Kung C, Martinac B, Sukharev S. **2010.** Mechanosensitive channels in microbes. *Annu.Rev.Microbiol.* **64:** 313-329.

Kupisz K, Trebacz K. **2011.** Effect of cold and menthol on membrane potential in plants. *Physiol Plant* **141:** 352-360.

Kurusu T, Hamada H, Koyano T, Kuchitsu K. **2012a.** Intracellular localization and physiological function of

a rice Ca^{2+} -permeable channel OsTPC1. *Plant Signal.Behav.* **7:** 1428-1430.

Kurusu T, Kuchitsu K, Nakano M, Nakayama Y, Iida H. **2013.** Plant mechanosensing and Ca^{2+} transport. *Trends Plant Sci.* **18:** 227-233.

Kurusu T, Nishikawa D, Yamazaki Y, Gotoh M, Nakano M, Hamada H, Yamanaka T, Iida K, Nakagawa Y, Saji H, Shinozaki K, Iida H, Kuchitsu K. **2012b.** Plasma membrane protein OsMCA1 is involved in regulation of hypo-osmotic shock-induced Ca^{2+} influx and modulates generation of reactive oxygen species in cultured rice cells. *BMC.Plant Biol.* **12:** 11.

Kurusu T, Sakurai Y, Miyao A, Hirochika H, Kuchitsu K. **2004.** Identification of a putative voltage-gated Ca^{2+} -permeable channel (OsTPC1) involved in Ca^{2+} influx and regulation of growth and development in rice. *Plant Cell Physiol* **45:** 693-702.

Kurusu T, Yagala T, Miyao A, Hirochika H, Kuchitsu K. **2005.** Identification of a putative voltage-gated Ca^{2+} channel as a key regulator of elicitor-induced hypersensitive cell death and mitogen-activated protein kinase activation in rice. *Plant J* **42:** 798-809.

Kurusu T, Yamanaka T, Nakano M, Takiguchi A, Ogasawara Y, Hayashi T, Iida K, Hanamata S, Shinozaki K, Iida H, Kuchitsu K. **2012c.** Involvement of the putative Ca^{2+}-permeable mechanosensitive channels, NtMCA1 and NtMCA2, in Ca^{2+} uptake, Ca^{2+}-dependent cell proliferation and mechanical stress-induced gene expression in tobacco (*Nicotiana tabacum*) BY-2 cells. *J.Plant Res.* **125:** 555-568.

Kusaka N, Maisch J, Nick P, Hayashi K, Nozaki H. **2009.** Manipulation of intracellular auxin in a single cell by light with esterase-resistant caged auxins. *Chembiochem.* **10:** 2195-2202.

Kutsuna N, Hasezawa S. **2002.** Dynamic organization of vacuolar and microtubule structures during cell cycle progression in synchronized tobacco BY-2 cells. *Plant Cell Physiol* **43:** 965-973.

Kutsuna N, Kumagai F, Sato MH, Hasezawa S. **2003.** Three-dimensional reconstruction of tubular structure of vacuolar membrane throughout mitosis in living tobacco cells. *Plant Cell Physiol* **44:** 1045-1054.

Laval V, Chabannes M, Carriere M, Canut H, Barre A, Rouge P, Pont-Lezica R, Galaud J. **1999.** A family of *Arabidopsis* plasma membrane receptors presenting animal beta-integrin domains. *Biochim.Biophys.Acta* **1435:** 61-70.

Le Dain AC, Saint N, Kloda A, Ghazi A, Martinac B. **1998.** Mechanosensitive ion channels of the archaeon *Haloferax volcanii*. *J.Biol.Chem.* **273:** 12116-12119.

Lee D, Polisensky DH, Braam J. **2005.** Genome-wide identification of touch- and darkness-regulated *Arabidopsis* genes: a focus on calmodulin-like and XTH genes. *New Phytol.* **165:** 429-444.

Legue V, Blancaflor E, Wymer C, Perbal G, Fantin D, Gilroy S. **1997.** Cytoplasmic free Ca^{2+} in *Arabidopsis* roots changes in response to touch but not gravity. *Plant Physiol* **114:** 789-800.

Leitz G, Kang BH, Schoenwaelder ME, Staehelin LA. **2009.** Statolith sedimentation kinetics and force

transduction to the cortical endoplasmic reticulum in gravity-sensing *Arabidopsis* columella cells. *Plant Cell* **21:** 843-860.

Lin C, Yu Y, Kadono T, Iwata M, Umemura K, Furuichi T, Kuse M, Isobe M, Yamamoto Y, Matsumoto H, Yoshizuka K, Kawano T. **2005.** Action of aluminum, novel TPC1-type channel inhibitor, against salicylate-induced and cold-shock-induced calcium influx in tobacco BY-2 cells. *Biochem.Biophys.Res.Commun.* **332:** 823-830.

Lintilhac PM. **1999.** Thinking of biology: toward a theory of cellularity-speculations on the nature of the living cell. *Bioscience.* **49:** 59-68.

Livak KJ, Schmittgen TD. **2001.** Analysis of relative gene expression data using real-time quantitative PCR and the $2^{-\text{Delta Delta C(T)}}$ Method. *Methods* **25:** 402-408.

Los DA, Murata N. **2004.** Membrane fluidity and its roles in the perception of environmental signals. *Biochim.Biophys.Acta* **1666:** 142-157.

Lovy-Wheeler A, Cardenas L, Kunkel JG, Hepler PK. **2007.** Differential organelle movement on the actin cytoskeleton in lily pollen tubes. *Cell Motil.Cytoskeleton* **64:** 217-232.

Lucas M, Kenobi K, von WD, Vobeta U, Swarup K, De S, I, Van DD, Lawrence T, Peret B, Moscardi E, Barbeau D, Godin C, Salt D, Guyomarc'h S, Stelzer EH, Maizel A, Laplaze L, Bennett MJ. **2013.** Lateral root morphogenesis is dependent on the mechanical properties of the overlaying tissues. *Proc.Natl.Acad.Sci.U.S.A* **110:** 5229-5234.

Lyford GL, Strege PR, Shepard A, Ou Y, Ermilov L, Miller SM, Gibbons SJ, Rae JL, Szurszewski JH, Farrugia G. **2002.** alpha_{1C} ($Ca_V1.2$) L-type calcium channel mediates mechanosensitive calcium regulation. *Am.J.Physiol Cell Physiol* **283:** C1001-C1008.

Lyman GH, Preisler HD, Papahadjopoulos D. **1976.** Membrane action of DMSO and other chemical inducers of friend leukaemic cell differentiation. *Nature* **262:** 361-363.

Lynch TM, Lintilhac PM. **1997.** Mechanical signals in plant development: a new method for single cell studies. *Dev.Biol.* **181:** 246-256.

Maisch J, Nick P. **2007.** Actin is involved in auxin-dependent patterning. *Plant Physiol* **143:** 1695-1704.

Mammoto T, Ingber DE. **2010.** Mechanical control of tissue and organ development. *Development* **137:** 1407-1420.

Marchler-Bauer A, Anderson JB, Cherukuri PF, DeWeese-Scott C, Geer LY, Gwadz M, He S, Hurwitz DI, Jackson JD, Ke Z, Lanczycki CJ, Liebert CA, Liu C, Lu F, Marchler GH, Mullokandov M, Shoemaker BA, Simonyan V, Song JS, Thiessen PA, Yamashita RA, Yin JJ, Zhang D, Bryant SH. **2005.** CDD: a conserved domain database for protein classification. *Nucleic Acids Res.* **33:** D192-D196.

Martinac B. **2001.** Mechanosensitive channels in prokaryotes. *Cell Physiol Biochem.* **11:** 61-76.

Martinac B. **2014.** The ion channels to cytoskeleton connection as potential mechanism of

mechanosensitivity. *Biochim.Biophys.Acta* **1838:** 682-691.

Martinac B, Adler J, Kung C. **1990.** Mechanosensitive ion channels of *E. coli* activated by amphipaths. *Nature* **348:** 261-263.

Martinac B, Rohde PR, Battle AR, Petrov E, Pal P, Foo AF, Vasquez V, Huynh T, Kloda A. **2010.** Studying mechanosensitive ion channels using liposomes. *Methods Mol.Biol.* **606:** 31-53.

Mathur J, Mathur N, Kernebeck B, Hulskamp M. **2003.** Mutations in actin-related proteins 2 and 3 affect cell shape development in *Arabidopsis*. *Plant Cell* **15:** 1632-1645.

Maurel C. **1997.** Aquaporins and water permeability of plant membranes. *Annu.Rev.Plant Physiol Plant Mol.Biol* **48:** 399-429.

McCann MC, Wells B, Roberts K. **1990.** Direct visualization of cross-links in the primary plant cell wall. *J.Cell Sci.* **96:** 323-334.

Meckel T, Hurst AC, Thiel G, Homann U. **2005.** Guard cells undergo constitutive and pressure-driven membrane turnover. *Protoplasma* **226:** 23-29.

Mirabet V, Das P, Boudaoud A, Hamant O. **2011.** The role of mechanical forces in plant morphogenesis. *Annu.Rev.Plant Biol.* **62:** 365-385.

Mogilner A, Keren K. **2009.** The shape of motile cells. *Curr.Biol.* **19:** R762-R771.

Monroy AF, Dhindsa RS. **1995.** Low-temperature signal transduction: induction of cold acclimation-specific genes of alfalfa by calcium at 25 degrees C. *Plant Cell* **7:** 321-331.

Monshausen GB, Bibikova TN, Weisenseel MH, Gilroy S. **2009.** Ca^{2+} regulates reactive oxygen species production and pH during mechanosensing in *Arabidopsis* roots. *Plant Cell* **21:** 2341-2356.

Monshausen GB, Gilroy S. **2009.** Feeling green: mechanosensing in plants. *Trends Cell Biol.* **19:** 228-235.

Monshausen GB, Haswell ES. **2013.** A force of nature: molecular mechanisms of mechanoperception in plants. *J.Exp.Bot.* **64:** 4663-4680.

Monshausen GB, Swanson SJ, Gilroy S. **2008.** Touch sensing and thigmotropism. In: Gilroy S, Masson PH, eds. *Plant Tropisms*. Oxford, UK.: Blackwell Publishing Ltd.

Moulia B, Coutand C, Lenne C. **2006.** Posture control and skeletal mechanical acclimation in terrestrial plants: implications for mechanical modeling of plant architecture. *Am.J.Bot.* **93:** 1477-1489.

Moulia B, Fournier M. **2009.** The power and control of gravitropic movements in plants: a biomechanical and systems biology view. *J.Exp.Bot.* **60:** 461-486.

Munnik T, Arisz SA, De VT, Musgrave A. **1995.** G protein activation stimulates phospholipase D signaling in plants. *Plant Cell* **7:** 2197-2210.

Nagata T, Nemoto Y, Hasezawa S. **1992.** Tobacco BY-2 cell-line as the hela-cell in the cell biology of higher-plants. *Internation Review of Cytology- A Survey of Cell Biology* **132:** 1-30.

Nakagawa Y, Katagiri T, Shinozaki K, Qi Z, Tatsumi H, Furuichi T, Kishigami A, Sokabe M, Kojima I, Sato S, Kato T, Tabata S, Iida K, Terashima A, Nakano M, Ikeda M, Yamanaka T, Iida H. **2007.** *Arabidopsis* plasma membrane protein crucial for Ca^{2+} influx and touch sensing in roots. *Proc.Natl.Acad.Sci.U.S.A* **104:** 3639-3644.

Nakamura M, Naoi K, Shoji T, Hashimoto T. **2004.** Low concentrations of propyzamide and oryzalin alter microtubule dynamics in *Arabidopsis* epidermal cells. *Plant Cell Physiol* **45:** 1330-1334.

Nakayama Y, Fujiu K, Sokabe M, Yoshimura K. **2007.** Molecular and electrophysiological characterization of a mechanosensitive channel expressed in the chloroplasts of *Chlamydomonas*. *Proc.Natl.Acad.Sci.U.S.A* **104:** 5883-5888.

Nesin OM, Pakhomova ON, Xiao S, Pakhomov AG. **2011.** Manipulation of cell volume and membrane pore comparison following single cell permeabilization with 60- and 600-ns electric pulses. *Biochim.Biophys.Acta* **1808:** 792-801.

Nick P. **2008.** Microtubules as sensors for abiotic stimuli. In: Nick P., ed. *Plant Microtubules*. Berlin: Springer-Verlag, 175-203.

Nick P. **2011.** Mechanics of the Cytoskeleton. In: Wojtaszek P, ed. *Mechanical Integration of Plant Cells and Plants*. Berlin: Springer Berlin Heidelberg, 53-90.

Nick P. **2013.** Microtubules, signalling and abiotic stress. *Plant J.* **75:** 309-323.

Nick P, Bergfeld R, Schafer E, Schopfer P. **1990.** Unilateral reorientation of microtubules at the outer epidermal wall during photo- and gravitropic curvature of maize coleoptiles and sunflower hypocotyls. *Planta* **181:** 162-168.

Nick P, Heuing A, Ehmann B. **2000.** Plant chaperonins: a role in microtubule-dependent wall formation? *Protoplasma* **211:** 234-244.

Nomura T, Cranfield CG, Deplazes E, Owen DM, Macmillan A, Battle AR, Constantine M, Sokabe M, Martinac B. **2012.** Differential effects of lipids and lyso-lipids on the mechanosensitivity of the mechanosensitive channels MscL and MscS. *Proc.Natl.Acad.Sci.U.S.A* **109:** 8770-8775.

Oda Y, Higaki T, Hasezawa S, Kutsuna N. **2009.** New insights into plant vacuolar structure and dynamics. In: Kwang WJ, ed. *International Review of Cell and Molecular Biology*. 103-135.

Okazaki Y, Ishigami M, Iwasaki N. **2002.** Temporal relationship between cytosolic free Ca^{2+} and membrane potential during hypotonic turgor regulation in a brackish water Charophyte *Lamprothamnium succinctum*. *Plant Cell Physiol* **43:** 1027-1035.

Orvar BL, Sangwan V, Omann F, Dhindsa RS. **2000.** Early steps in cold sensing by plant cells: the role of actin cytoskeleton and membrane fluidity. *Plant J.* **23:** 785-794.

Ovecka M, Lang I, Baluska F, Ismail A, Illes P, Lichtscheidl IK. **2005.** Endocytosis and vesicle trafficking during tip growth of root hairs. *Protoplasma* **226:** 39-54.

Palmer CP, Zhou XL, Lin J, Loukin SH, Kung C, Saimi Y. **2001.** A TRP homolog in *Saccharomyces cerevisiae* forms an intracellular Ca^{2+}-permeable channel in the yeast vacuolar membrane. *Proc.Natl.Acad.Sci.U.S.A* **98:** 7801-7805.

Peaucelle A, Braybrook SA, Le GL, Bron E, Kuhlemeier C, Hofte H. **2011.** Pectin-induced changes in cell wall mechanics underlie organ initiation in *Arabidopsis*. *Curr.Biol.* **21:** 1720-1726.

Peiter E, Maathuis FJ, Mills LN, Knight H, Pelloux J, Hetherington AM, Sanders D. **2005.** The vacuolar Ca^{2+}-activated channel TPC1 regulates germination and stomatal movement. *Nature* **434:** 404-408.

Pelletier S, Van OJ, Wolf S, Vissenberg K, Delacourt J, Ndong YA, Pelloux J, Bischoff V, Urbain A, Mouille G, Lemonnier G, Renou JP, Hofte H. **2010.** A role for pectin de-methylesterification in a developmentally regulated growth acceleration in dark-grown *Arabidopsis* hypocotyls. *New Phytol.* **188:** 726-739.

Petrasek J, Schwarzerova K. **2009.** Actin and microtubule cytoskeleton interactions. *Curr.Opin.Plant Biol* **12:** 728-734.

Pickard BG. **2008.** "Second extrinsic organizational mechanism" for orienting cellulose: modeling a role for the plasmalemmal reticulum. *Protoplasma* **233:** 7-29.

Pickard BG, Ding JP. **1993.** The mechanosensory calcium-selective ion channel: key component of a plasmalemmal control centre? *Aust.J Plant Physiol* **20:** 439-459.

Pickard BG, Fujiki M. **2005.** Ca^{2+} pulsation in BY-2 cells and evidence for control of mechanosensory Ca^{2+}-selective channels by the plasmalemmal reticulum. *Functional Plant Biology* **32:** 863-879.

Pivetti CD, Yen MR, Miller S, Busch W, Tseng YH, Booth IR, Saier MH, Jr. 2003. Two families of mechanosensitive channel proteins. *Microbiol.Mol.Biol.Rev.* **67:** 66-85, table.

Plieth C, Trewavas AJ. **2002.** Reorientation of seedlings in the earth's gravitational field induces cytosolic calcium transients. *Plant Physiol* **129:** 786-796.

Poppinga S, Hartmeyer SR, Seidel R, Masselter T, Hartmeyer I, Speck T. **2012.** Catapulting tentacles in a sticky carnivorous plant. *PLoS.One.* **7:** e45735.

Potocka I, Szymanowska-Pulka J, Karczewski J, Nakielski J. **2011.** Effect of mechanical stress on Zea root apex. I. Mechanical stress leads to the switch from closed to open meristem organization. *J.Exp.Bot.* **62:** 4583-4593.

Preuss ML, Kovar DR, Lee YR, Staiger CJ, Delmer DP, Liu B. **2004.** A plant-specific kinesin binds to actin microfilaments and interacts with cortical microtubules in cotton fibers. *Plant Physiol* **136:** 3945-3955.

Qiao F, Chang XL, Nick P. **2010.** The cytoskeleton enhances gene expression in the response to the Harpin elicitor in grapevine. *J Exp.Bot.* **61:** 4021-4031.

Ranf S, Wunnenberg P, Lee J, Becker D, Dunkel M, Hedrich R, Scheel D, Dietrich P. **2008.** Loss of the vacuolar cation channel, AtTPC1, does not impair Ca^{2+} signals induced by abiotic and biotic stresses. *Plant J* **53:** 287-299.

Reddy AS. **2001.** Calcium: silver bullet in signaling. *Plant Sci.* **160:** 381-404.

Reddy VS, Reddy AS. **2004.** Proteomics of calcium-signaling components in plants. *Phytochemistry* **65:** 1745-1776.

Reisen D, Marty F, Leborgne-Castel N. **2005.** New insights into the tonoplast architecture of plant vacuoles and vacuolar dynamics during osmotic stress. *BMC.Plant Biol.* **5:** 13.

Reuzeau C, Pont-Lezica RF. **1995.** Comparing plant and animal extracellular matrix-cytoskeleton connections-are they alike? *Protoplasma* **186:** 113-121.

Richter GL, Monshausen GB, Krol A, Gilroy S. **2009.** Mechanical stimuli modulate lateral root organogenesis. *Plant Physiol* **151:** 1855-1866.

Ringli C. **2010.** Monitoring the outside: cell wall-sensing mechanisms. *Plant Physiol* **153:** 1445-1452.

Rodakowska E, Derba-Maceluch M, Kasprowicz A, Zawadzki P, Szuba A, Kierzkowski D, Wojtaszek P. **2009.** Signaling and Cell Walls. In: Baluska F, Mancuso S, eds. *Signaling in Plants*. Berlin: Springer Berlin Heidelberg, 173-193.

Royle SJ, Murrell-Lagnado RD. **2003.** Constitutive cycling: a general mechanism to regulate cell surface proteins. *Bioessays* **25:** 39-46.

Ruthardt N, Gulde N, Spiegel H, Fischer R, Emans N. **2005.** Four-dimensional imaging of transvacuolar strand dynamics in tobacco BY-2 cells. *Protoplasma* **225:** 205-215.

Sachs F, Morris CE. **1998.** Mechanosensitive ion channels in nonspecialized cells. *Rev.Physiol Biochem.Pharmacol.* **132:** 1-77.

Saito C, Ueda T, Abe H, Wada Y, Kuroiwa T, Hisada A, Furuya M, Nakano A. **2002.** A complex and mobile structure forms a distinct subregion within the continuous vacuolar membrane in young cotyledons of *Arabidopsis*. *Plant J.* **29:** 245-255.

Sangwan V, Foulds I, Singh J, Dhindsa RS. **2001.** Cold-activation of *Brassica napus* BN115 promoter is mediated by structural changes in membranes and cytoskeleton, and requires Ca^{2+} influx. *Plant J.* **27:** 1-12.

Sangwan V, Orvar BL, Beyerly J, Hirt H, Dhindsa RS. **2002.** Opposite changes in membrane fluidity mimic cold and heat stress activation of distinct plant MAP kinase pathways. *Plant J.* **31:** 629-638.

Sano T, Higaki T, Oda Y, Hayashi T, Hasezawa S. **2005.** Appearance of actin microfilament 'twin peaks' in mitosis and their function in cell plate formation, as visualized in tobacco BY-2 cells expressing GFP-fimbrin. *Plant J.* **44:** 595-605.

Schmelzer E. **2002.** Cell polarization, a crucial process in fungal defence. *Trends Plant Sci.* **7:** 411-415.

Schmidt GW, Delaney SK. **2010.** Stable internal reference genes for normalization of real-time RT-PCR in tobacco (*Nicotiana tabacum*) during development and abiotic stress. *Mol.Genet.Genomics* **283:** 233-241.

Schwartz MA, DeSimone DW. **2008.** Cell adhesion receptors in mechanotransduction. *Curr.Opin.Cell Biol.* **20:** 551-556.

Schwuchow J, Sack FD, Hartmann E. **1990.** Microtubule distribution in gravitropic protonemata of the moss Ceratodon. *Protoplasma* **159:** 60-69.

Seibicke T. 2002. Untersuchungen zur induzierten Resistenz an *Vitis* spec. Dr. rer. nat., University of Freiburg.

Seifert GJ, Blaukopf C. **2010.** Irritable walls: the plant extracellular matrix and signaling. *Plant Physiol* **153:** 467-478.

Shigematsu H, Iida K, Nakano M, Chaudhuri P, Iida H, Nagayama K. **2014.** Structural Characterization of the Mechanosensitive Channel Candidate MCA2 from *Arabidopsis thaliana*. *PLoS.One.* **9:** e87724.

Shlomovitz R, Gov NS. **2008.** Exciting cytoskeleton-membrane waves. *Phys.Rev.E.Stat.Nonlin.Soft.Matter Phys.* **78:** 041911.

Shope JC, DeWald DB, Mott KA. **2003.** Changes in surface area of intact guard cells are correlated with membrane internalization. *Plant Physiol* **133:** 1314-1321.

Somerville C, Bauer S, Brininstool G, Facette M, Hamann T, Milne J, Osborne E, Paredez A, Persson S, Raab T, Vorwerk S, Youngs H. **2004.** Toward a systems approach to understanding plant cell walls. *Science* **306:** 2206-2211.

Spector I, Shochet NR, Blasberger D, Kashman Y. **1989.** Latrunculins-novel marine macrolides that disrupt microfilament organization and affect cell growth: I. Comparison with cytochalasin D. *Cell Motil.Cytoskeleton* **13:** 127-144.

Spedding M, Paoletti R. **1992.** Classification of calcium channels and the sites of action of drugs modifying channel function. *Pharmacol.Rev.* **44:** 363-376.

Starr DA, Fridolfsson HN. **2010.** Interactions between nuclei and the cytoskeleton are mediated by SUN-KASH nuclear-envelope bridges. *Annu.Rev.Cell Dev.Biol.* **26:** 421-444.

Strohm AK, Baldwin KL, Masson PH. **2012.** Molecular mechanisms of root gravity sensing and signal transduction. *Wiley.Interdiscip.Rev.Dev.Biol.* **1:** 276-285.

Sukharev S, Corey DP. **2004.** Mechanosensitive channels: multiplicity of families and gating paradigms. *Sci.STKE.* **2004:** re4.

Svyatyna K, Jikumaru Y, Brendel R, Reichelt M, Mithofer A, Takano M, Kamiya Y, Nick P, Riemann M. **2013.** Light induces jasmonate-isoleucine conjugation via OsJAR1-dependent and -independent pathways in rice. *Plant Cell Environ.*

Taiz L, Zeiger E. **2002.** Water and Plant Cells. In:*Plant Physiology*.

Tavernarakis N, Driscoll M. **1997.** Molecular modeling of mechanotransduction in the nematode *caenorhabditis elegans*. *Annu.Rev.Physiol.* **59:** 659-689.

Telewski FW. **2006.** A unified hypothesis of mechanoperception in plants. *Am.J.Bot.* **93:** 1466-1476.

Torres MA, Dangl JL. **2005.** Functions of the respiratory burst oxidase in biotic interactions, abiotic stress and development. *Curr.Opin.Plant Biol.* **8:** 397-403.

Toyota M, Furuichi T, Tatsumi H, Sokabe M. **2008.** Cytoplasmic calcium increases in response to changes in the gravity vector in hypocotyls and petioles of *Arabidopsis* seedlings. *Plant Physiol* **146:** 505-514.

Toyota M, Gilroy S. **2013.** Gravitropism and mechanical signaling in plants. *Am.J.Bot.* **100:** 111-125.

Trewavas A, Knight M. **1994.** Mechanical signalling, calcium and plant form. *Plant Mol.Biol.* **26:** 1329-1341.

Tsunozaki M, Bautista DM. **2009.** Mammalian somatosensory mechanotransduction. *Curr.Opin.Neurobiol.* **19:** 362-369.

Uemura T, Yoshimura SH, Takeyasu K, Sato MH. **2002.** Vacuolar membrane dynamics revealed by GFP-AtVam3 fusion protein. *Genes Cells* **7:** 743-753.

Uyttewaal M, Burian A, Alim K, Landrein B, Borowska-Wykret D, Dedieu A, Peaucelle A, Ludynia M, Traas J, Boudaoud A, Kwiatkowska D, Hamant O. **2012.** Mechanical stress acts via katanin to amplify differences in growth rate between adjacent cells in *Arabidopsis*. *Cell* **149:** 439-451.

Varki A. **1993.** Biological roles of oligosaccharides: all of the theories are correct. *Glycobiology* **3:** 97-130.

Veley KM, Marshburn S, Clure CE, Haswell ES. **2012.** Mechanosensitive channels protect plastids from hypoosmotic stress during normal plant growth. *Curr.Biol.* **22:** 408-413.

Vogel V, Sheetz M. **2006.** Local force and geometry sensing regulate cell functions. *Nat.Rev.Mol.Cell Biol.* **7:** 265-275.

Wang N, Tytell JD, Ingber DE. **2009.** Mechanotransduction at a distance: mechanically coupling the extracellular matrix with the nucleus. *Nat.Rev.Mol.Cell Biol.* **10:** 75-82.

Wang QY, Nick P. **1998.** The auxin response of actin is altered in the rice mutant Yin-Yang. *Protoplasma* **204:** 22-33.

Wang YJ, Yu JN, Chen T, Zhang ZG, Hao YJ, Zhang JS, Chen SY. **2005.** Functional analysis of a putative Ca^{2+} channel gene TaTPC1 from wheat. *J Exp.Bot.* **56:** 3051-3060.

Wayne R, Tazawa M. **1988.** The actin cytoskeleton and polar water permeability in *Characean* cells. *Protoplasma* **Suppl. 2:** 116-130.

Wei ZM, Laby RJ, Zumoff CH, Bauer DW, He SY, Collmer A, Beer SV. **1992.** Harpin, elicitor of the hypersensitive response produced by the plant pathogen *Erwinia amylovora*. *Science* **257:** 85-88.

Welsh MJ, Price MP, Xie J. **2002.** Biochemical basis of touch perception: mechanosensory function of degenerin/epithelial Na^+ channels. *J.Biol.Chem.* **277:** 2369-2372.

Wolf S, Hematy K, Hofte H. **2012.** Growth control and cell wall signaling in plants. *Annu.Rev.Plant Biol.* **63:** 381-407.

Wolfe J, Dowgert MF, Steponkus PL. **1985.** Dynamics of membrane exchange of the plasma membrane and the lysis of isolated protoplasts during rapid expansions in area. *The Journal of Membrane Biology* **86:** 127-138.

Wolfe J, Dowgert MF, Straessner R. **1986.** Mechanical study of the deformation of the plasma membranes of protoplasts during osmotic expansions. *J Membr Biol* **93:** 63-74.

Wymer CL, Wymer SA, Cosgrove DJ, Cyr RJ. **1996.** Plant cell growth responds to external forces and the response requires intact microtubules. *Plant Physiol* **110:** 425-430.

Xu T, Qu Z, Yang X, Qin X, Xiong J, Wang Y, Ren D, Liu G. **2009.** A cotton kinesin GhKCH2 interacts with both microtubules and microfilaments. *Biochem.J.* **421:** 171-180.

Yahraus T, Chandra S, Legendre L, Low PS. **1995.** Evidence for a mechanically induced oxidative burst. *Plant Physiol* **109:** 1259-1266.

Yamanaka T, Nakagawa Y, Mori K, Nakano M, Imamura T, Kataoka H, Terashima A, Iida K, Kojima I, Katagiri T, Shinozaki K, Iida H. **2010.** MCA1 and MCA2 that mediate Ca^{2+} uptake have distinct and overlapping roles in *Arabidopsis*. *Plant Physiol* **152:** 1284-1296.

Zeiger E, Hepler PK. **1977.** Light and stomatal function: blue light stimulates swelling of guard cell protoplasts. *Science* **196:** 887-889.

Zhang Y, Hamill OP. **2000.** On the discrepancy between whole-cell and membrane patch mechanosensitivity in *Xenopus* oocytes. *J.Physiol* **523 Pt 1:** 101-115.

Zhou XL, Batiza AF, Loukin SH, Palmer CP, Kung C, Saimi Y. **2003.** The transient receptor potential channel on the yeast vacuole is mechanosensitive. *Proc.Natl.Acad.Sci.U.S.A* **100:** 7105-7110.

5. Appendix

5.1 Suspension cultures used in this study and its cultivation conditions

Name of the cell line	Volume for Subcultivation	Antibiotics	Sources
Vitis rupestris	10 ml	none	(Seibicke T., 2002)
Vitis riparia	10 ml	none	(Seibicke T., 2002)
BY-2 Wild Type	1 ml	none	(Nagata *et al.*, 1992)
BY-2 GF-11	1.5 ml	Hygromycin 30 µg/ml	(Sano *et al.*, 2005)
BY-2 *β*-Tub6	1.5 ml	Kanamycin 50 µg/ml	(Nakamura *et al.*, 2004)
NtTPC1A-GFP ox	1.5 ml	Kanamycin 100 µg/ml	This work
NtTPC1A-RFP ox	1.5 ml	Hygromycin 45 µg/ml	This work
GFP-NtMCA2 ox	1.5 ml	Kanamycin 100 µg/ml	This work

5.2 Coding sequences of the two putative calcium channel genes under investigation

5.2.1 NtTPC1A (735AA GenBank: AB124646.1)

MEEYLLSGESSNSGRTRRRIGSIFDRRDAIAHGSAYQKAAALVDLAEDGIGLPEEILEGASFEKAA
ELYFIFTRFDFLWSLNYLALVVLNFFEKPLWCSKHLAESCNNRDYYYLGELPFLTGAESLIFEGVTL
LLLIIHILFPISYEGFNLYWRSLLNRVKVILLLILVADIVVYILFLADFYYLPFRIAPYLRVVFFILNIRELR
DSFFILAGMLGTYLNVVALSALFLLFSSWLAYVFFEDTRQGKTTFTSYGTTLYQMFVLFTTSNNPD
VWIPAYKDSRWYCLFFVLYVLLGVYFVTNLILAVVYDSFKSELVKQVADKDRLRLRTLKKAFSLIDE
ANNGHLNEKQCTLLFEELNKYRTLPKISGDDFKSIFSELDDTGDFKINLDEFADLCTAIGLRFQKE
DSLPIFEACPNFYHSPASEKLRGFVRGATFEYIIVFVLLVNLVAVIIETTLDIQNNSGQTFWQKVEFT
FGWLYVIEMALKVYTYGFENYWRDGQNRFDFVVTWVIVIGETATFVAPDGLTFLSNGEWIRYLLIA
RMLRLIRLLMHVERYRAFVATFFTLIPSLVPYLGTIFCILCFYCSLGLQIFGGIVNTGNPNLAQTDLA
GNDYLLFNFNDYPNGMVTLFNILVMGNWQVWMQSYKELTGTAWTYAYFVSFYLISVLWLLNLIVA
FVLEAFQAEVDLEASARCVDGDDKEAKSERRRNVGTKTRSQRVDFLLHHMLRSELTECSNENP

5.2.2 NtMCA2 (419AA GenBank: AB622812.1)

MASWEHFGEIANVAQLTGIDAVRLIGMIVKAATTARMHKKNCRQFAQHLKLIGNLLEQLKITELKRY
PETREPLEQLEDALRRSYILVKSCQDRSYLYLLAMGWNIVYQFRRAQNEIDQYLKIIPLITLVDNAR
VRERLEFIERDQHEYTLEAEDMKVQEVIMKPEPSKDDTIILTKNLSCSYPRVPINEAIKKENEKLQL

ELQRSQANLDVGQCEFIQHLLDVTEVVATNSLSLKSSPIKPPKKLDESYSNVDSYTDHYVESYAK
NDEKQATSRNASSVSSKHELLSSKGSHRYEEWHSDLLGCCSEPLLCIKTVFFPCGTFSKVASVA
ADRHISSAEACNELMAYSLILSCCCYTCCIRRKLRKKLNIMGGFVDDFLSHLMCCCCALVQEWRE
VEIRGTHGLEKTKVRPPTSQLMES

5.3 Primers used for Gateway® cloning

Primers	Sequences (5'- 3')
NtTPC1A Fw	GGGGACAAGTTTGTACAAAAAAGCAGGCTTCATGGAAGAATATCT ACTGTCAGGG
NtTPC1A Re N-terminal	GGGGACCACTTTGTACAAGAAAGCTGGGTCTTATGGATTCTCATT GGAGCATTCTG
NtTPC1A Re C-terminal	GGGGACCACTTTGTACAAGAAAGCTGGGTCTGGATTCTCATTGG AGCATTCTG
NtMCA2 Fw	GGGGACAAGTTTGTACAAAAAAGCAGGCTTCATGGCTTCATGGG AACATTTTGGG
NtMCA2 Re N-terminal	GGGGACCACTTTGTACAAGAAAGCTGGGTCTCAGGATTCCATTAA CTGAGAGGTTG
NtMCA2 Re C-terminal	GGGGACCACTTTGTACAAGAAAGCTGGGTCGGATTCCATTAACT GAGAGGTTGGAG

5.4 PCR reaction for Gateway® cloning

Amplification of NtTPC1A and NtMCA2 from BY-2 cDNA	
Ingredients	**Volume in µl**
Template DNA (cDNA)	1
Forward primer (10 µM)	2
N or C- terminal Reverse primer (10 µM)	2
dNTPs (10 mM)	1
HF-Buffer (5x)	10
NEB Phusion-Polymerase	0.5
Betaine (5M)	5
DMSO	2
ddH_2O	26.5
Total Volume	**50**

PCR Program:

Pre-Heating		98°C, 30 sec
38 cycles	Denaturation Annealing Extension	98°C, 10 sec 56°C, 35 sec 72°C, 45 sec
Final Extension		72°C, 7 min
End		4°C, Hold

5.5 Gateway® destination vectors constructed

Overview of the constructs generated from this study:

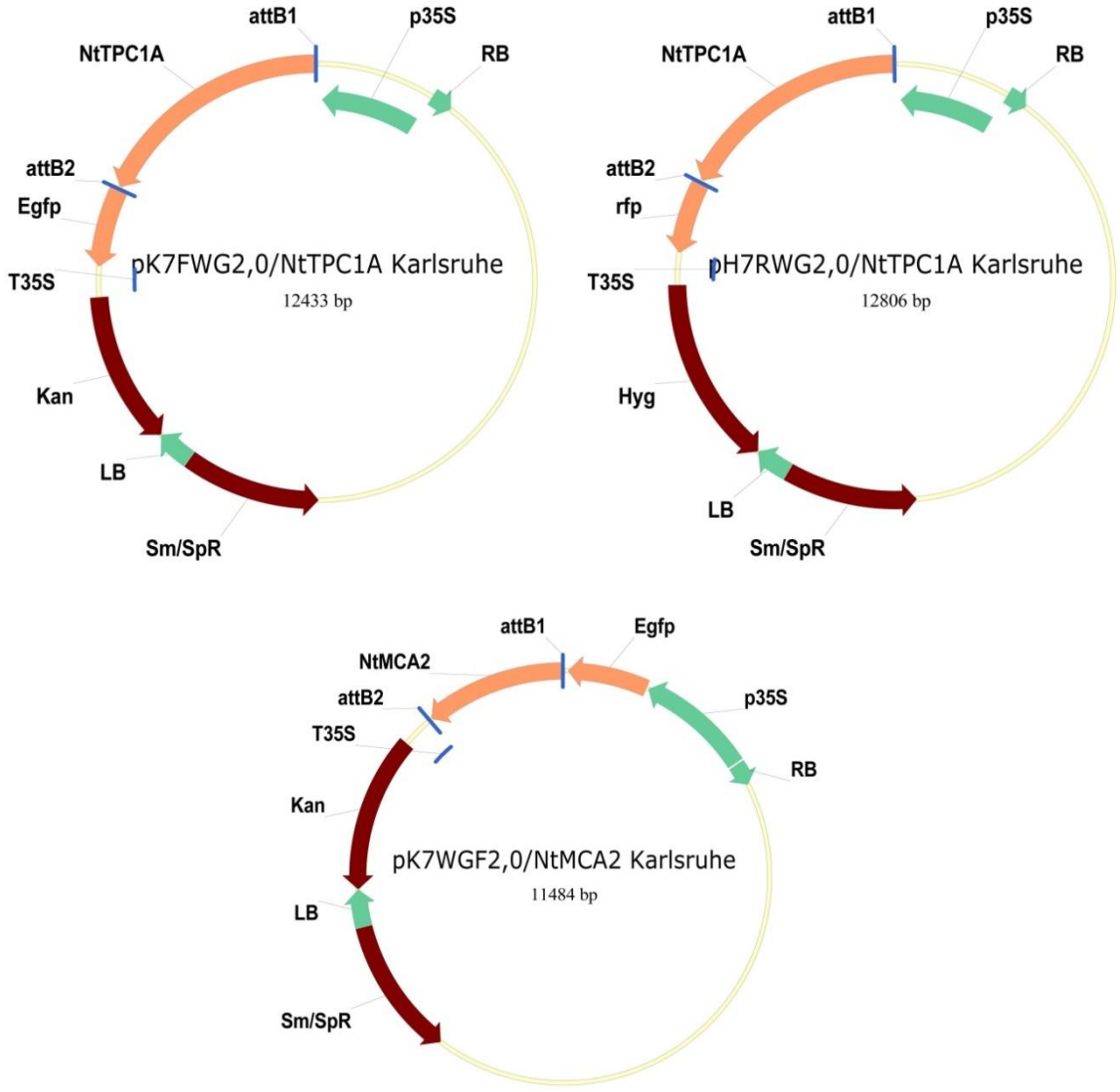

5.6 Preparation of DNA-coated gold particles for biolistic transformation

120 mg of gold particles (1.5-3.0 µm; Sigma-Aldrich) were suspended in 1 ml 50 % (v/v) sterile glycerol by mixing on a platform vortexer (Bender & Hobein, Zurich, Switzerland). Continuous agitation of the suspended gold particles was needed for uniform DNA precipitation onto gold particles maximizing uniform sampling. For each sample, 12.5 µl of gold suspension was removed to a 1.5 ml reaction tube.

While mixing vigorously, the following components were added successively: 1 µg of DNA, 12.5 µl of 2.5 M sterile $CaCl_2$, and 5 µl of 0.1 M sterile spermidine (Roth, Karlsruhe, Germany).

Following supplementary mixing for 3 minutes, the DNA-coated gold particles were spun down briefly, and the supernatant was discarded. Subsequently, the gold particles were washed with 125 µl of ice-cold absolute ethanol and resuspended in 40 µl of ice-cold absolute ethanol. DNA-coated gold particles were loaded onto the macrocarrier (Bio-Rad, Hercules, CA, USA) in 10 µl steps. Particle bombardment was performed immediately after complete evaporation of the ethanol.

This protocol was taken and modified from the doctoral thesis of Dr. Jan Maisch (Botanical Institute I, KIT, Karlsruhe; Maisch J., 2007).

5.7 Primers for expression analysis using qPCR

Primers	Sequences (5'- 3')
GAPDH Fw	ACAAATTGCCTTGCTCCCTTGGC
GAPDH Re	CCTCCAGTCCTTGGCTGATGG
L25 Fw	GTTGCCAAGGCTGTCAAGTCAGG
L25 Re	GCACTAATACGAGGGTACTTGGGG
qNtTPC1A Fw	GAGTAGTAATTCGGGTCGGACTCG
qNtTPC1A Re	GCAGACCAATGCCATCTTCAGC
qNtMCA2 Fw	GGGGAAATCGCAAATGTCGCCC
qNtMCA2 Re	GAGATGCTGCGCAAACTGCCTGC

5.8 Gateway® recombination reactions technology overview

The Gateway® technology (Invitrogen Corporation, Paisley, UK) uses the bacteriophage site-specific lambda recombination system to facilitate transfer of heterologous DNA sequences between vectors (Hartley *et al.*, 2000). The components of the lambda recombination sites (*att* sites) are modified to improve the specificity and efficiency of the system (Bushman *et al.*, 1985).

Two recombination reactions constitute the basis of this technology:

1. BP reaction: Facilitates recombination of an *attB* substrate (attB-PCR product) with an *attP* substrate (called “donor vector”) to create an *attL*-containing entry clone. This reaction is catalysed by BP Clonase™ II enzyme mix (Invitrogen).

2. LR reaction: Facilitates recombination of an *attL* substrate (called “entry clone”) with an *attR* substrate (called “destination vector”) to create an *attB*-containing expression clone. This reaction is catalysed by LR Clonase™ II enzyme mix (Invitrogen).

The presence of the *ccdB* gene within this system allows negative selection of the donor and destination vectors in E. coli following recombination and transformation. The CcdB protein interferes with E. coli DNA gyrase (Bernard and Couturier, 1992), thereby inhibiting growth of most *E. coli* strains. When recombination occurs (i.e. between an attB-PCR product and a donor vector or between an entry clone and a destination vector), the *ccdB* gene is replaced by the gene of interest. Cells that take up unreacted vectors carrying the *ccdB* gene or by-product molecules retaining the *ccdB* gene will fail to grow. This allows high-efficiency recovery of the desired clones. For more information concerning the Gateway® technology, refer to the manual “Gateway® Technology with Clonase™ II” (Invitrogen; http://www.invitrogen.com). This summary of the Gateway® technology was taken from the doctoral thesis of Dr. Jan Maisch (Botanical Institute I, KIT, Karlsruhe; Maisch, 2007).

5.9 Effect of localized release of caged auxin on actin organization and membrane curvature

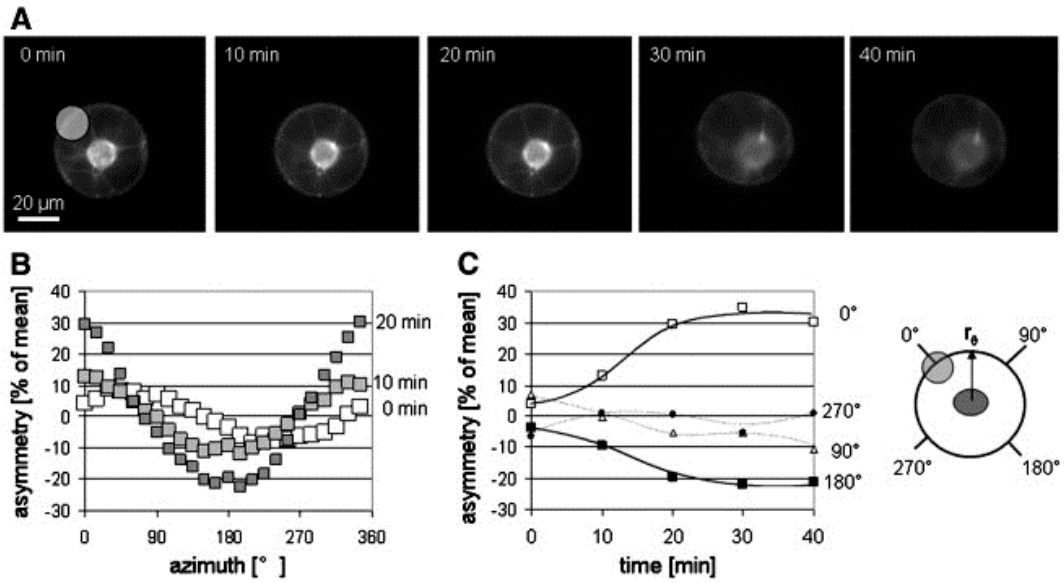

A. Time series of a cell expressing the fluorescent actin marker fimbrin actin-binding domain 2 (FABD2) in fusion with GFP preloaded with 5 µM of caged auxin in slightly hypotonic medium (0.3 M). Auxin was released at time 0 min by a light beam at the indicated position. Note the displacement of the nucleus, the dissolution of transvacuolar actin cables, and the deformation of the protoplast. B Azimuthal plot of the asymmetry defined as relative difference $(r - r_0)/r_0$ at a given azimuth and r_0 as mean radius over the whole circumference of the cell. B. Time course of asymmetry for different azimuthal angles. Note that the most rapid response of asymmetry is observed at the site of auxin release (= 0, see graphical scheme).

Publications

1. **Liu Q**, Qiao F, Ismail A, Chang X, Nick P. 2013. The plant cytoskeleton controls regulatory volume increase. *Biochim.Biophys.Acta* 1828: 2111-2120.

2. Kühn S, **Liu Q**, Eing C, Frey W, Nick P. 2013. Nanosecond electric pulses affect a plant-specific kinesin at the plasma membrane. *J.Membr.Biol. 246:* 927-938.